INVESTIGATION OF INSULATING PROPERTIES OF VACUUM UNDER HIGH VOLTAGE

by

MUHAMMAD ABDUL GOFFAR KHAN

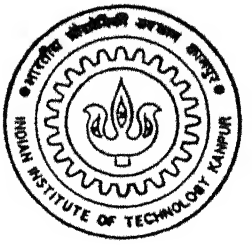

DEPARTMENT OF ELECTRICAL ENGINEERING

INDIAN INSTITUTE OF TECHNOLOGY KANPUR

DECEMBER, 1995

INVESTIGATION OF

INSULATING PROPERTIES OF VACUUM

UNDER HIGH VOLTAGE

A Thesis Submitted
In Partial Fulfillment of the Requirements
for the Degree of

DOCTOR OF PHILOSOPHY

by

Muhammad Abdul Goffar Khan

to the

DEPARTMENT OF ELECTRICAL ENGINEERING

INDIAN INSTITUTE OF TECHNOLOGY KANPUR

December, 1995

10 JUL 1998
CENTRAL LIBRARY
I. I. T., KANPUR
Acc. No. A 125681

EE-1995-D-KHA-INV

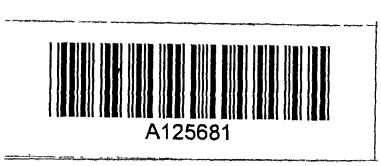

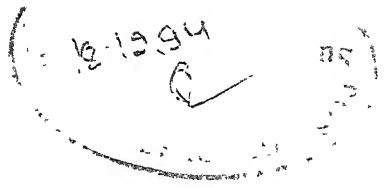

CERTIFICATE

It is certified that the work contained in the thesis entitled "Investigation of Insulating Properties of Vacuum Under High Voltage" by Muhammad Abdul Goffar Khan, has been carried out under my supervision.

Dr. Ravindra Arora

Professor, EE

IIT Kanpur

December, 1995.

ACKNOWLEDGEMENTS

I wish to acknowledge my deep sense of gratitude to Dr. Ravindra Arora for his invaluable guidance, necessary education and encouragement throughout the course of this work.

My sincere thanks to Dr. S.C.Srivastava for his cordial help in different ways.

I wish to thank Major Rajiv Shahwany, Sunil Prem and my friend N.K.Verma for their help, valuable suggestions and support throughout the work. My thanks to Mr.Deshpande for his help in designing different electronic parts of the setup.

My sincere thanks to Mr.S.V.Ghorpade of our lab for his cooperation and assistance during experiments. I also thank to Mr.Brij Kishore for his prompt service.

I wish to thank Mr.Tewary of EE workshop who took lot of pain in fabricating numbers of delicate parts of the setup according to the desired high accuracy. I also thank Mr.Imran Khan for his help.

I am thankful to the authorities of Bangladesh Institute of Technology, Rajshahi and Indian Council for Cultural Relations for the financial help.

At the end I wish to thank my family members specially my wife, nagging daughter Nazia and little Sarim for their loving attention and advice, without whom the work would have completed much earlier.

December 1995. M.A.G.Khan

SYNOPSIS

Name of Student	: Muhammad Abdul Goffar Khan
Roll No.	: 9120463
Degree for which submitted	: Doctor of Philosophy
Department	: Electrical Engineering
Thesis Title	: Investigation of Insulating Properties of Vacuum Under High Voltage.
Name of Supervisor	: Dr.Ravindra Arora
Month & Year of submission	: December, 1995.

Vacuum has very old history of being used as electrical insulation. It was used in X-Ray tubes, electronic valves, high frequency capacitors and interrupters etc. It has good arc quenching property also. For this reason it is being now used widely in power circuit breakers. Other proposed applications are in vacuum insulated fuses, lightning arresters and cryocables. The most recent application of vacuum is in space based high voltage apparatus, such as satellites and space stations. The advantages of use of vacuum as electrical insulation are that it reduces the weight and volume of the system considerably and offers no manufacturing and aging problems. It is also safe and self healing.

While going through the international literature, it was found that most of the experiments performed for the investigation of insulating properties of vacuum under high voltage have been on highly clean conditions of vacuum where sophisticated methods of cleaning and electrode preparation were adopted. This may have been possible for a few number of electrodes to be tested under ideal conditions in the laboratory. However, it is not practically feasible in case of large manufacturing process. It is also questionable if it is maintained

over the life time of an apparatus of 40-50 years. Different electrode conditioning and baking methods are reported which have given rise to very high breakdown strength temporarily. Most of the results are reported for a particular pressure by individual authors. Moreover, different shapes and sizes of electrodes have been used with different types of applied voltages in different publications. Hence, it was not feasible to make a comparative statement of these results. It was also found that different terminologies were adopted to define an electric field configuration. The concept of weakly nonuniform field was not mentioned in any publication. Keeping all these in mind, it was proposed to investigate the insulating properties of vacuum under normal conditions in practice adopting simple methods of cleaning and without electrode conditioning and baking. Experiments were carried out at a wide range of pressure between 0.34 and 10^{-6} Torr. Same electrode pairs were investigated for both ac and impulse voltages. Electrode shape and size were chosen to remain within weakly nonuniform field configuration still having wide range of degree of uniformity, η. The objectives of the work were (a) to investigate the insulating properties of vacuum under practical conditions (b) to estimate the degree of uniformity by Charge Simulation Method and (c) to find the dependency of the breakdown strength with ac power frequency and lightning impulse voltages and the degree of uniformity. A brief description of the work follows.

In Chapter 1 a comprehensive literature survey is reported and some of the experimental work, performed earlier by other researchers, under different conditions of vacuum are described. Different factors influencing the breakdown strength are discussed. After a critical examination of earlier research work, the scope of the present work is

described in this chapter.

In Chapter 2, the suitability of the Charge Simulation Method (CSM) for the estimation of electric fields is described. This method has been applied to investigate the electric field and the degree of uniformity of twelve different electrode pair configurations under two different conditions of voltage application, (a) symmetrically applied voltage of ±U/2 and (b) asymmetrically applied voltage of U and 0. Only point charges were adopted to simulate the equipotential electrode surfaces although different types of charges and their combinations such as line charge, ring charge etc. have been used by other workers. The results are in good agreement with others. Numerical value of degree of uniformity, η has been estimated for different electrode configurations having a unit gap distance. The results obtained enable to estimate the effects, such as that of grounding of one of the electrodes on the field, by calculating the value of η. The method applied in this work for electrodes having rotational symmetry can be conveniently extended to any electrode used in practice. It may be useful in designing GIS and space based systems more confidently.

The development of the experimental setup is described in Chapter 3. A vacuum chamber (test vessel) was needed to be fabricated as the commercially available chambers, made of stainless steel, were not compatible to the specific needs for this work. The detailed of this vacuum chamber are furnished. A mechanism was fabricated which helped to set a desired gap distance between the electrodes without disturbing the vacuum conditions. A commercially available vacuum pumping system was procured for the work which was not suitable for high voltage applications. Several modifications had to be made to

this pumping system which include the design and fabrication of a heater and a solenoid operated valve which is used to minimize the backstreaming of oil. This way a know how for making conventional vacuum pumping system compatible for high voltage application was developed. Fabrication and cleaning of the electrodes with the help of commercially available methods are also described in this chapter.

The experimental results under alternating power frequency voltage (ac) and lightning impulse voltage (li) are discussed in Chapters 4 and 5 respectively. Photographs showing stages of glow phenomena observed at low vacuum levels are given. Variation of breakdown voltage of vacuum has been investigated with changing gap distance and pressure. Characteristic curves have been measured revealing the typical behaviour of vacuum as a dielectric medium. It is interesting to observed from the measured results how the breakdown strength of vacuum first decreases from a high value at slightly less than atmospheric pressure to very low values at low vacuums (ambient plasma state) and then rises again to very high values at high vacuums (10^{-4} to 10^{-6} Torr). The results obtained under high vacuum have been analyzed for their dependency with the degree of uniformity, η of the field.

In Chapter 6, the results obtained from the present investigations have been compared with those obtained by other workers. It can be seen that the breakdown strength of practical vacuum are slightly lower than that obtained under ideal conditions by others. The experimental setup developed in this work could be used for further investigations under switching impulse voltages and with solid insulators in vacuum. Suggestions and the scope for a continued research has been discussed at the end of this chapter.

LIST OF SYMBOLS

U_b	Breakdown voltage
U_{b50}	50% breakdown voltage
ac (voltage)	Alternating power frequency (voltage)
li (voltage)	Lightning impulse (voltage)
si (voltage)	Switching impulse voltage
dc	Direct current
E	Electric field intensity
E_{bmax}	Maximum electric field intensity at breakdown
E_{bav}	Average electric field intensity at breakdown
d	Gap distance between electrodes
η	Degree of uniformity, Schwaiger factor
s	Second
ms	Millisecond
μs	Microsecond
mPa	10^{-3} Pascal
mBar	10^{-3} Bar
HV	High voltage
V	Volt
kV	10^{3} Volt
A	Ampere
kA	10^{3} Ampere
mm	Millimeter
cm	Centimeter
μm	Micrometer
CSM	Charge Simulation Method
SPSP50	Sphere-sphere electrode pair, diameter 50 mm
SP25PL	Sphere-plane electrode pair, sphere diameter 25 mm
SP50PL	Sphere-plane electrode pair, sphere diameter 50 mm
RODPL	Rod-plane electrode pair
PLPL	Plane-plane electrode pair

CONTENTS

CHAPTER 1
INTRODUCTION AND LITERATURE SURVEY

1.1	Introduction	1
1.2	Literature survey	2
1.3	Prebreakdown phenomenon in vacuum	3
1.3.1	Electron emission from metallic surfaces	4
1.3.2	Nonmetallic emission process	7
1.4	Investigation on space as electrical insulation	9
1.5	Area effect and shape factor of electrodes	10
1.6	Effect of front time of switching impulse	12
1.7	Comparison of dc and ac breakdown voltage	12
1.8	Effect of conditioning of electrodes	13
1.9	Investigations reported on vacuum circuit breakers	14
1.10	Review of literature survey	15
1.11	Objective of the thesis	16
1.12	Scope of present research	17
	References	18

CHAPTER 2
ESTIMATION OF ELECTRIC FIELD BY NUMERICAL METHODS

2.1	Introduction	22
2.2	Classification of electric fields	23
2.3	The degree of uniformity, η	23
2.4	Numerical methods	25
2.4.1	Charge Simulation Method	26
2.4.2	Surface Charge Simulation Method	26
2.5	Application of CSM for the estimation of field	26
2.5.1	The mathematical analysis	27
2.5.2	Electrodes configuration considered for investigation	29
2.5.3	Estimation of E and η	32
2.5.4	Results and discussions	34
2.5.4.1	Effect of symmetrically applied voltage on the distribution of equipotential lines	34

2.5.4.2 Effect of asymmetrically applied voltage on the distribution of equipotential lines 47

2.5.4.3 Effect of the mode of applied voltage on the distribution of electric field intensity 48

2.5.4.4 Effect of applied voltage on the degree of uniformity, η 55

2.5.5 Conclusion 57

References 58

CHAPTER 3

DEVELOPMENT OF THE EXPERIMENTAL SETUP

3.1 Introduction 60

3.2 High voltage ac supply 61

3.3 Impulse generator 61

3.4 Oscilloscope 64

3.5 Current viewing resistor 64

3.6 Vacuum pumping system 64

3.6.1 The rotary vane pump 68

3.6.2 Diffusion pump 72

3.6.3 Measurement of pressure 74

3.7 Modification of vacuum pumping system for high voltage use 77

3.7.1 Modification of solenoid 77

3.7.2 Modification of heating arrangement of diffusion pump 79

3.8 Design and fabrication of vacuum chamber 82

3.9 Design and fabrication of gap adjustment mechanism 85

3.10 Electrode preparation 88

3.11 Cleaning of electrodes and vacuum chamber 88

References 90

CHAPTER 4

INVESTIGATION WITH ALTERNATING POWER FREQUENCY VOLTAGE

4.1 Introduction 91

4.2 Investigation at low vacuum 92

4.2.1 Experimental setup 93

4.2.2 Adjustment of pressure 93

4.2.3	Observations	95
4.2.4	Measurement of conduction current with increasing voltage	104
4.2.5	pd versus breakdown voltage	106
4.3	Investigation at high vacuum	108
4.3.1	Electrodes used for investigation	108
4.3.2	Experimental procedure	109
4.3.3	Experimental results	109
4.4	Comparison of breakdown strength of different electrode pairs	123
	References	129

CHAPTER 5

INVESTIGATION WITH LIGHTNING IMPULSE VOLTAGE

5.1	Introduction	130
5.2	Experimental setup	130
5.3	Experimental procedure	132
5.4	Determination of 50% breakdown voltage	132
5.5	Occurrence of partial breakdown	133
5.6	Time required for breakdown	136
5.6.1	The phenomenon of statistical time lag as observed in vacuum	136
5.6.2	Time required to bridge the gap distance for breakdown	138
5.7	Investigation at low vacuum	142
5.8	Investigation at high vacuum	147
5.8.1	Comparison of breakdown voltages measured for different electrode pairs	151
5.9	Effect of pressure on breakdown voltage	151
5.10	Comparison of positive and negative impulse voltage	155

CHAPTER 6

CONCLUSIONS

6.1	Introduction	156
6.2	Conclusions	157
6.3	Scope of further research	160
	References	161

CHAPTER 1

INTRODUCTION AND LITERATURE SURVEY

1.1 Introduction

The idea of using vacuum for insulating purpose is very old. Electrical Phenomena in vacuum have been studied since 1897 [1.1]. It has found wide applications in electronic valves, X-Ray tubes, high frequency capacitors, controlled nuclear devices, electrostatic generators and now also for high power vacuum capacitors and interrupters.

Vacuum has good insulating as well as arc quenching properties. For this reason it has found use for current breaking in high voltage apparatus. In the year of 1960, vacuum circuit breakers, capable of breaking respectable short circuit currents were designed for the first time. Other applications of vacuum in power system are in vacuum insulated fuses, lightning arresters and cryocables [1.2]. It is the insulation that at the same time provides a good thermal insulation which satisfies the design of cryogenically cooled cables.

The most recent application of vacuum as insulation is thought of for space applications, for example, in satellites and space stations. Many space observation methods require electricity at ~5 kV for supplying power to analyzers, spectroscopes and cameras. Communication satellites use travelling wave tubes which need high power HV supplies at voltages >15 kV. Application of a carbon dioxide

gas laser, for studying earth's atmosphere, requires safe operation at voltage >100 kV [1.3]. Vacuum a weightless insulation, can serve the purpose best for these applications.

As an insulator, vacuum has the following advantages :-

(a) Use of vacuum is safe. In case of any accident, no fear of fire hazard or leaking of poisonous by-products.

(b) It is self healing. Occasional flashover do not result in permanent damage.

In case of space application,

(c) It reduces the weight and volume of the system.

(d) It allows easy assembly, testing, repairing etc. because all parts are accessible in space.

(e) There is no manufacturing and aging problem as vacuum is naturally available in space.

1.2 Literature survey

The field of electrical discharges in vacuum has been a subject of intensive theoretical and experimental investigation for many years. Two bibliographies were published by H.Craig Miller in 1990 and 1991 respectively [1.4, 1.5]. The total number of articles enlisted in these are about 3000. The first one, covers the field of electrical discharges in vacuum, contains all references from 1877 through 1979 while the second one contains from 1980 to 1990. The references were first grouped by year, then within a year alphabetically by the first author. Along with an author index was also given which allows to find all papers with which a particular author was associated.

While going through the titles of the papers of these two bibliografic references, about one hundred papers were chosen which

described different laboratory experiments performed to understand the insulating properties of vacuum under high voltage, which are of interest of this work. A study of these references revealed that in most of the experiments, very complicated setup were used to simulate the most ideal conditions for experimental setup. The results show very high voltage withstand capabilities. However in practice the condition in which vacuum is subjected to high voltage, is quite different and far away from the ideal conditions. Adsorbates, metal oxides, contaminants etc. are introduced to the vacuum from the pumping system, which affect the insulating property causing a lower breakdown strength. Considering these, a few number of papers were chosen to be discussed here which are closely related to practical conditions. These involve comparatively simpler experimental setup and the results are in good agreement with the practical conditions. The extension of these works appeared to be possible within the facilities available in our laboratory.

The subject of electrical breakdown in vacuum has been thoroughly discussed in a recent book by R.V.Latham [1.9]. Other good recent reviews of vacuum breakdown have been written by Chatterton [1.10] (184 references) and Farral [1.11, 1.12] (160,163 references). Surface flashover of insulators in vacuum has been reviewed by Latham [1.9] and Miller [1.13] (99 references).

1.3 Prebreakdown phenomenon in vacuum

A fairly good number of papers have been published which describe different prebreakdown phenomenon in vacuum. They can be broadly divided into two categories, (a) Electron emission from metallic surfaces, (b) Nonmetallic emission process.

1.3.1 Electron emission from metallic surfaces

Initially it was thought that the prebreakdown current in vacuum is due to field emission, field assisted thermionic emission or thermionic emission. The results of the experiments performed under highly clean conditions and at very low pressure (10^{-9} Torr) for small gap distances (fraction of mm to mm range) agree with this theory. Some of such experiments and their results are described below.

In 1966, D.K.Devis and M.A.Biondi reported the results of their experiment in extremely high vacuum, 10^{-9} Torr [1.14]. They measured the prebreakdown current between two parallel plane copper electrodes, which were thoroughly outgassed by a tedious process. The electrode preparation was also very complicate before they were placed for experiment. The experiments were conducted for a gap range of 0.3 to 2 mm. The measured current was found to be in good agreement with Fowler-Nordhim theory of field emission from the pure metal surface. From combined measurements of prebreakdown currents and breakdown voltages at different electrode separations, it was concluded that the "cathode microscopic field" at breakdown was constant and was of magnitude of the order of $(6 \pm 1)\times10^{7}$ v/cm.

Two papers were published in 1967 [1.15, 1.16], describing theoretical and the experimental work, by F.M.Charbonnier and his co-workers. Their experiments were for very short gap lengths, 1/1000 to 1/10 inch under dc voltage. They attempted to prove the complicated theory given in the first paper.

A more comprehensive work was reported by T.Utsumi in the same year [1.17]. He investigated the problem whether the breakdown between

two parallel plane electrodes in vacuum was an anode induced or cathode induced breakdown. He also tried to investigate the conditions under which the above mentioned type of breakdown dominate. The critical anode current density for an anode induced breakdown and critical cathode current density for a cathode induced breakdown were measured by using very complicated set up comprising optical microscope etc.

In 1972, R.Hackam and S.K.Salman measured the prebreakdown currents for short gaps (2.8 mm) in high vacuum, at 10^{-9} Torr, between aluminium electrodes under dc voltage. The prebreakdown currents were found to follow Fowler-Nordhim field emission theory. For gap separation larger than 0.89 mm, a large increase in the prebreakdown current was observed at a particular applied voltage. The current sensing voltage was determined as a function of the gap spacing and was found to increase with increasing gap separation. The variation of breakdown voltage and its effect on subsequent current emission was also investigated by the same author and reported in another paper [1.20]. The breakdown voltage was found to increase linearly with gap distance upto a gap = 0.7 mm. After completion of first series of breakdown, the prebreakdown current-voltage characteristic were measured and it was found that the field enhancement factor, β decreases after breakdown presumably due to conditioning.

A work to investigate the electrical insulation properties of vacuum with silver alloy electrodes was reported by R.Hackam and S.K.Salman in 1975 [1.18]. They measured the prebreakdown currents between a pair of parallel plane sterling silver (an alloy of silver and copper, silver 92.5% and copper 7.5%) electrodes having 11 mm

diameter. The electrodes were given a surface roughness of 25 μm, cleaned with methanol and acetone and placed in a vacuum chamber which was evacuated to a pressure ~10^{-9} Torr by running a sorption pump backed by triode ion pump for five days. They found that the prebreakdown current follow the Fowler-Nordhim field emission theory. The field enhancement factor, β was found to increase with the increase of gap length. The value of β was determined before and after breakdown. It was observed that the effect of sparking is to decrease the value of β at a fixed gap length. It was also found that repeated sparking of electrodes resulted in a considerable decrease in the emitted current at a fixed gap length and a fixed applied voltage. The breakdown voltage was found to increase linearly with gap spacing upto d = 1.5 mm at which a transition to the Cranberg clump [1.19] mechanism of vacuum breakdown ensues. The critical electrical field intensity at microprotrusions at breakdown voltage was $(7.7 \pm 0.7)\times10^{9}$ V/m in the range d = 0.25 to 2.54 mm.

In the year 1982, a group of six workers [1.22] reported another interesting experimental work conducted to study the field emission characteristics and its dependency on breakdown with copper electrodes in vacuum under switching impulse voltage. They used two different electrode configurations, (a) sphere-sphere , diameter = 80 mm, and (b) rod-plane, tip diameter of rod = 5 mm, diameter of plane was not mentioned. The gap distance was 12 mm. They described these field configurations as uniform and nonuniform field respectively, while both are actually weakly nonuniform fields [1.6, 1.7]. The impulse voltage waveshape was 280/2000 μs. The surfaces of the electrodes were machined to ±2 μm smoothness. The vacuum chamber, made of pyrex glass, was evacuated to a pressure of 1×10^{-6} Torr with the help of an ion

pump and Ti-getter pump. While evacuating, the vessel was baked in a furnace at 350° C for 20 hours. A shunt of 1 kΩ was used to measure the prebreakdown current by a CRO. The current was found to follow the Fowler-Nordhim field emission theory. They explained the breakdown of sphere-sphere gap by anode heating hypothesis. They also found that breakdown between rod-plane gap depended on the polarity of applied voltage. For the given dimensions of the rod and gap distance, the effect of polarity on breakdown could have been observed as the field configuration approached the extremely nonuniform field.

In 1983, K.Tsuruta [1.24] studied the mechanism of prebreakdown field emission current and breakdown voltage of small vacuum gaps. He used parallel plane copper electrodes, for very small gap range between 0.002 to 0.2 mm. The voltage waveform was 550/5500 μs. The breakdown field strength, effective field enhancement factor and field emission current just prior to breakdown were found to be a function of gap spacing. It was noticed that with a decrease in gap spacing, the field emission current just prior to breakdown increased sharply.

1.3.2 Nonmetallic emission process

The conduction currents between vacuum insulated high voltage electrodes were attributed to a field emission process occurring at isolated metallic microprotrusions for over a century. However as a result of new evidences, in 1983 R.V.Latham [1.23] proposed that the localized emission currents could actually stem from some form of complex non-metallic emission mechanism. The phenomenon is associated with some form of insulating/semiconducting surface oxide or impurity concentrations. He has given a brief review of the experimental evidences in support of the above contention, in which the breakdown

strength was found to be as low as 10^6 V/m for contaminated electrodes while that for ideal case it could be $3x10^9$ V/m.

J.Halbritter [1.25] explained the theoretical background of how the breakdown strength of practical vacuum becomes low. He described that the oxides, adsorbates and dust present on broad area electrodes, especially in technical systems, limit electric field in three respects (i) by enhancing field emission, (ii) by enhancing secondary field emission and (iii) simulated desorption of molecules and ions. Because of these phenomena, breakdown strength could be as low as 10^6 V/m.

As a continuation of earlier works, [1.14-1.18, 1.24], K.Tsuruta [1.28] investigated prebreakdown currents for a long duration impulse voltage. He used parallel plane copper electrodes having diameters 12 and 14 mm in a vacuum of $2.25x10^{-7}$Torr. The experimental setup was very simple. It consisted a vacuum chamber made of pyrex glass, having diameter 150 mm and length 250 mm. The vessel was evacuated with an oil diffusion pump backed by a rotary pump and liquid Nitrogen trap. The electrode surfaces were polished to give a mirror finish using 4000 grit emery paper. They were rinsed with water and then with alcohol before placing in vacuum. To set the gap distance, a screw mechanism was used which could be adjusted by the rotation angle for which one degree corresponded to 0.0028 mm of gap spacing. The component of the prebreakdown current due to field emission, measured against a 500 Ω resistor, was found to follow Fowler-Nordhim field emission theory. The field enhancement factor, β was found to increase from 15 to 230 with increasing electrode separation from 0.003 to 2.5 mm while the average breakdown field strength decreased from $7x10^8$ V/m to $3.3x10^7$ V/m with increasing electrode separation.

1.4 Investigation on space as electrical insulation

High voltage and high current power systems require electrical insulation against breakdown and discharge. Ground systems can use solid, liquid or gaseous insulation techniques. However placing these systems in space requires light weight insulation techniques. Among the traditional ground insulators, only electronegative gases appear to be light enough for use in space, but the containers needed to hold the various components and gases are large and heavy.

Strategic Defense Initiative Organization (SDIO) [1.3] has been investigating the use of vacuum (ambient plasma) as electrical insulation in low earth orbit (LEO) environment. The LEO environment is not perfect vacuum but is actually a low density gas or plasma. It contains charged particles, electrons and ions in addition to neutral molecules and atoms. This ambient plasma causes problems such as breakdown, excessive power drain, outgassing, component malfunction and spacecraft charging etc. while the spacecraft moves through LEO environment. SDIO has performed a number of experiments, called Space Power Experiments Abroad Rockets (SPEAR), to establish the basis for treating the problems in the areas of high voltage insulation and to develop pulsed power system that use space vacuum as electrical insulation. SPEAR-I was launched in 1987 to understand the formation of plasma sheath around the spacecraft at 12 kV. The results of SPEAR-I demonstrated that light weight, high voltage systems could be operated in LEO environment. SPEAR-II was designed to validate the space vacuum insulation technology by exposing two separate systems in LEO environment, (a) a 100 kV high voltage system, (b) a 150 kA high current system.

1.5 Area effect and Shape factor of electrodes

A number of researchers have reported the so called "Area effect" of electrodes on breakdown in vacuum. It states that the breakdown strength of a vacuum gap decreases as the effective area of the electrode increases. By "effective area", it is meant the area of the electrode surface in which the electric field intensity is 90% to 100% of the maximum electric field in the dielectric.

This concept of effective area of electrode surface was introduced by H.Toya and his co-workers [1.21] in 1981. They conducted a detailed experiment to study the statistical property of breakdown with metal electrodes in vacuum. Parallel plane copper electrodes were used for gap lengths between 3 to 20 mm. Three pairs of electrodes having diameters of 50, 100 and 200 mm with different radius of curvatures at the edge, 7.5, 15 and 30 mm respectively were investigated. The electrode surface was polished to 1 μm smoothness and degreased with acetone by an ultrasonic vibrator. The test chamber was of stainless steel having diameter 60 cm and length 75 cm. It required 4 hours of continuous run of a oil diffusion pump backed by a rotary pump to create a vacuum of 2×10^{-6} Torr. Before the experiment was started, the electrodes were subjected to "glow conditioning". The results have been summarized by expressing the cumulative probability of breakdown as a function of applied voltage and gap length. They used a slow impulse voltage of waveform 0.5/10 ms. The 50% breakdown voltage, U_{b50} was expressed by $U_{b50} \propto \sqrt{d}$, where d is the gap distance.

Later, T.Shioiri and co-workers [1.22] proposed a method to find the effective area, S_{eff} of the electrode and found a relation between effective area and the voltage. The area effect on breakdown field

strength was analytically described to be $E_b \propto (S_{eff})^{-1/4}$ [1 12]

B Mazurek and J D Cross [1 29] presented energy explanation of the so called "area effect" [1 8 in 1 29, 1 22] in electrical breakdown in vacuum They used point-plane electrode for their experiment The diameter of tip of the point electrode was 3 mm and that of the plane was 100 mm The electrode surfaces were mechanically polished and cleaned in hot water and detergent solution in an ultrasonic cleaner It was found that a capacitor connected in parallel with the electrode gap reduces the electrical strength in a manner similar to that observed with increasing electrode area

The concept of "shape factor" was introduced by T Shioiri [1 22] for rod-plane electrode The shape factors of rod and plane were defined as $\alpha_r = E_r / E_{av}$ and $\alpha_p = E_p / E_{av}$, where E_r and E_p are the maximum field intensities at the rod and plane respectively and E_{av} is the average field intensity

The area effect was verified by M Okawa and his friends in 1988 [1 30] Total six numbers of different electrode configurations were investigated by them The pressure was $0\ 75 \times 10^{-6}$ Torr The waveshape of the voltage used was 450/2300 μs and the gap length was 15 mm (variable) They concluded that the breakdown field strength, $E_b = \alpha U_b/d$, depends on the effective area S_{eff} and can be expressed by a single experimental equation $E_b = K_1 (S_{eff})^{-n}$, where K_1 is a constant, n is about 0 24 [1 22], S_{eff} is the electrode area subjected to more than 90% of maximum field strength, α is the "shape factor" [1 22] Similarly the field enhancement factor, β can also be expressed as $\beta = K_2 (S_{eff})^n$

1.6 Effect of front time of switching impulse

In 1985, K V Srinivasa and G R Nagabhusana investigated prebreakdown conduction in vacuum gaps under switching impulse voltage [1 26] The electrode configurations used in their experiments were (a) hemisphere-plane, diameter of hemispheres were 3, 10, 20 and 30 mm, that of plane was 30 mm with edge rounded off to a radius of 1 5 mm, (b) needle-plane, needle tip diameter was 0 1 mm, (c) needle-needle The gap distances were 0 5, 1, 1 5 mm All electrodes were of stainless steel polished to mirror finish with micron size alumina powder and ultrasonically cleaned before experiment Slow switching impulse voltages with front times of 200 μs, 750 μs, 1 7 ms, 3 ms and 5 ms were used for the investigation The pressure was below 0 1 mPa ($\cong$ 7 5x10^{-7} Torr) They measured the prebreakdown current for each set of electrodes and si voltages It was always found that there was a time lag between the voltage peak and current peak, varying from 0 3 to 0 5 ms The time lag increased with the front time

1.7 Comparison of dc and ac breakdown voltage

A comparative study of vacuum breakdown under 50 Hz ac and dc voltages was conducted by R Hackam [1 27] He measured the dc breakdown voltage for high vacuum using silver alloy electrodes The breakdown voltage with dc was found to increase to the level of the peak ac 50 Hz voltage after conditioning of both electrodes Over a range of gap distance of 0 2 to 1 mm, the equality of dc and ac breakdown voltage was confirmed by him

1.8 Effect of conditioning of electrodes

Different methods of conditioning of electrodes have been adopted by researchers while performing the experiments The net effect of all the conditioning methods adopted was found to increase the breakdown voltage temporarily

Glow conditioning was introduced by H Toya [1 21] in 1981 His experiment was with slow impulse voltage of waveform 0 5/10 ms. Before the breakdown, he produced glow discharge in the volume of the vacuum chamber by applying low voltage at a comparatively higher pressure He described that by doing so, the adsorbed gases are removed from the chamber and the vacuum is cleaned According to him this was the reason for measuring higher withstand voltages compared to without conditioning

The method of "arc conditioning" was described by H Pursch and his co-workers [1 33] They used parallel plane electrodes of diameter 25 mm, the gap distance was variable between 1 to 3 mm The experiment was carried out in a stainless steel vessel, evacuated by an ion pump to a pressure below 0 75x10^{-7} Torr While being evacuated, the vessel was heated to 400°C in order to remove gases Prebreakdown current measurements were carried out at different stages of conditioning, fresh electrodes, after several hundred dc breakdown, after arc conditioning and after mechanical disruption of electrodes jointed together by passing a high current pulse across the electrodes kept in contact with each other Their results showed that the dielectric strength strongly depends upon surface conditions of the electrode material With the help of arc conditioning, the breakdown strength can be increased by a factor ~ 5

K Tsuruta [1 28] adopted "spark conditioning" by applying

impulse voltage through current limiting resistors for about 100 times before applying the actual test voltage He concluded that the sharp projections on the electrodes were blunted off by this process which caused higher withstand voltage

T Tsutsumi [1 32] treated his electrodes by "current conditioning" method The parallel plane electrode surfaces were conditioned by letting impulse currents of several kA flow for a few times

N C Jaitly et al [1 34] adopted DC step conditioning procedure Their experiment was with dc voltage Before reaching the breakdown voltage, it was increased in a step of 4-6 kV and held for 90 seconds O Yammoto [1 35] also used same conditioning method but at a step of 10 kV Step conditioning with impulse voltage was used by H H Zhong [1 37] He applied 4-6 pulses at a step of 10 kV It appears that the step conditioning method has been adopted in case of solid insulators in vacuum The use of step conditioning for vacuum as insulation has not been reported

1.9 Investigations reported on vacuum circuit breakers

The test report of a commercial 24 kV vacuum interrupter with butt contacts was presented by L M J Vries and G C Damstra in 1988 [1 31] They used three different contact materials, OFHC copper, stainless steel and Cu/Cr (75/25) At a constant distant of 1, 2, 3 mm , the critical breakdown field was computed based on the prebreakdown emission current measurements They proposed an experimental formula to find critical breakdown field, $E_c = \beta U_b/d$

H.Toya et al [1 37], developed a model for vacuum interrupter of 72 kV rating Their experiments were conducted on two different

electrode configurations, (a) a pair of hemispherical copper electrodes of diameter 80 mm and gap 5 mm (b) a pair of parallel plane electrodes of diameter 50 mm, gap was variable between 10 to 40 mm Switching impulse voltage of 250/2000 μs and lightning impulse voltage of 1/40 μs were used in the experiment They developed a numerical model which can be used to evaluate withstand voltage of HV vacuum interrupters

1.10 Review of literature survey

From detailed study of publications investigating vacuum as an insulation following conclusions can be drawn

(a) The shape, size and dimensions of the electrodes used by the workers are different from each other The gap distances are also vary over a wide range between a few μm to a few tens of mm Therefore it is very difficult to compare the results drawn by different workers

(b) The pressure range in which the majority of experiments have been conduced varies over a wide range between 10^{-3} to 10^{-9} Torr

(c) Different methods of conditioning have been adopted which could result in a very high breakdown voltage An increase even by a factor of 5 is reported The breakdown strength of vacuum used in practice is much less than these values

(d) In most of the work with impulse voltage, standard lightning wave shape has not been used Often the polarity of the wave shape has not been mentioned

(e) Different sophisticated methods were adopted to prepare the electrodes before experiments Expensive coating of electrodes (for example, gold plating etc) and cleaning techniques (ultrasonic cleaning) were adopted in some of the experiments These methods of electrode preparation, cleaning and coating may be possible for a few

electrodes to be used in the laboratory However such sophisticated techniques may not be possible for commercial production of equipments Besides the condition of the electrodes in due course of life of the equipment may not remain that ideal in practice

(f) A very important conclusion could be drawn that the concept of uniform and nonuniform electric field is not clear among the workers so far Since the behaviour of dielectrics strongly depends upon the type of field, it is necessary to first classify the field configurations Investigations according to the classification of fields on the basis of Schwaiger factor have not been made so far

1 11 Objective of the thesis

On the basis of the literature survey and the possible laboratory facilities, following investigations are proposed for this work -

(a) The insulating property of vacuum is proposed to be studied over a wide range of pressure beginning near the Paschen's minimum to 10^{-6} Torr

(b) The suitability of the application of Charge Simulation Method (CSM) is proposed to be investigated for the estimation of electric field intensity in the gap between the electrodes and for the estimation of the degree of uniformity (also known as the Schwaiger factor, η) of the electrode system

(c) The insulating property of vacuum is proposed to be studied under ac and li voltage using the same electrodes during experiments

(d) Comparatively simpler, commercially available and less costly methods would be adopted for electrode preparation, cleaning and polishing The results obtained could thus be useful in practice

1.12 Scope of present research

The results of the research are expected to be used in the following fields

(a) The results could be helpful in designing vacuum circuit breakers (VCB) of higher voltage rating Presently vacuum circuit breakers are available upto 33 kV only Higher voltage VCB are still being developed (b) The investigation of the insulating properties of low vacuum near Paschen's minimum (ambient plasma) may be helpful in designing space based apparatus using high voltage such as analyzers, spectroscopes etc It could be used in designing space based high voltage power supply system

(c) Vacuum insulation is not only a good electrical but also a good thermal insulator Therefore it can be successfully used in cryogenically cooled cables and other apparatus

(d) A complete vacuum insulated substation (VIS) can be designed

REFERENCES

1 1 R W Wood, "A new form of cathode discharge and the production of X-Rays together with some notes on diffraction", Physics Review, vol 5, No 1, pp 1-10, 1897

1 2 Peter Graneau, "Underground Power Transmission", John Wiley & Sons, 1979

1 3 L Rustan Jr , "SDIO space insulation techniques", Conference record of the IEEE International Symposium on Electrical Insulation, Baltimore, USA, 1992

1 4 H Craig Miller, "Electrical discharges in vacuum 1980-1990", IEEE Trans on Electrical Insulation, vol 26, pp 949-1043, 1991

1 5 H Craig Miller, "Electrical discharges in vacuum 1877-1989", IEEE Trans on Electrical Insulation, vol 25, pp 765-860, 1990

1 6 R Arora and W Mosch, "High voltage insulation engineering", Wiley Eastern Ltd , India, 1995

1 7 M A G Khan and R Arora, "Application of charge simulation method (CSM) for the estimation of field between HV and grounded electrodes", Proc of 3rd workshop and conference on EHV technology, Bangalore, India, 1995

1 8 D J Simon and R Michelier, "Electrostatic separator development", Proc III DEIV conference, pp 263-273, 1968

1.9 R V Latham, "High voltage vacuum insulation", Academic Press, London, New York, 1981

1 10 P A Chatterton, "Vacuum Breakdown", John Wiley, New York, 1978

1 11 G A Farral, "Electrical breakdown in vacuum", John Wiley, New York, 1980

1 12 G A Farral, "Electrical breakdown in vacuum", IEEE Trans on Electrical Insulation, vol EI-20, pp 815-841, 1985

1 13 H C Miller, "Surface flashover of insulators", IEEE Trans on Electrical Insulation, vol EI-24, pp 765-786, 1989

1 14 D K Davis and M A Biondi, "Vacuum electrical breakdown between parallel plane copper electrodes", J Applied Physics, vol 37, pp 2969-2977, 1966

1 15 F M Charbonnier, C J Bennette and L W Swanson, "Electrical breakdown between metal electrodes in high vacuum, I - Theory", J Applied Physics, vol 38, pp 627-633, 1967

1 16 F M Charbonnier, C J Bennette and L W Swanson, "Electrical breakdown between metal electrodes in high vacuum, II - Experiment", J Applied Physics, vol 38, pp 634-640, 1967

1 17 T Utsumi, "Cathode and anode induced electrical breakdown in vacuum", J Applied Physics, vol , pp 2989-2997, 1967

1 18 R Hackam and S K Salman, "Electrical insulating properties of sterling silver electrodes in ultrahigh vacuum", IEEE Trans on Electrical Insulation, vol EI-10, pp 9-13, 1975

1 19 L Cranberg, "The initiation of electrical breakdown in vacuum", J Applied Physics, vol 23, pp 518-522, 1952

1 20 R Hackam and S K Salman, "Vacuum breakdown and its effect of subsequent current emission", Proc of IEE vol 119, No 3, pp 1747-1750, 1972

1 21 H Toya, N Veno, T Okeda and Y Murai, "Statistical property of breakdown between metal electrodes in vacuum", IEEE

Trans on PAS, vol 100,- pp 1932-1939, 1981

1 22 T Shioiri, I Ohshima, M Honda, H Okumura, H Takahasi, H Yoshida, "Impulse voltage field emission characteristics and breakdown dependency upon field strength in vacuum gaps", IEEE Trans on PAS, vol PAS-101, pp 4178-4184, 1982

1 23 R V Latham, "Prebreakdown electron emission", IEEE Trans on Electrical Insulation, vol EI-18, pp 194-203, 1983

1 24 K Tsuruta, "Prebreakdown field emission current and breakdown mechanism of a small vacuum gap", IEEE Trans on Electrical Insulation, vol EI-18, pp 204-208, 1983

1 25 J Halbritter, "On contamination on electrode surfaces and electric field limitations", IEEE Trans on Electrical Insulation, vol EI-20, pp 671-681, 1985

1 26 K V Srinivasa and G R Nagabhusana, "Prebreakdown conduction in vacuum gaps under switching impulse excitations", IEEE Trans on Electrical Insulation, vol EI-20, pp 691-695, 1985

1 27 R Hackam, "Comparison between 50 Hz ac and dc vacuum breakdown", J of Physics, Sec-D Appl Physics, vol 8, pp L53, 1975

1 28 K Tsuruta, "Impulse electrical breakdown fields of short vacuum gaps", IEEE Trans on Electrical Insulation, vol EI-22, pp 77-79, 1987

1 29 B Mazurek, and J D Cross, "An energy explanation of the area effect in electrical breakdown in vacuum", IEEE Trans on Electrical Insulation, vol EI-22, pp 341-346, 1987

1 30 M Okawa, T Shioiri, H Okubo, and S Yanabu, "Area effect on electrical breakdown of copper and stainless steel

electrodes in vacuum", IEEE Trans on Electrical Insulation, vol EI-23, pp 77-81, 1988

1 31 L M J Vries and G C Damstra, "Prebreakdown emission current measurements in a 24 kV vacuum interrupter with butt contacts",IEEE Trans on Electrical Insulation, vol EI-23, pp 97-100, 1988

1 32 T Tsutsumi, T Shioiri, H Okubo and S Yanabu, "The effect of mechanical contact on breakdown characteristics in vacuum", IEEE Trans on Electrical Insulation, vol EI-24, pp 921-924, 1989

1 33 H Pursch, P Siemroth and B Juttner, "On the nature of prebreakdown emission currents in vacuum interrupters", IEEE Trans on Electrical Insulation, vol EI-24, pp 917-920, 1989

1 34 N C Jaitly, T S Sudarshan, R A Dougal, "Degradation due to Hydrogen firing on the HV performance of Alumina insulators in vacuum applications", IEEE Trans on Electrical Insulation, vol EI-22, 1987, pp 447-452

1 35 O Yamamoto, T Hara, T Nakae and M Hayashi, "Effects of spark conditioning, insulator angle and length on surface flashover in vacuum", IEEE Trans on Electrical Insulation, vol EI-24, pp 991-994, 1989

1 36 H H Zhong, H C Karner and M Gollor, "Time characteristics of fast pulsed flashover in vacuum", IEEE Trans on Electrical Insulation, vol. EI-27, pp 496-503, 1992

1 37 H Toya, T Hayashi, M Yorita and Y Murai, "Numerical modeling to evaluate the withstand voltage of a HV vacuum interrupter", IEEE Trans on Electrical Insulation, vol EI-24, pp 21-30, 1989

CHAPTER 2

ESTIMATION OF ELECTRIC FIELD BY NUMERICAL METHODS

2 1 Introduction

Exact knowledge of potential distribution and electric field intensity,"E" in a dielectric between any two electrodes is necessary for the investigation of the behavior of the insulation The Schwaiger factor or the degree of uniformity, η is an important parameter to asses the distribution of field intensity Estimation of electric field and potential distribution across the gap between spheres of equal and unequal diameters by direct solution of the Laplace's equation have been reported by several workers [2 1] Different electrode shapes such as, sphere-plane, rod-plane, point-plane, hemisphere-hemisphere etc are also used by a number of workers [2 1 to 2 6] But analytical solution of Laplace's equation for these electrode arrangements are not possible because of non availability of any suitable coordinate system Therefore different numerical methods are successfully used to solve this problem

Unlike the case of electrodes in free air, for compressed gas insulated systems (GIS) and in space borne HV apparatus, it is extremely important to achieve more uniformity in fields within different parts of the apparatus as far as possible The exact knowledge of electrostatic fields in three dimensional unsymmetrical electrode systems became a necessity for providing appropriate shapes

to the electrodes and thus optimizing the size of these apparatus Numerical methods for the estimation of electrostatic fields have since received considerable attention

2.2 Classification of Electric Fields

While going through the international literatures, it is revealed that different terminologies such as divergent field, convergent field, slightly nonuniform field, quasi uniform field, homogeneous field, sharply nonuniform field etc are adopted to define the electric fields This reflects that the concept of "Weakly nonuniform field" as described in a recent book [2 7], originated in Germany, is yet not conceived by the English speaking world Therefore it is necessary to explain the classification of electric fields in this new light

Electric fields can be broadly divided into two types, the uniform field and the nonuniform field [2 7] In uniform field, no stable partial discharges occur before breakdown, i e $U_b = U_i$, where U_b is the breakdown voltage and U_i is the PD inception voltage Depending upon to severity, the nonuniform field can be subdivided into two types, weakly nonuniform field and extremely nonuniform field Like in uniform field, in case of weakly nonuniform field also, $U_b = U_i$, however in extremely nonuniform field, $U_b > U_i$, i e , stable partial discharges always occur before the breakdown, Fig 2 1

2.3 The degree of uniformity, η

The degree of uniformity of a particular field comprising by a pair of electrodes can be well estimated by the factor η, also known as Schwaiger factor It is defined as

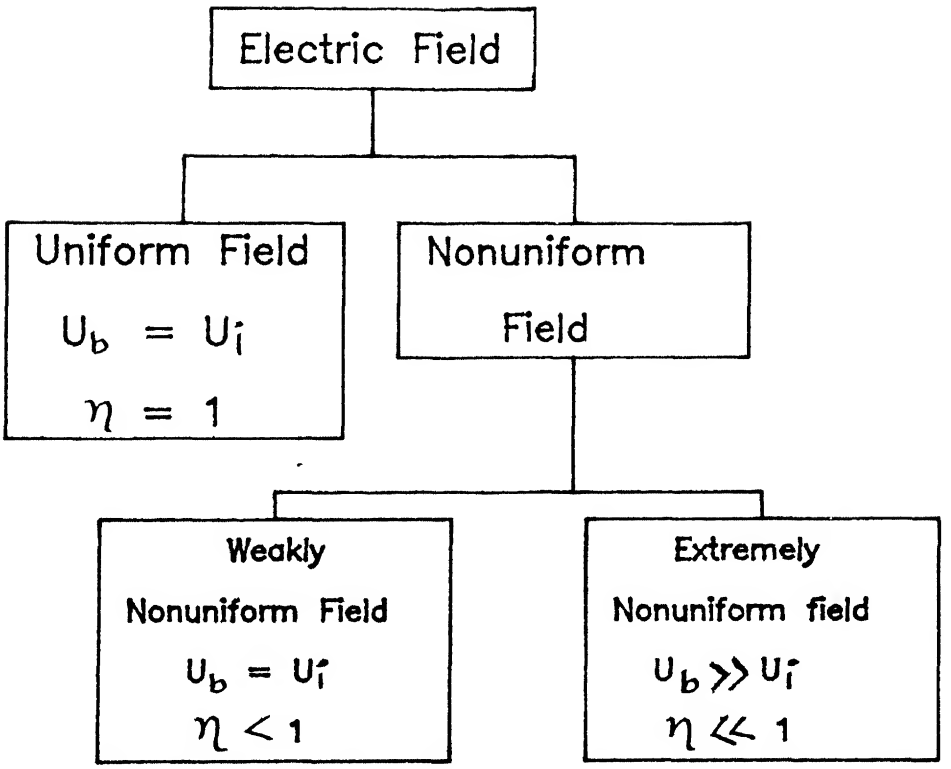

Fig.2.1 Classification of Electric Fields

$$\eta = \frac{U}{d \; E_{max}} \qquad (2\ 1)$$

where U is the applied voltage, d the gap distance and E_{max} the maximum electric field intensity in the dielectric between the electrodes For a uniform field η is equal to unity, whereas for weakly nonuniform fields, η is less than 1 but not too small compared to unity For extremely nonuniform fields, η has considerably smaller value

2.4 Numerical methods

Physical systems are so complex that the analytical solution of Laplace's or Poisson's equations is very difficult, if not impossible Application of numerical methods involves the solution of partial differential equations including Laplace's equation, by systematic approximation A number of methods, for example, Finite Difference Method (FDM), Finite Element Method (FEM), Charge Simulation Method (CSM) and its later version, Surface Charge Simulation Method (SCSM) have been developed ever since the application of modern computers

Among all the methods mentioned above, FEM is widely used by the researchers But in case of high voltage application it has got some limitations It requires more computational time and memory compared to CSM if the results are to be fairly accurate, specially in case of very sharp corners or bends of the electrodes In comparison to that application of CSM is simple and it requires less computational time and memory [2 8] CSM has been developed for the estimation of high voltage fields only whereas FEM is a generalized method which can be used in structural analysis, heat flow, fluid flow etc also

2.4.1 Charge Simulation Method

The basic principle of this method lies in the concept that the field under consideration is formed by superposition of many individual fields The distribution of charge on the surface of the electrode is replaced by n number of discrete fictitious charges arranged suitably inside the conductor, outside the space in which the field is to be estimated The potential function of the field at any point due to individual charges can be found by the summation of scalar potentials resulting from these individual charges

2.4 2 Surface Charge Simulation Method

In this method a finely distributed surface charge is used directly to simulate the complete equipotential surface, the "electrode contour", as the surface charge is distributed on the contour surface itself The existing surface charge on the electrode configuration is simulated by integration of ring charges placed on the electrode contour and dielectric boundaries Thus it leads to a physically correct reproduction of the whole electrode configuration

Because of various practical difficulties, the SCSM is not used as frequently as CSM

2.5 Application of CSM for the estimation of field

CSM is used to estimate the electric field and the distribution of equipotential lines in the dielectric between two electrodes subjected to high voltage In this work the method has been extended to find the variation of electric field intensity along the shortest distance between the electrodes The maximum field intensity, E_{max} has been estimated for each pair of electrode configurations The degree

of uniformity, also known as the Schwaiger factor, η has been estimated and variation of η with the change of electrode configuration reported

Estimation of E_{max} for a pair of spherical electrodes has been proposed by G W Carter [2 9] which involves the analytical solution of Laplace's equation by means of dipolar co-ordinates, which cannot be applicable to other electrode shapes and three dimensional unsymmetrical electrodes used in practice

2.5.1 The mathematical analysis

In CSM, for the computation of the electrostatic fields, the distributed charge on the equipotential electrode surfaces are replaced by n fictitious charges arranged inside the conductor, i e, outside the space where the electric field is desired to be estimated These charges may be in the form of a point, finite line, ring or a combination of them depending upon the suitability The positions and types of these charges are allocated but their magnitude is unknown The magnitudes and positions of these charges are such that their integrated effect, together with the field of those charges existing inside the space (if any), satisfies the boundary conditions The field equations for an electrostatic field in a homogeneous medium is given by the well known Poisson's equation -

$$\nabla^2\phi = -\frac{\rho}{\varepsilon} \qquad (2\ 2)$$

where, ϕ = potential,

ρ = space charge density,

ε = permittivity of the medium

For zero charge density, above equation becomes the Laplace's equation -

$$\nabla^2\phi = 0 \qquad (2\ 3)$$

Any function that satisfies these equations can be taken as a solution, provided the boundary conditions are satisfied

The potential function of any charge satisfies Laplace's equation outside its volume Therefore the fictitious charges are placed outside the space in which the field is to be computed, the combined potential function due to these and real space charges automatically satisfy the required Laplace's or Poisson's equation everywhere in the space The important point is that if some classical charge distribution are chosen, explicit analytical expressions are obtained for the potential field distribution as given by -

$$\Phi(r) = \sum_j p_j(r)\, q_j \qquad (2\ 4)$$

$$E(r) = -\nabla\Phi(r) = \sum_j \{\nabla p_j(r)\} q_j \qquad (2\ 5)$$

where, q_j represents the magnitude of the charge, which is not known, on the j^{th} distribution, and $p_j(r)$ is a coefficient that depends only on the type of the distribution and the position of the point r The potential defined by Eq 2 4 satisfies Laplaces equation Boundary conditions are represented by imposed at a set of collocation points on the electrode surfaces For each electrode as many collocation points are chosen as there are inner charges These conditions lead to a linear system given as

$$Pq = \Phi \qquad (2\ 6)$$

where, $P_{ij} = p_j(r_i)$ The linear equations (Eq 2 6) are solved by standard methods and the charges q_j calculated The potential and field at all points, including the electrode surfaces, may then be calculated from Eq 2 4 and 2 5

2.5 2 Electrode configurations considered for investigation

A number of different electrode configurations were chosen to investigate the applicability of CSM for the estimation of η Two different cases of the method of voltages applications, (i) Symmetrically applied voltage of +U/2 & -U/2 and (ii) Asymmetrically applied voltage of U & 0 were considered on the electrodes The shape of different electrode combinations considered along with the mode of application of voltage and the number of point charges used to simulate the electrode surfaces are shown in Table 2 1 The two electrodes are placed symmetrically above and below the horizontal plane The gap distance is considered to be unity for all cases Diameter of spheres and hemispheres is 1, the tip diameter of the rod is 1, and the plane electrode has the overall diameter of 5 25, edges rounded with radius of 0 3 In case of unequal spheres, the smaller sphere has diameter 90% of that of larger sphere

Although different types of complicated charge combinations have been used to simulate the equipotential surfaces by other workers, in this work only point charge is considered due to its simplicity The results are found to be in good agreement with those reported by others The point charges were located at positions symmetrically distributed below the electrode surface

Rotational symmetry exists for each pair of electrodes investigated The location of contour points, charge positions and check points [refer to 2 10] for a pair of equal spheres is shown in Fig 2 2 The same pattern is followed in case of other electrode pairs also The displacement ratio [2 10], β = df/ds as explained in Fig 2 2, is kept between 0 7 to 1 5 throughout the work The accuracy of CSM largely depends upon the positioning and the number of the

Table 2.1 : Electrode arrangement, applied voltage and no. of point charges considered in simulation.

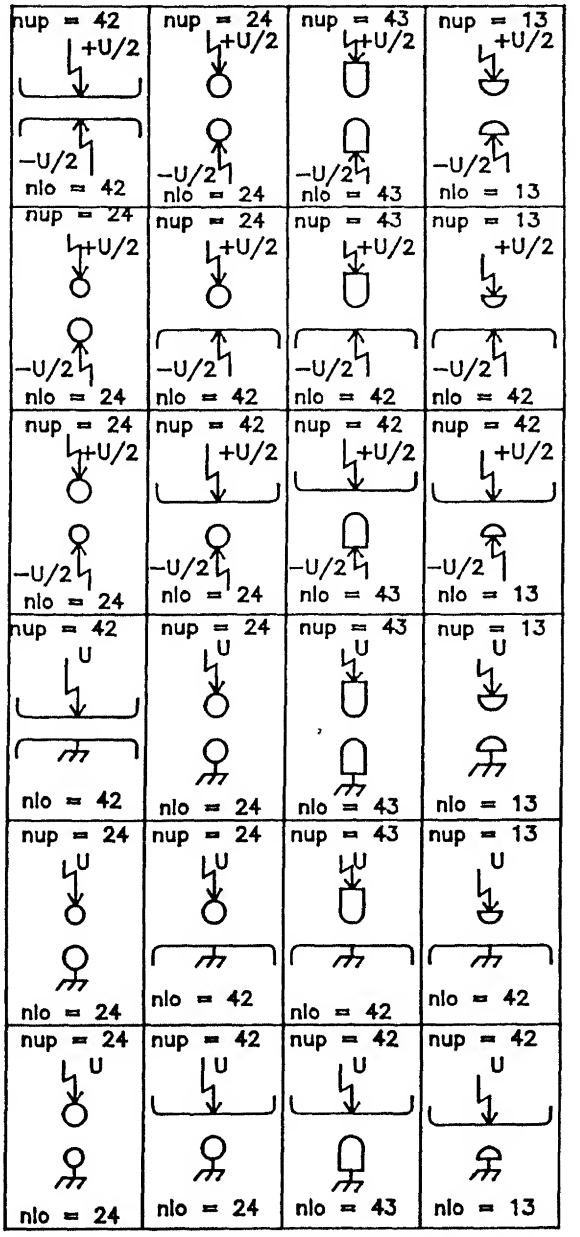

nup = no of charges for upper electrode
nlo = no of charges for lower electrode

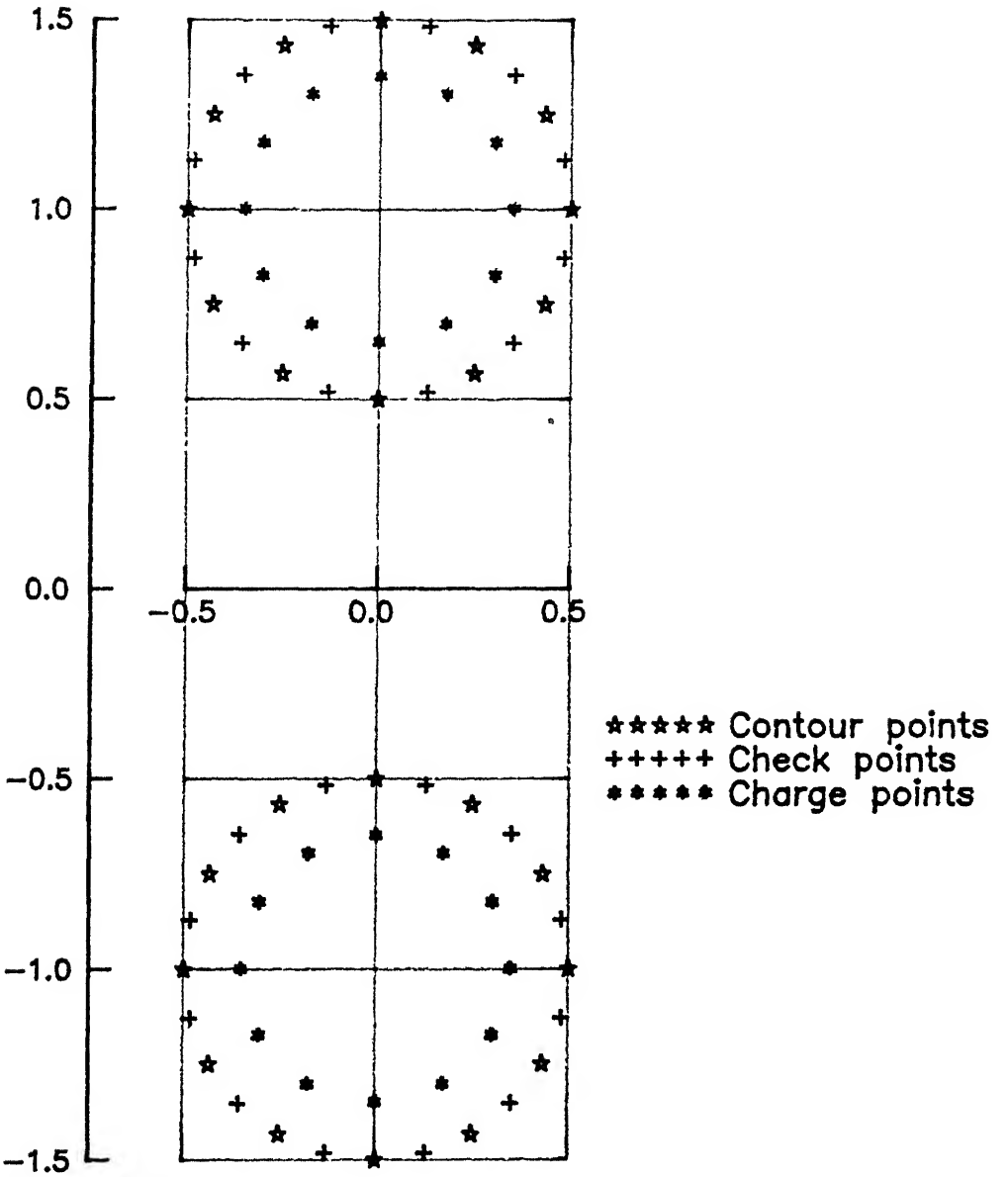

Fig.2.2 : Positions of contour points, check points and charges for sphere–sphere electrode.

charges and the corresponding contour points used in the simulation One of the measure of the accuracy of this simulation is "potential error", [2 11 in 2 1] defined as the difference between the known (applied) potentials and the computed potentials at the electrode surfaces at various check points The permissible potential error in this work was less than 0 01% at the surfaces for both the symmetrically and asymmetrically applied voltages

2 5.3 Estimation of E and η

The electric field intensity E has been calculated at a number of points along the shortest distance between the two electrodes, known as the electrode axis [2 10] by using the following equation -

$$E_p = \sum_{i=1}^{n} \frac{Q_i^*}{4 \Pi \varepsilon_o R_{ip}^2} \qquad (2\ 7)$$

where E_p is the value of E at any point p in the dielectric, R_{pi} is the distance between point p and the position of i^{th} charge Q_i For the sake of convenience of calculation , the value of potential difference between the two electrodes is considered as U = 1 The gap distance is considered to be unity (Fig 2 2) Therefore, $\eta = U/d\ E_{max}$ reduces to $\eta = 1/E_{max}$, where E_{max} is the maximum value of E calculated as described above The flowchart of the computer program used is shown in Fig 2 3

FLOWCHART OF CSM TO ESTIMATE η

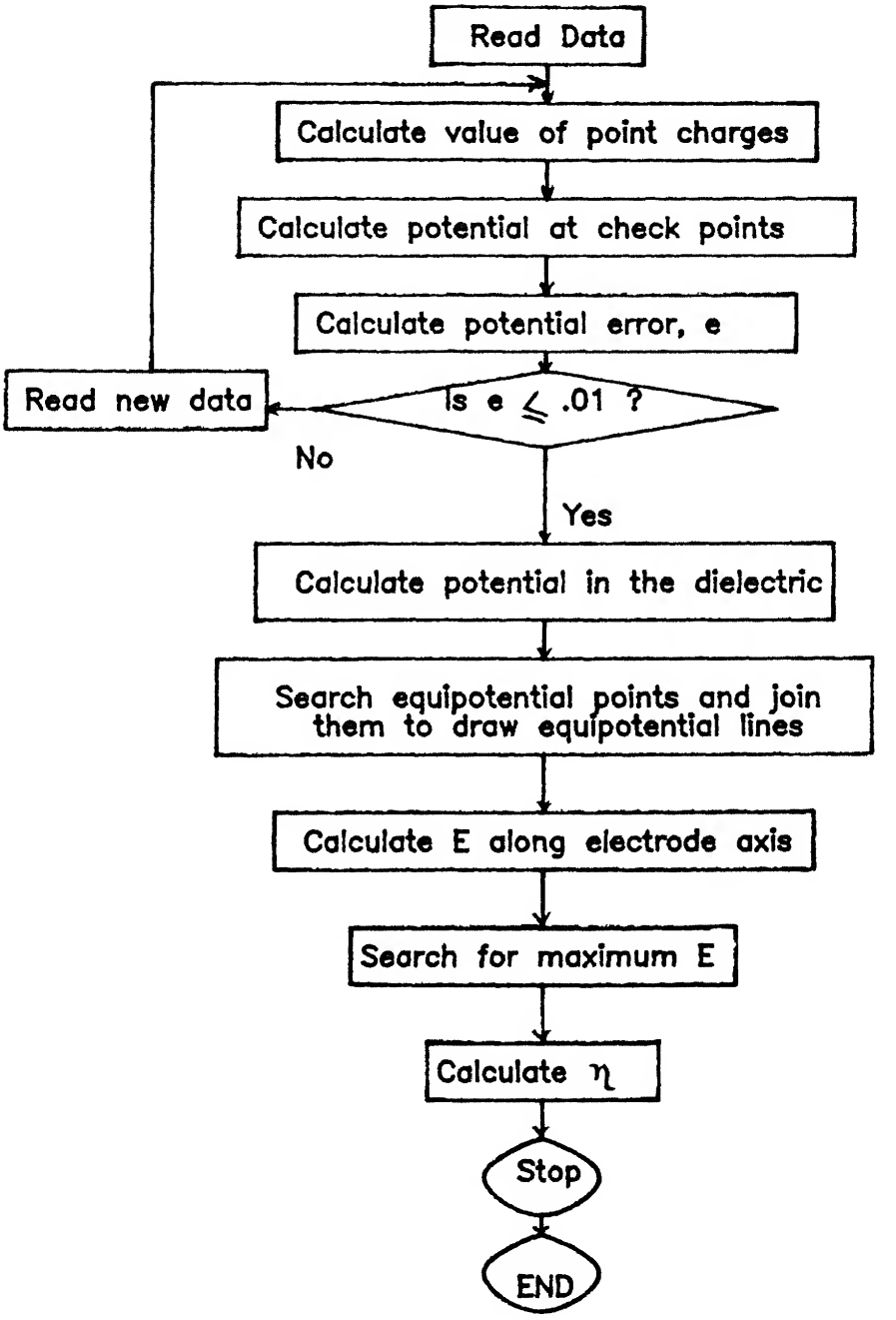

Fig.2.3

2.5.4 Results and discussions

The distribution of the equipotential lines in a two dimensional plane in the dielectric between the electrodes for different electrode configurations considered are shown in Fig 2 4 and 2 5 The equipotential lines have been calculated at a difference of 10% of the applied voltage Variation of electric field intensity along the electrode axis for all these electrode configurations are shown in Fig 2 6

2.5.4.1 Effect of symmetrically applied voltage on the distribution of equipotential lines

Distribution of the equipotential lines in the dielectric between different pairs of electrodes on applying the voltage symmetrically are shown in Fig 2 4(a) to 2 4(l) It can be seen from these figures that for symmetrical electrode pairs such as plane-plane, sphere-sphere, rod-rod etc , the equipotential lines are symmetrically distributed above and below the horizontal plane The 0% voltage line, a straight line, falls exactly at the middle of the gap between the electrodes But for unsymmetrical electrode pairs such as rod-plane or plane-rod, the equipotential lines are not distributed symmetrically Fig 2 4(e) to 2 4(l) In all these cases the 0% voltage line is shifted towards the electrode having lower radius of curvature Even in case of the electrodes of similar shape but of different size, as shown in Fig 2 4(e) and 2 4(f), where the smaller sphere has a diameter equal to 90% of that of the larger one, the equipotential lines have a tendency to fall closer towards the smaller sphere indicating that the field intensity is higher there

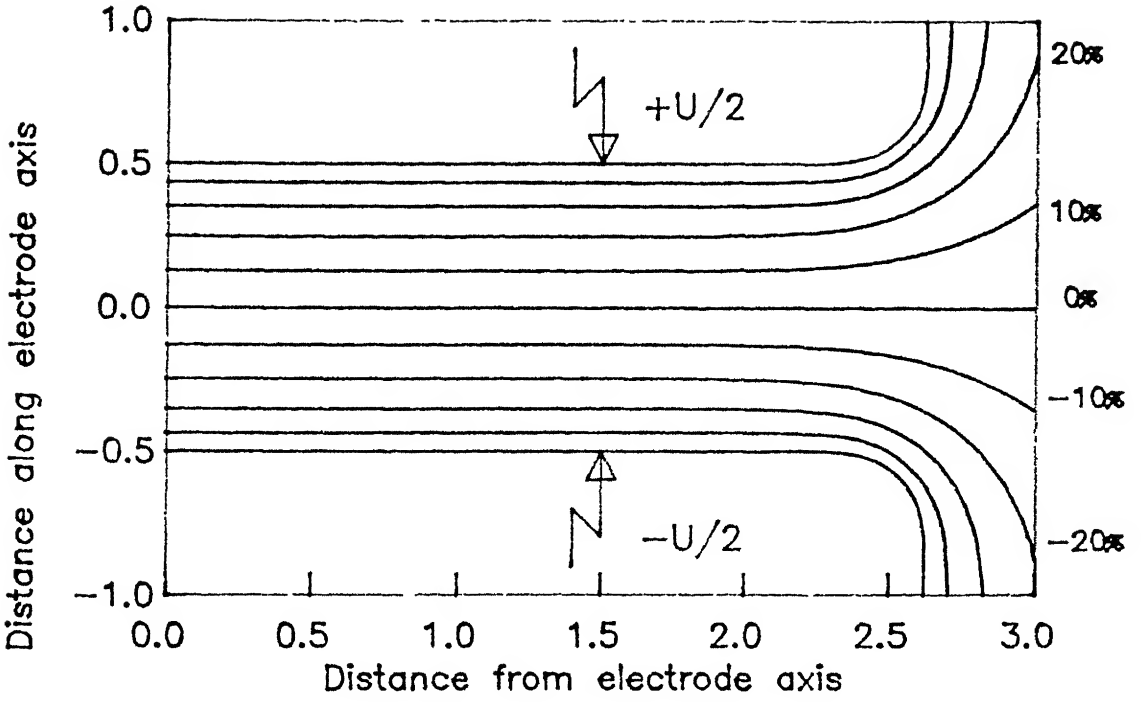

Fig.2.4(a) Equipotential lines for Plane–Plane electrode ; Symmetrical voltage.

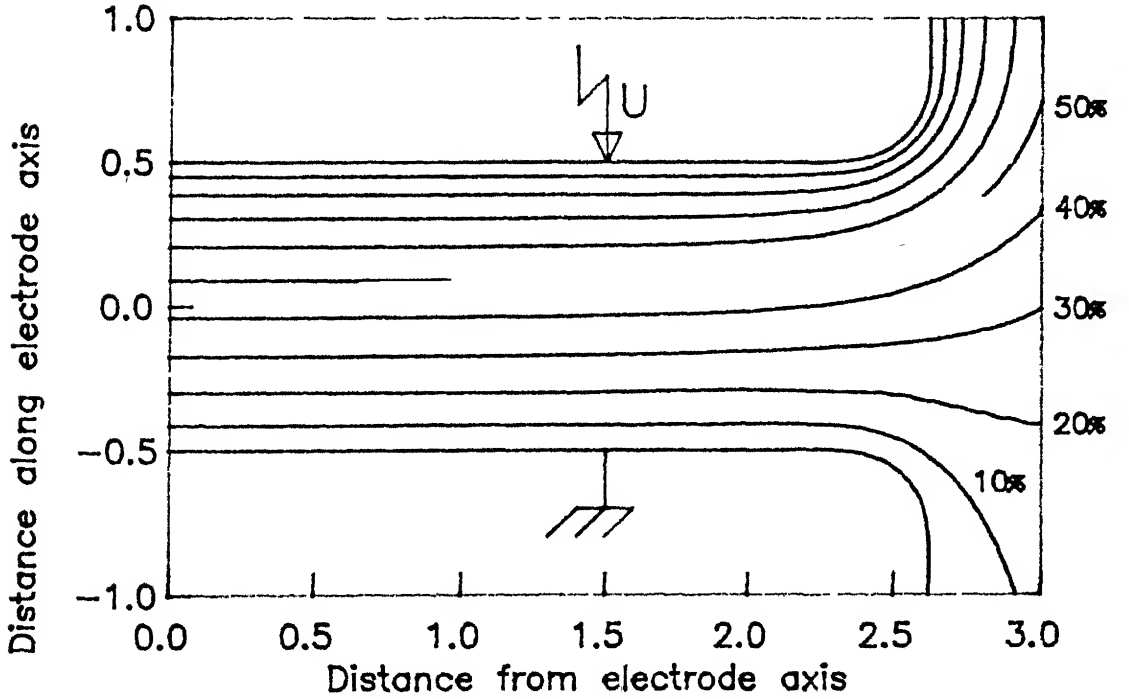

Fig.2.5(a) Equipotential lines for Plane–Plane electrode ; Asymmetrical voltage.

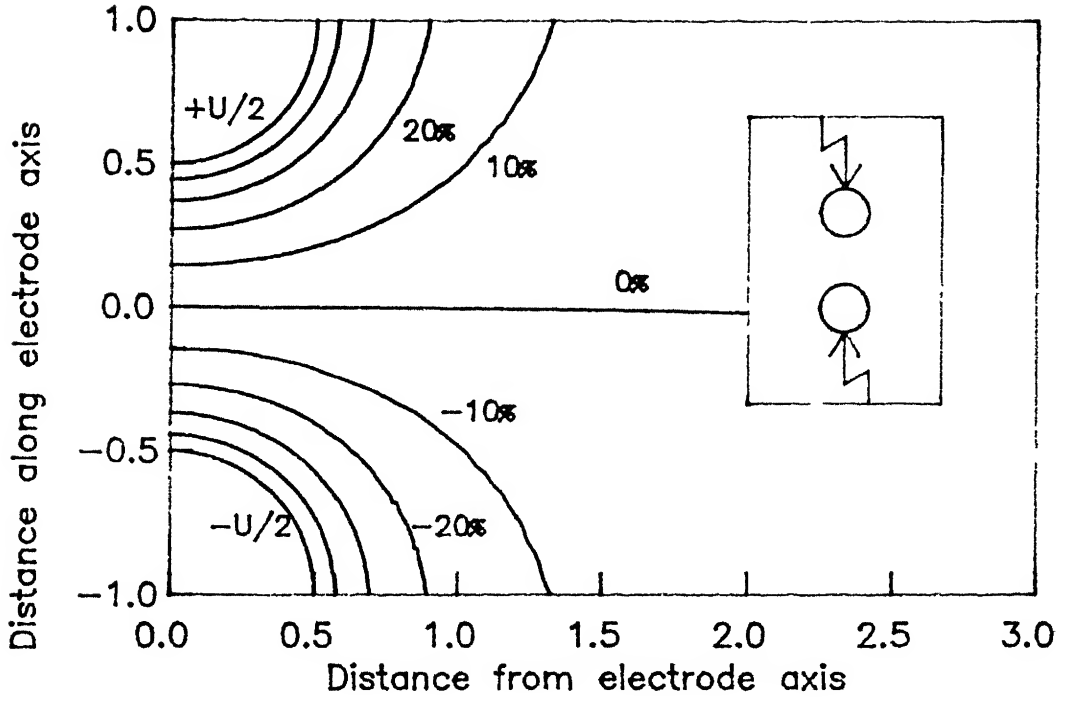

Fig.2.4(b) Equipotential lines for Sphere–Sphere electrode ; Symmetrical voltage.

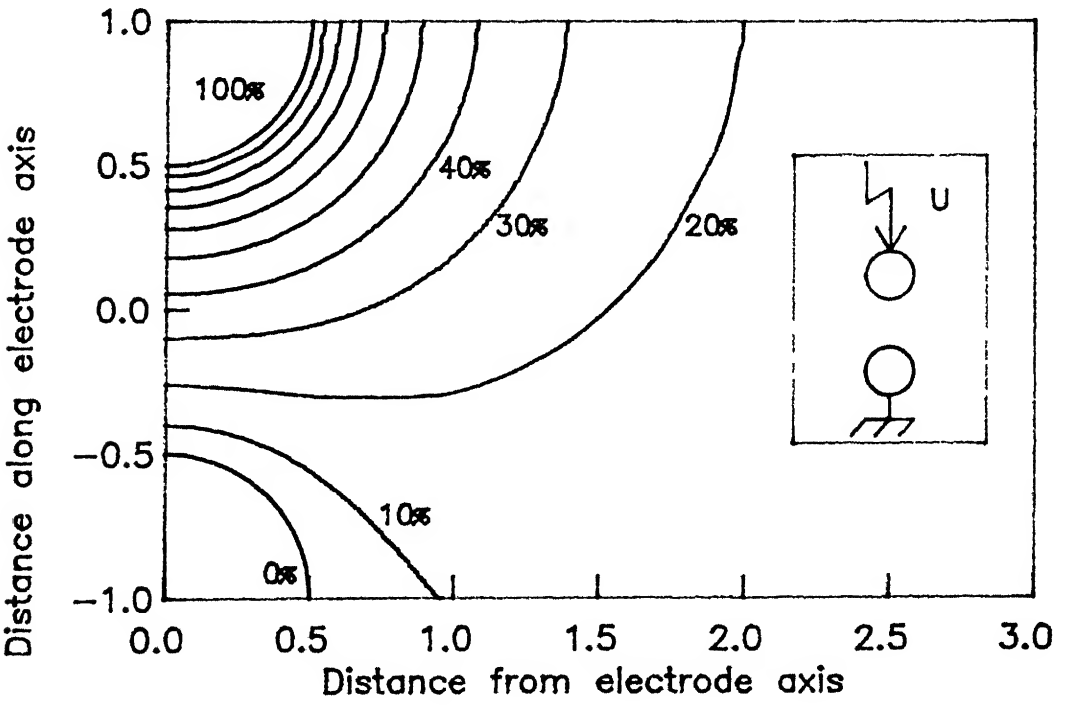

Fig.2.5(b) Equipotential lines for Sphere–Sphere electrode ; Asymmetrical voltage.

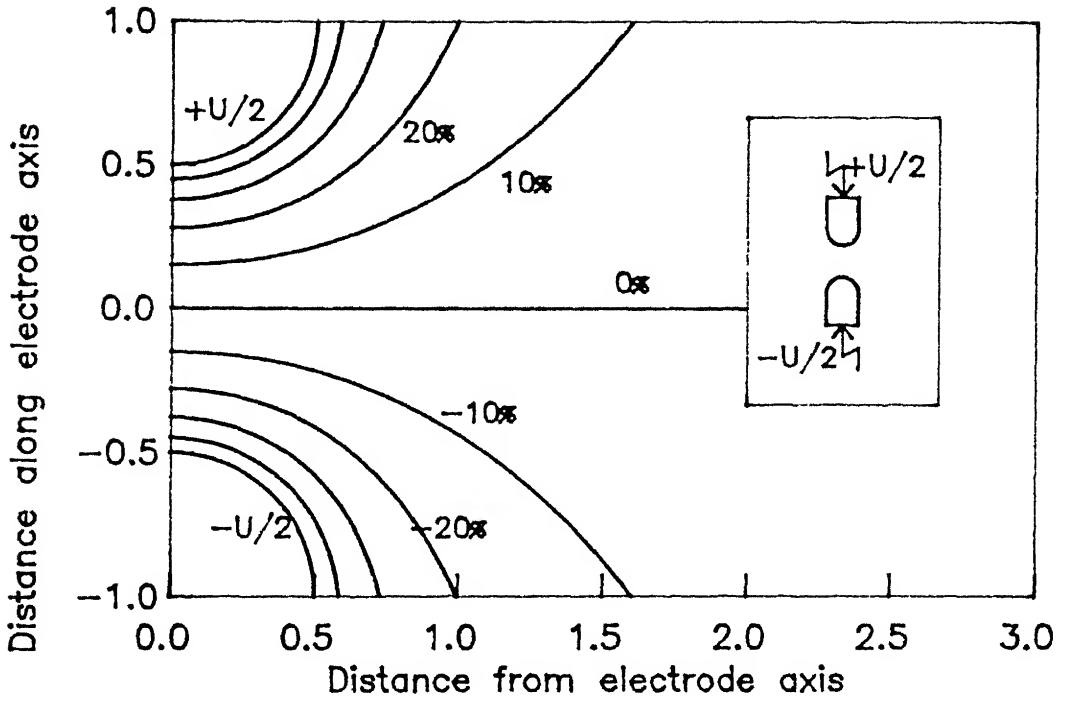

Fig.2.4(c) Equipotential lines for Rod–Rod electrode ; Symmetrical voltage.

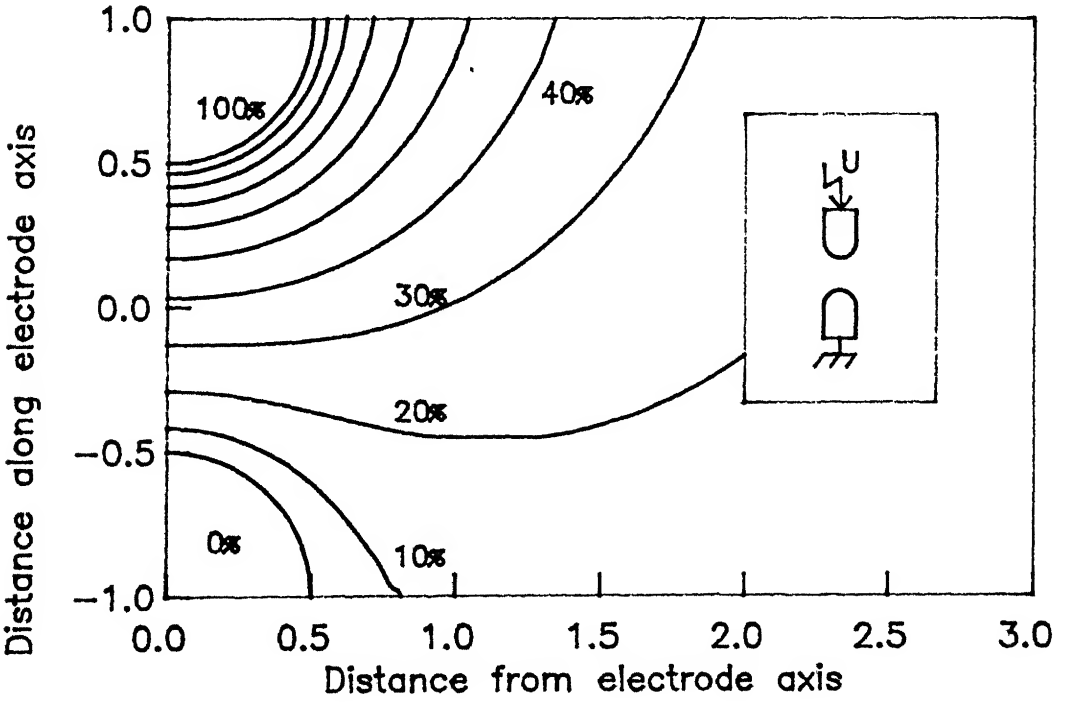

Fig.2.5(c) Equipotential lines for Rod–Rod electrode ; Asymmetrical voltage.

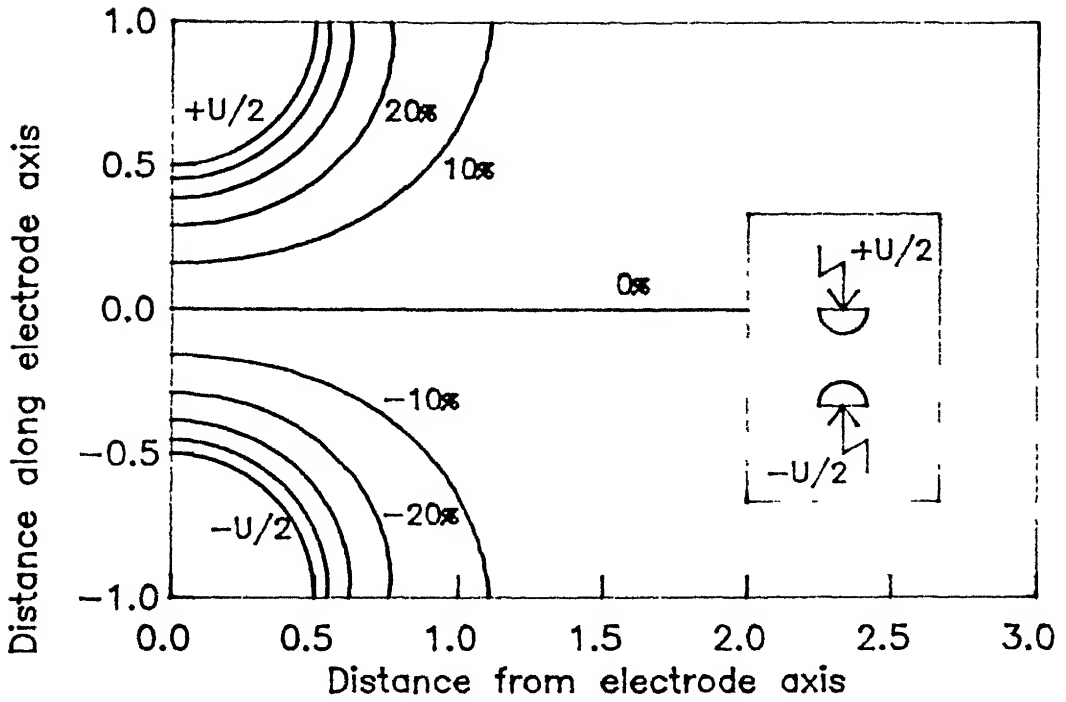

Fig.2.4(d) Equipotential lines for Hemisphere–Hemisphere electrode ; Symmetrical voltage.

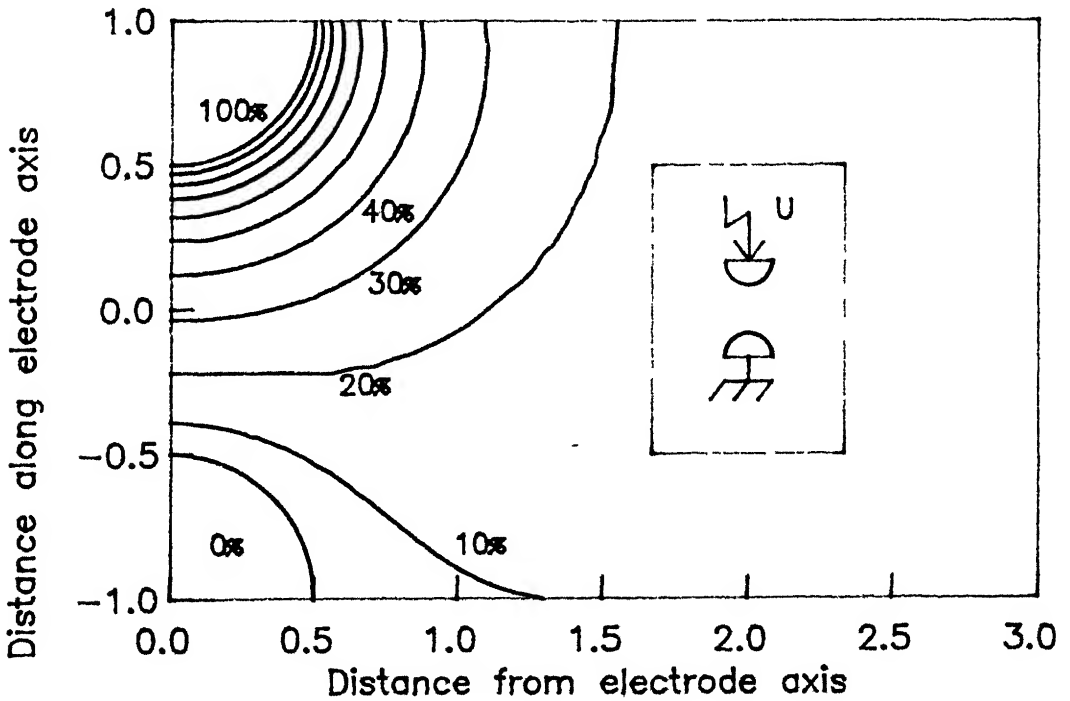

Fig.2.5(d) Equipotential lines for Hemisphere–Hemisphere electrode ; Asymmetrical voltage.

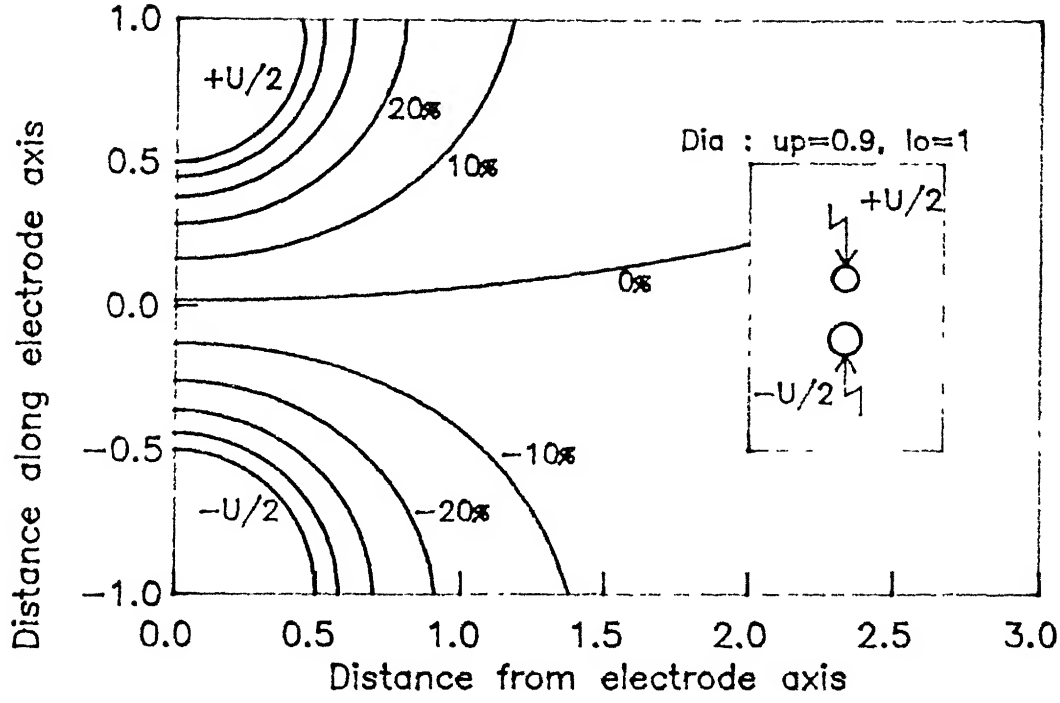

Fig.2.4(e) Equipotential lines for Unequal Sphere electrode ; Symmetrical voltage.

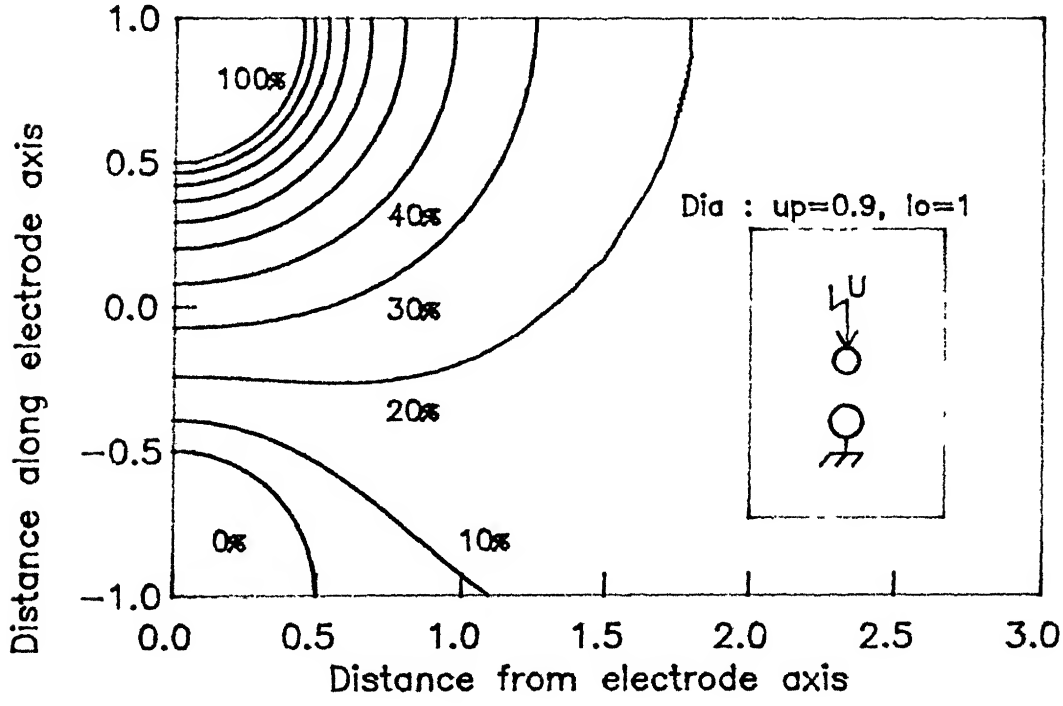

Fig.2.5(e) Equipotential lines for Unequal Sphere electrode ; Asymmetrical voltage.

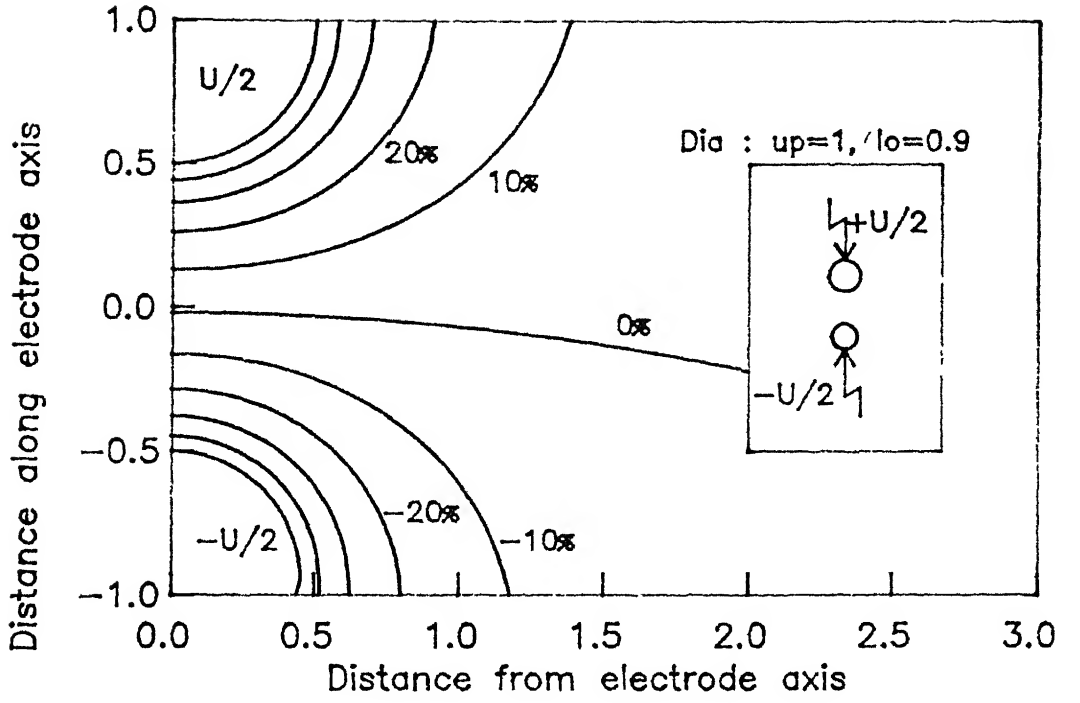

Fig.2.4(f) Equipotential lines for Unequal Sphere electrode ; Symmetrical voltage.

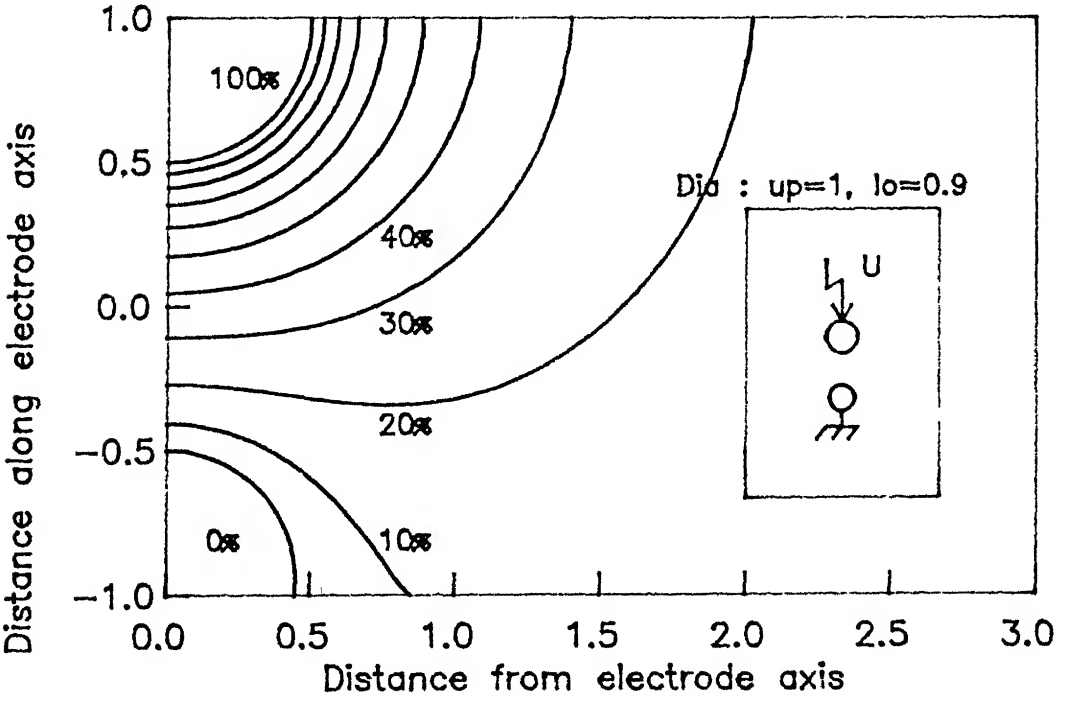

Fig.2.5(f) Equipotential lines for Unequal Sphere electrode ; Asymmetrical voltage.

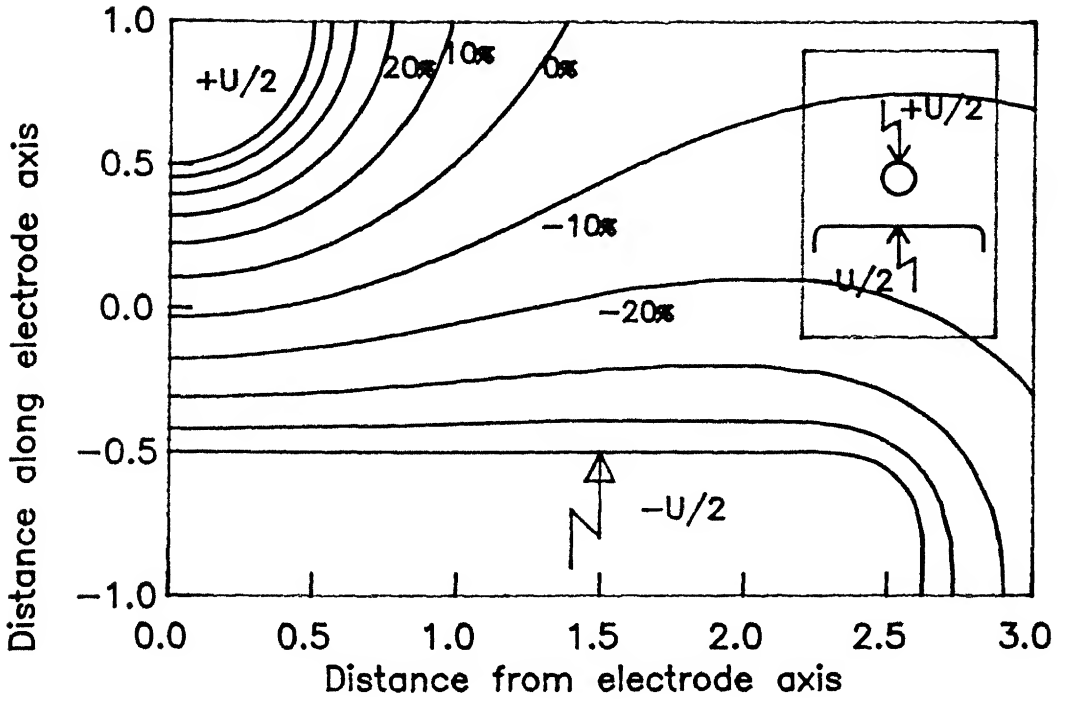

Fig.2.4(g) Equipotential lines for Sphere–Plane electrode ; Symmetrical voltage.

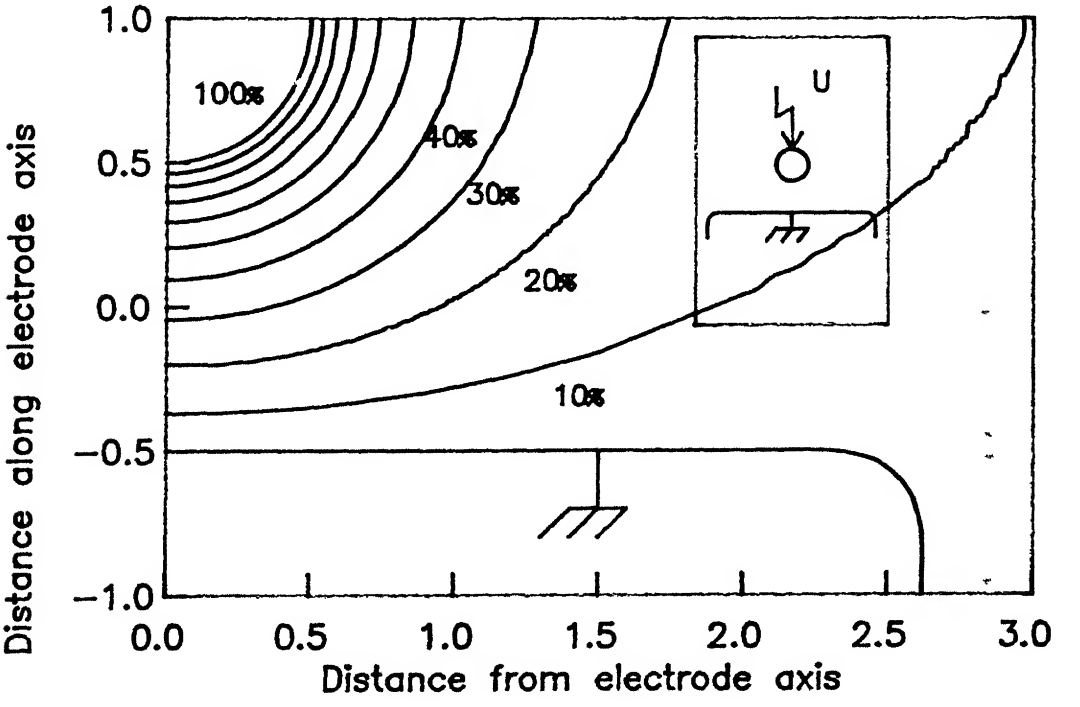

Fig.2.5(g) Equipotential lines for Sphere–Plane electrode ; Asymmetrical voltage.

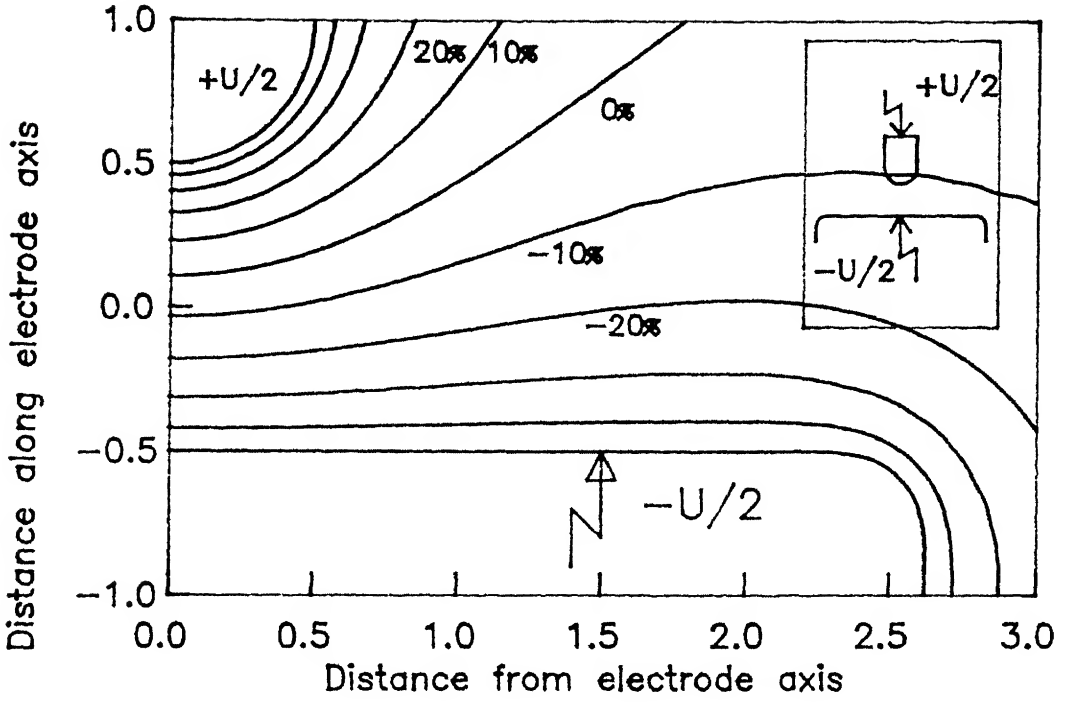

Fig.2.4(h) Equipotential lines for Rod–Plane electrode ; Symmetrical voltage.

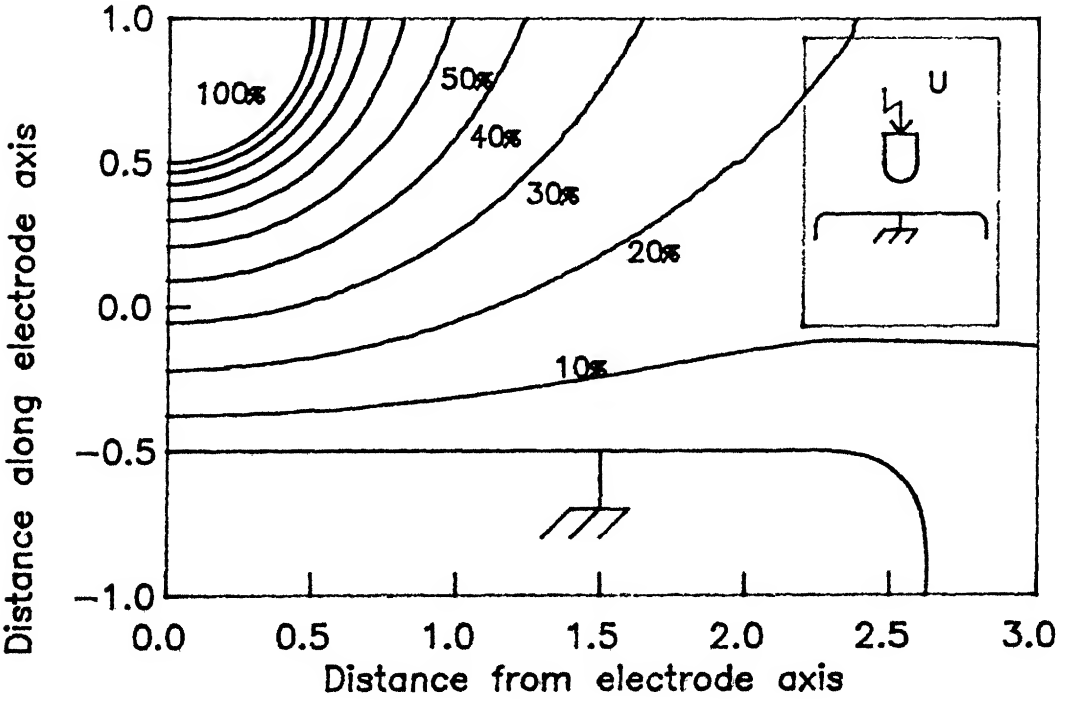

Fig.2.5(h) Equipotential lines for Rod–Plane electrode ; Asymmetrical voltage.

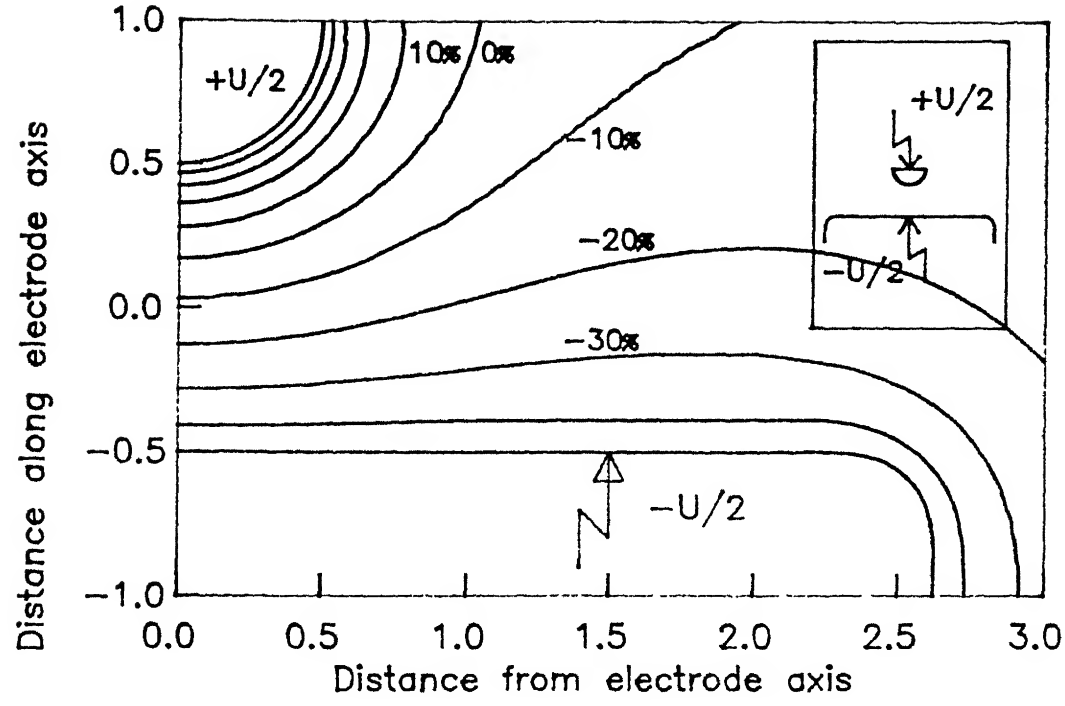

Fig.2.4(i) Equipotential lines for Hemisphere–Plane electrode ; Symmetrical voltage.

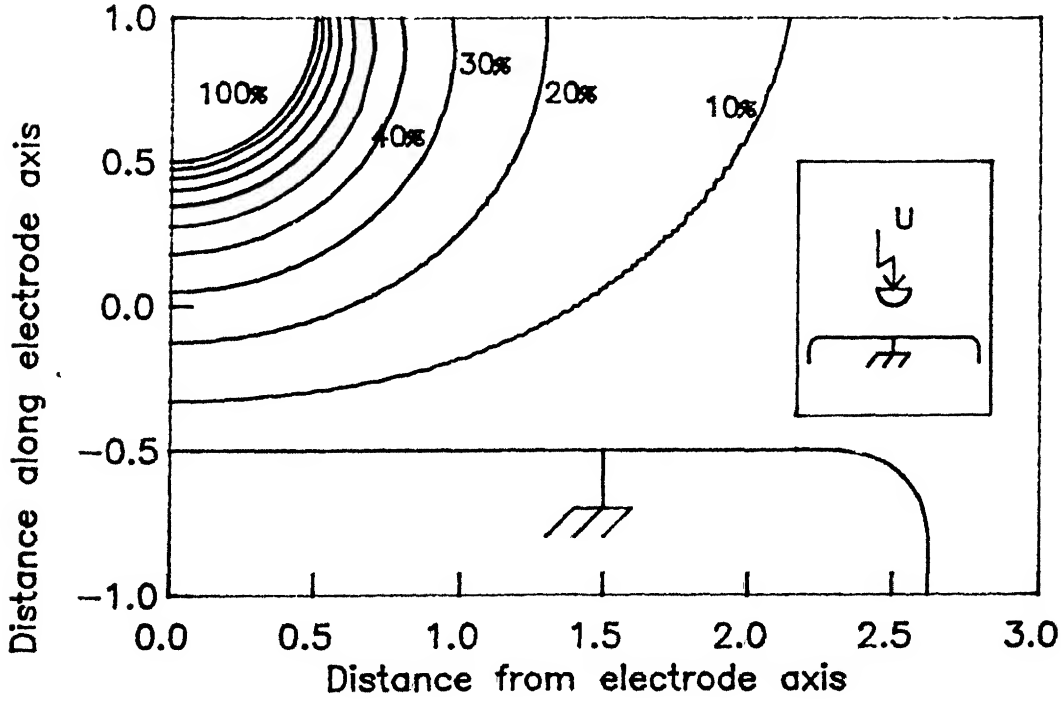

Fig.2.5(i) Equipotential lines for Hemisphere–Plane electrode ; Asymmetrical voltage.

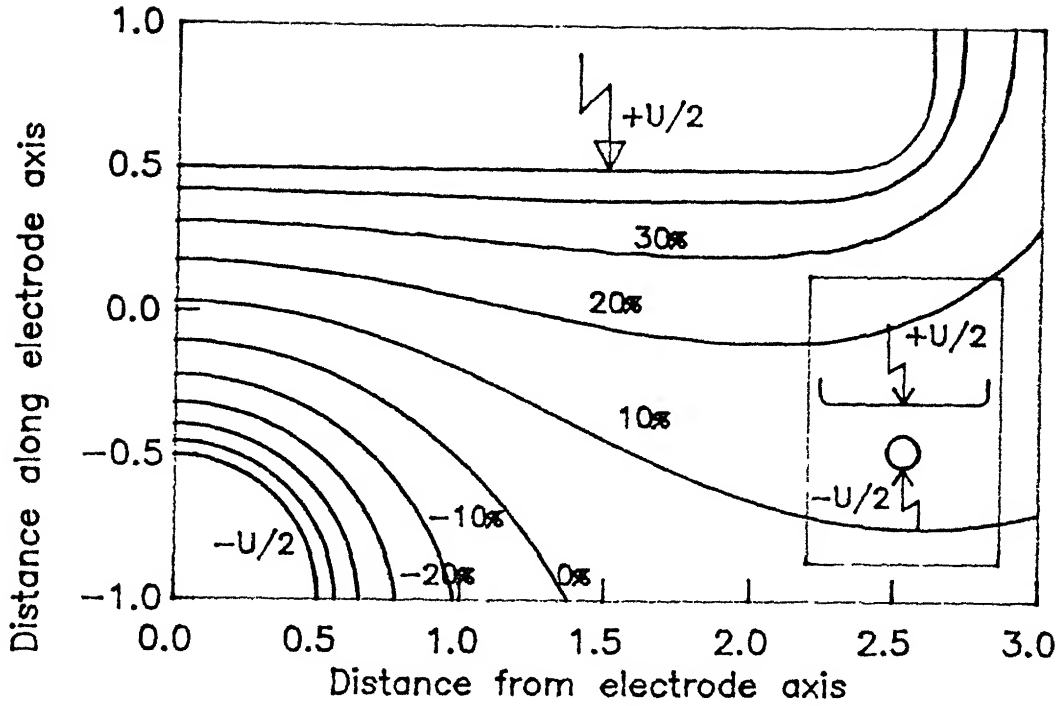

Fig.2.4(j) Equipotential lines for Plane–Sphere electrode ; Symmetrical voltage.

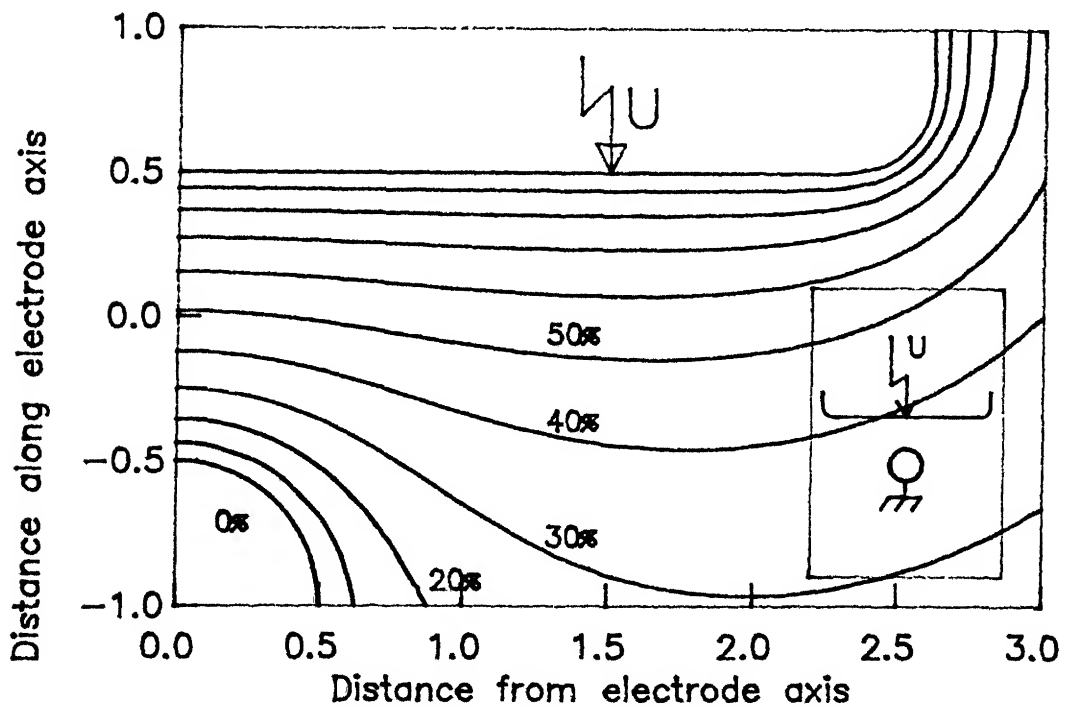

Fig.2.5(j) Equipotential lines for Plane–Sphere electrode ; Asymmetrical voltage.

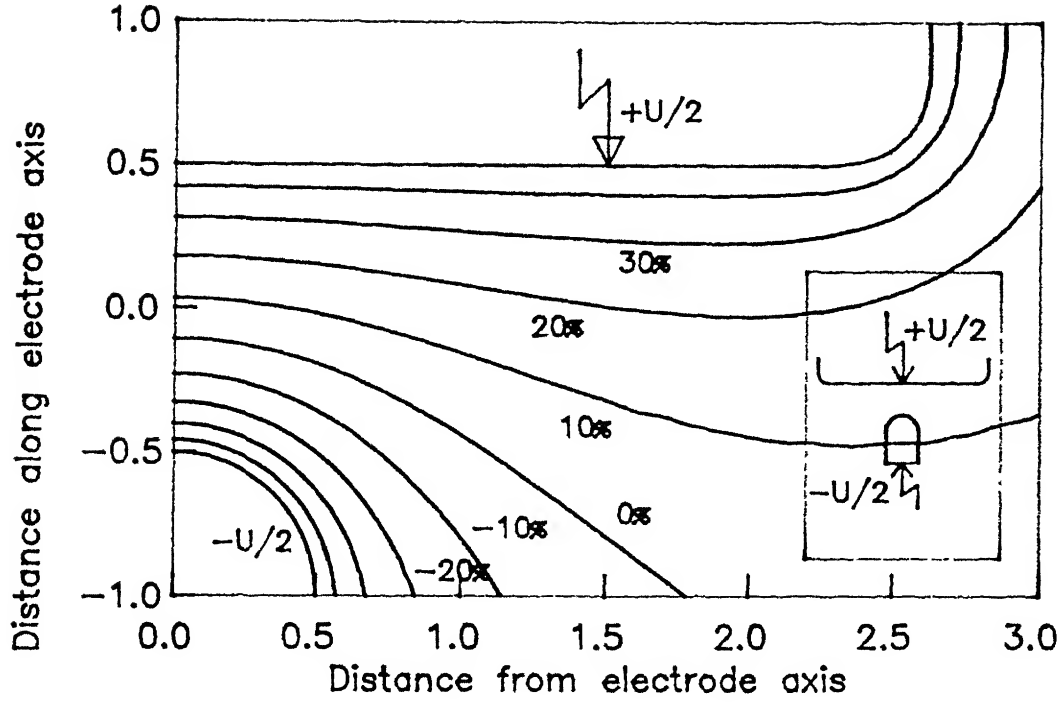

Fig.2.4(k) Equipotential lines for Plane–Rod electrode ; Symmetrical voltage.

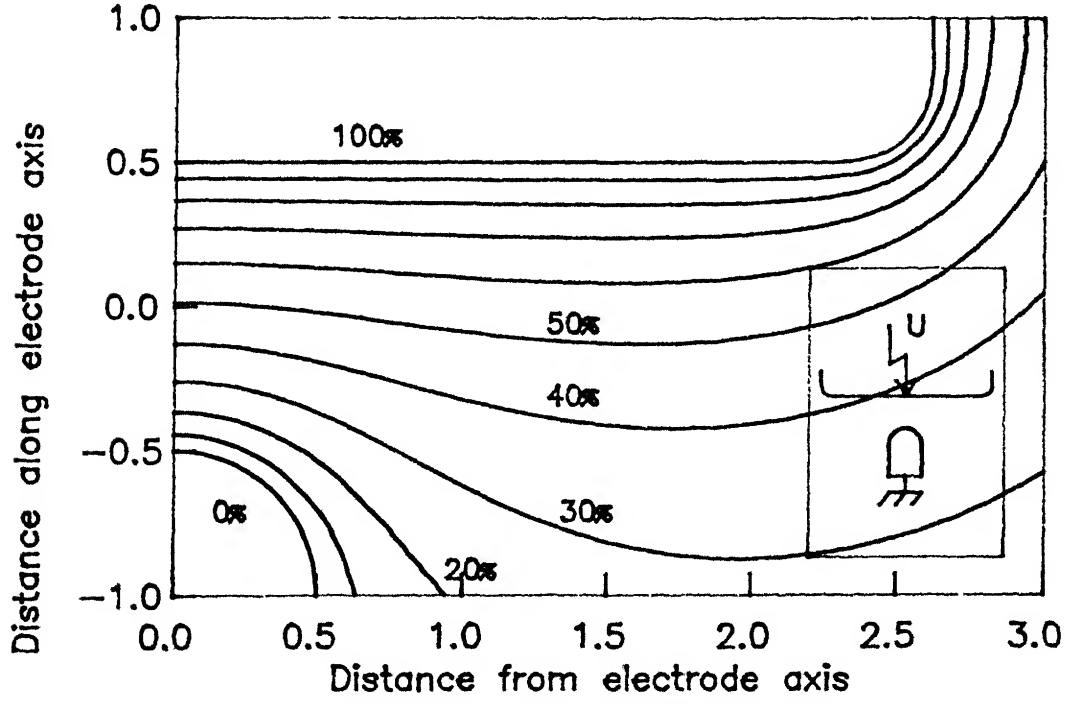

Fig.2.5(k) Equipotential lines for Plane–Rod electrode ; Asymmetrical voltage.

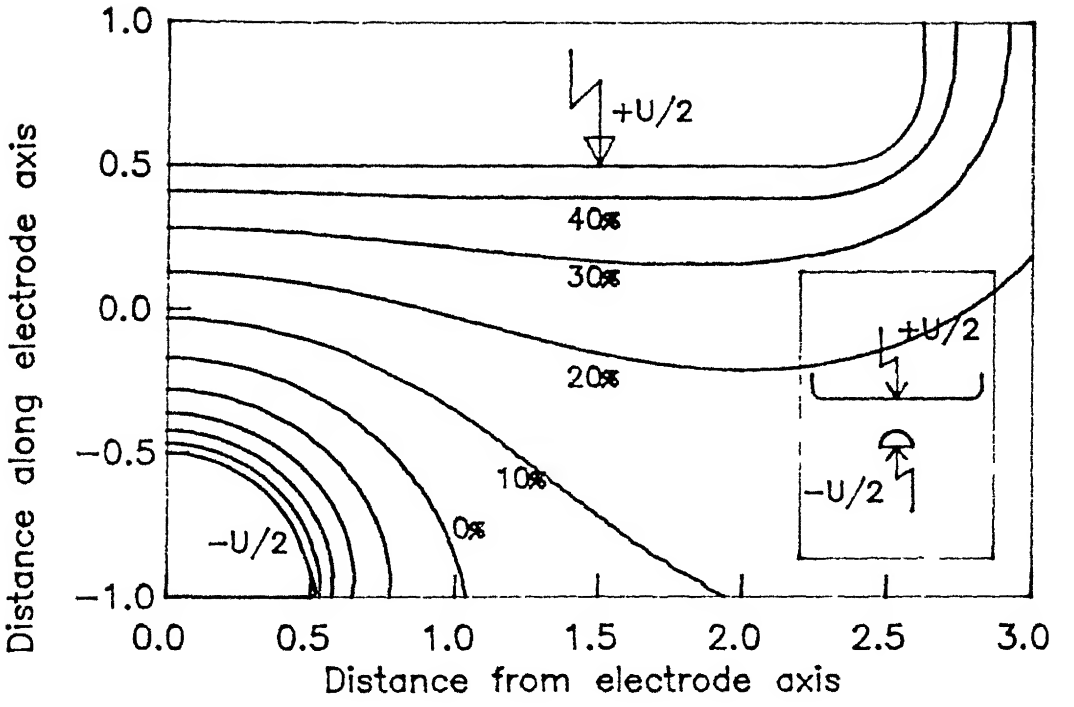

Fig.2.4(L) Equipotential lines for Plane–Hemisphere electrode ; Symmetrical voltage.

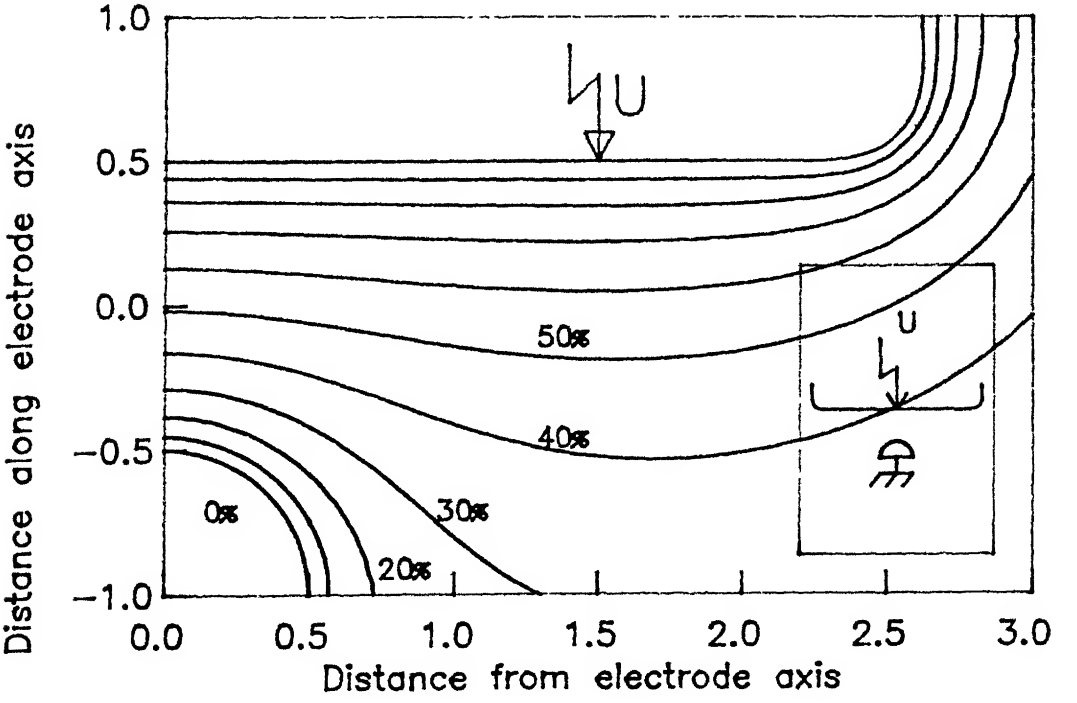

Fig.2.5(L) Equipotential lines for Plane–Hemisphere electrode ; Asymmetrical voltage.

2.5 4.2 Effect of asymmetrically applied voltage on the distribution of equipotential lines

Distribution of the equipotential lines in the dielectric between the same pairs of electrodes, as described above, on applying the voltage asymmetrically are shown in Fig 2 5(a) to 2 5(l) It can be seen from these figures that in all the cases almost all equipotential lines , except the 10% voltage line, have a tendency to follow the curvature of the HV electrode For symmetrical electrode pair such as plane-plane, sphere-sphere, rod-rod etc , the 50% voltage line does not fall at the middle of the gap (Fig 2 5(a) to 2 5(d)), rather it is shifted towards the HV electrode In case of rod-plane electrode, (Fig 2 5(h)), the 50% voltage line is shifted significantly towards the rod, however in case of plane-rod electrodes the 50% line is almost at the middle of the gap

Comparing the two cases of voltage application in Fig 2 4(a-l) and 2 5(a-l) it can be observed that for all the electrode arrangements the equipotential lines are more evenly distributed in the dielectric in case of symmetrically applied voltage than in asymmetrically applied voltage In practice, the case of symmetrically applied voltage is rarely present and of less interest For example in a transmission line, the dielectric (air) is stressed by the high voltage conductor and ground which is a case of asymmetrically applied voltage It was a limitation of the analytical calculations that symmetrically applied voltage had to be considered in such calculations From this investigation with the help of CSM it can be observed that in case of asymmetrically applied voltage to unsymmetrical electrode systems, the equipotential lines are more concentrated towards the HV electrode This means that the dielectric in the vicinity of this electrode is stressed much more than in the

-rest of- the volume Hence the possibility of PD as well as the initiation of breakdown process is more near the HV electrode in the dielectric

2.5.4.3 Effect of the mode of applied voltage on the distribution of electric field intensity

Computation of electric field intensity was made as described in Sec 2 5 3 for all the pairs of electrodes on applying the two modes of the voltage Variation of the electric field intensity along the shortest distance between the electrodes, the electrode axis, are shown in Fig 2 6(a-l) for all electrode pairs

It could be observed that for symmetrically applied voltage, the electric field intensity, E in the dielectric near both the electrodes are equal and acquire its maximum value identically near the two electrodes in case of symmetrical electrode pairs, Fig 2 6(a-d) For these cases, the minimum field intensity occurs exactly at the middle of the gap However, for unsymmetrical electrode pairs, such as, sphere-plane, rod-plane or plane-rod etc , E is maximum near the electrode having lower radius of curvature, Fig 2 6(e-l) Even if the electrodes are of similar shape but of different sizes, as in Fig 2 6(e-f), E near the two electrodes are unequal, and E_{max} is near the smaller sphere In these cases, the minimum field intensity does not occur at the middle of the gap, rather at a point closer towards the electrode having larger radius of curvature

In case of asymmetrically applied voltage, in case of all electrode pairs the maximum field intensity occurs near the HV electrode, irrespective of their shape and size The minimum field intensity occurs at a point in the dielectric not at the middle of the gap but closer towards the grounded electrode.

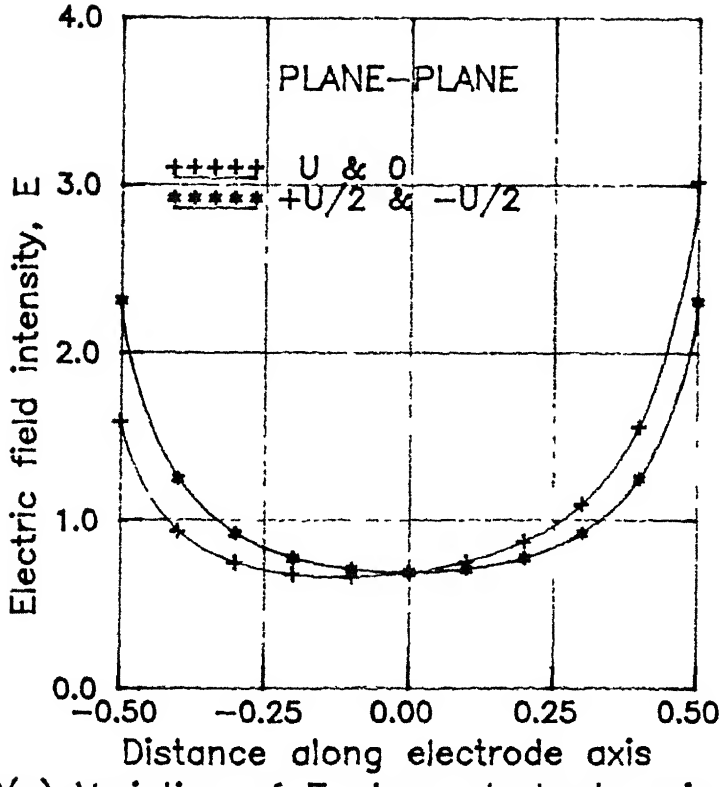

Fig.2.6(a) Variation of E along electrode axis for Plane–Plane electrode.

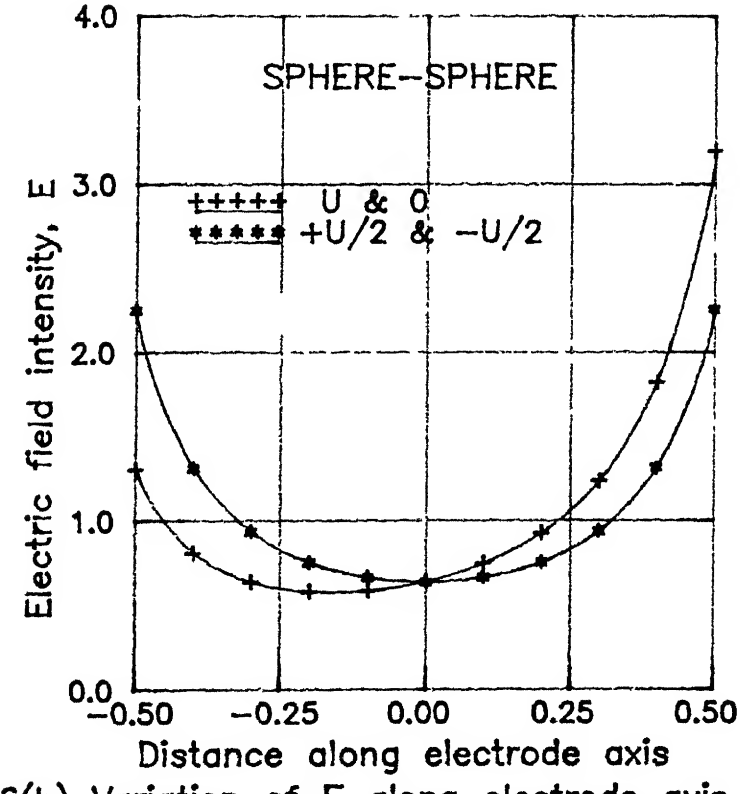

Fig.2.6(b) Variation of E along electrode axis for Sphere–Sphere electrode.

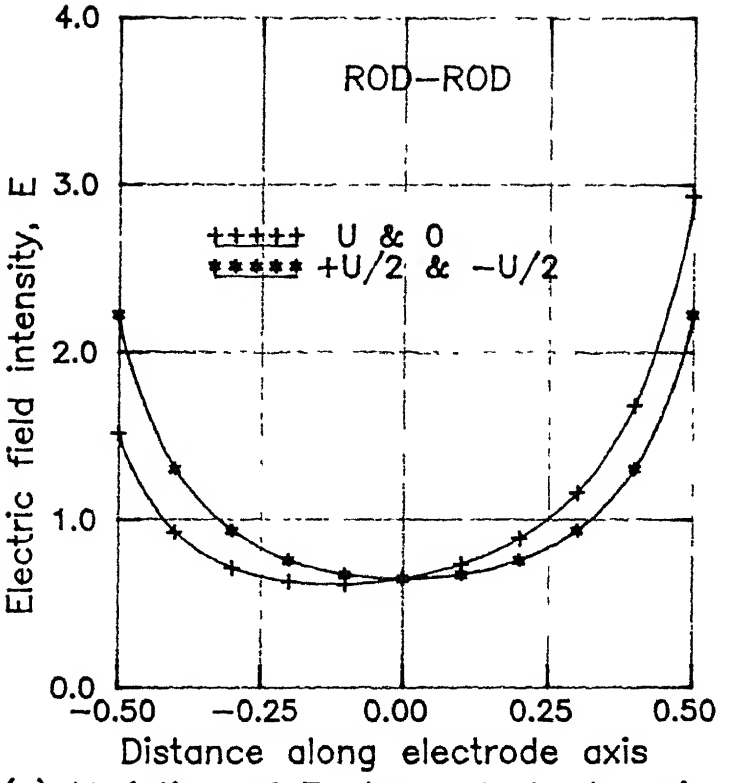

Fig.2.6(c) Variation of E along electrode axis for Rod–Rod electrode.

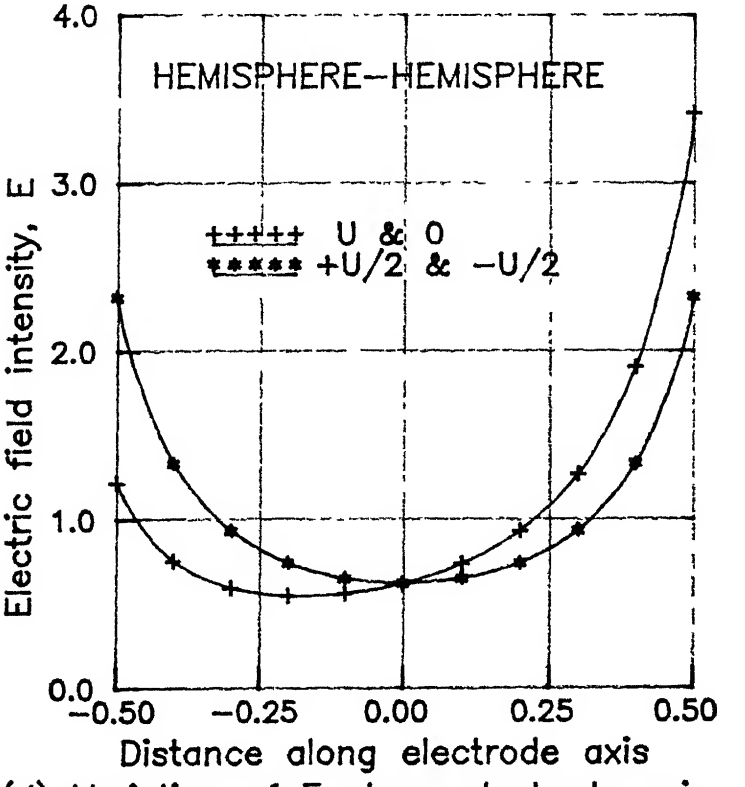

Fig.2.6(d) Variation of E along electrode axis for Hemisphere–Hemisphere electrode.

No. A 125681

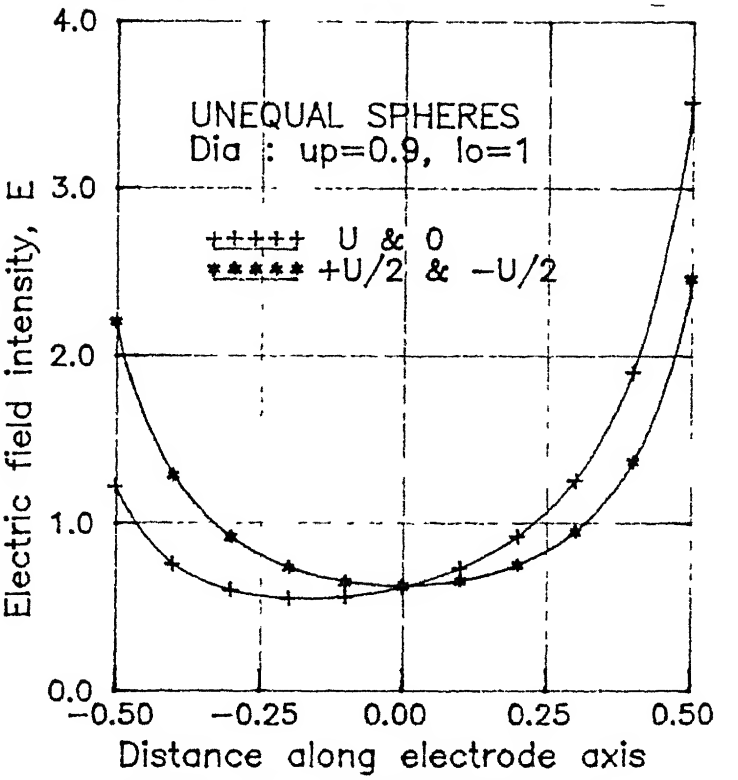

Fig.2.6(e) Variation of E along electrode axis for Unequal sphere electrode.

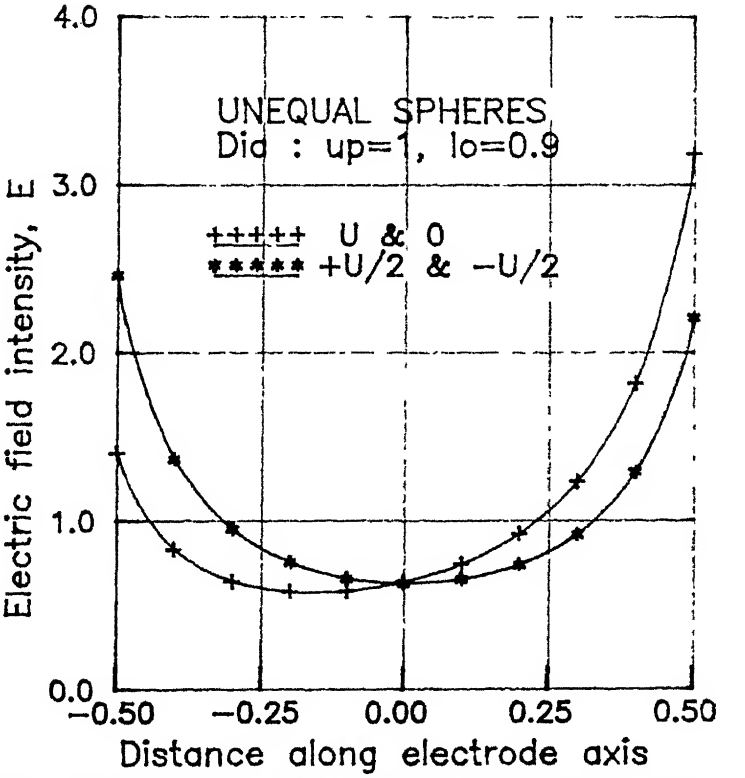

Fig.2.6(f) Variation of E along electrode axis for Unequal sphere electrode.

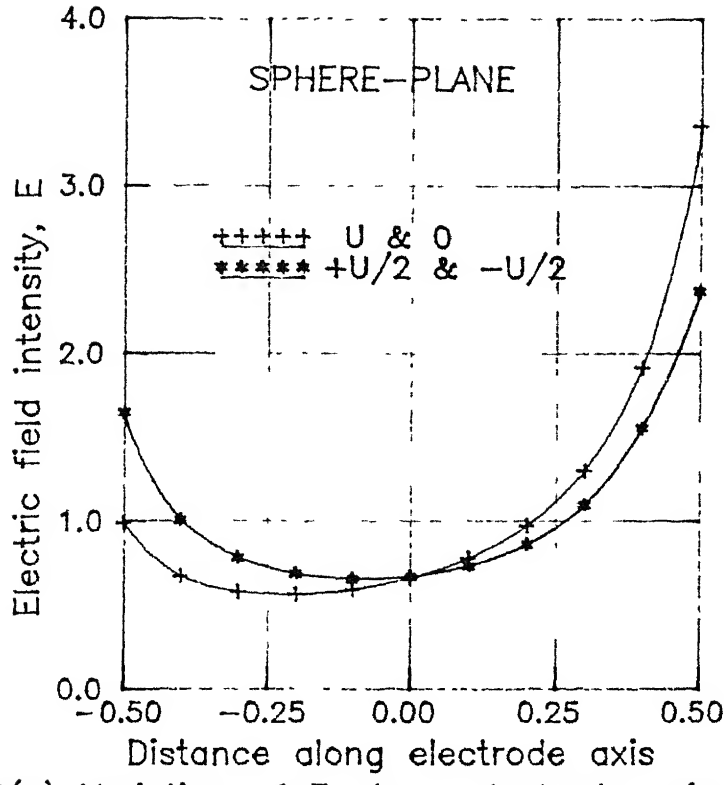

Fig.2.6(g) Variation of E along electrode axis for Sphere–Plane electrode.

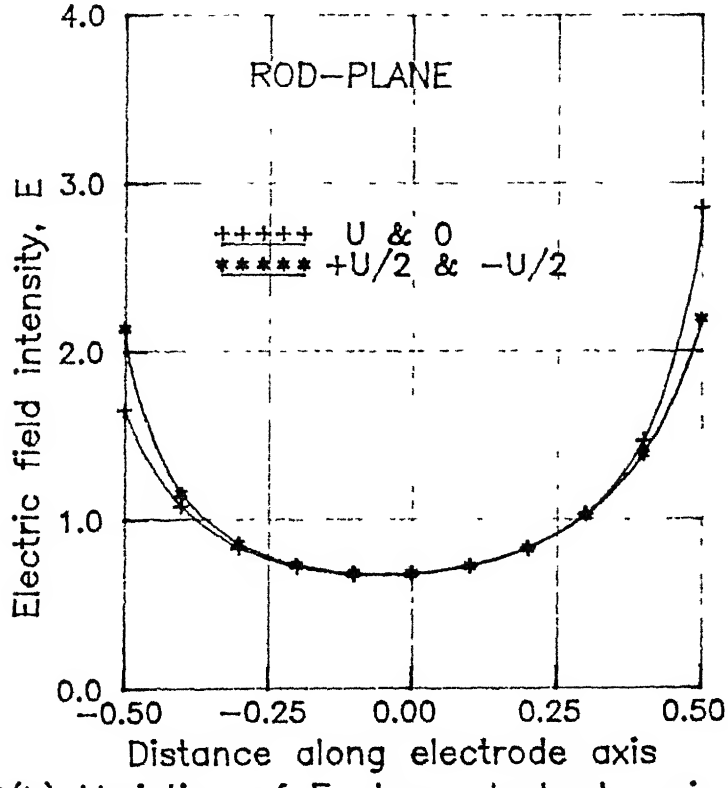

Fig.2.6(h) Variation of E along electrode axis for Rod–Plane electrode.

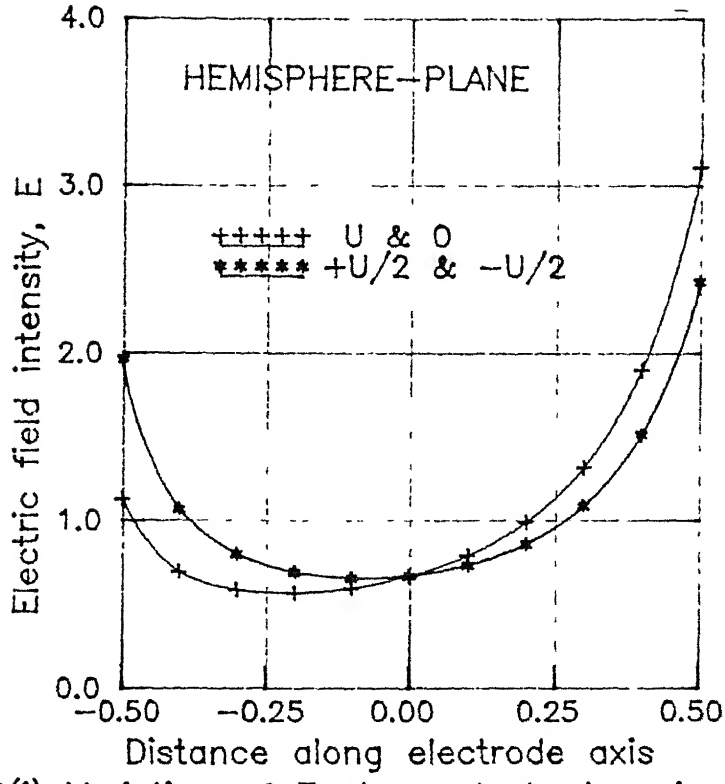

Fig.2.6(i) Variation of E along electrode axis for Hemisphere–Plane electrode.

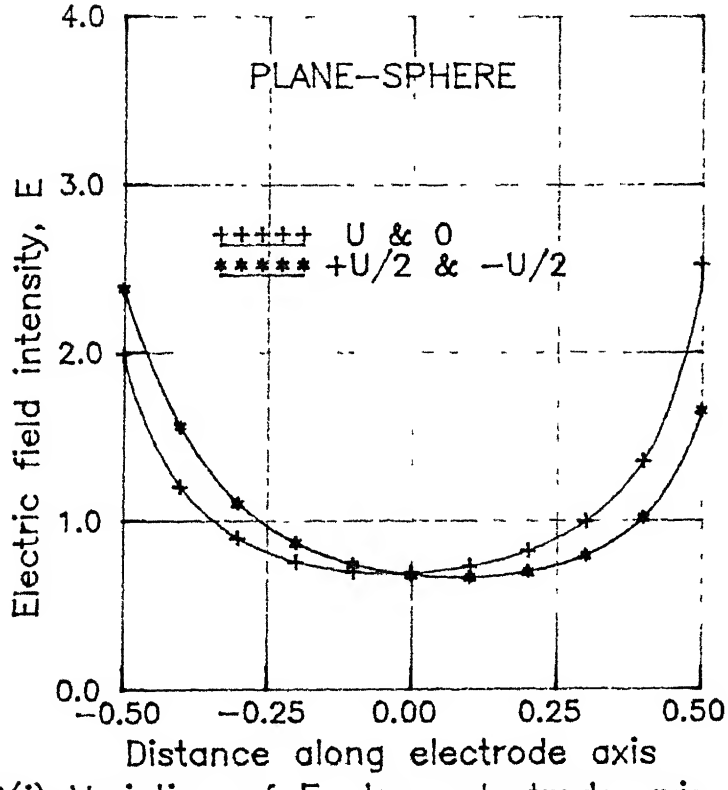

Fig.2.6(j) Variation of E along electrode axis for Plane–Sphere electrode.

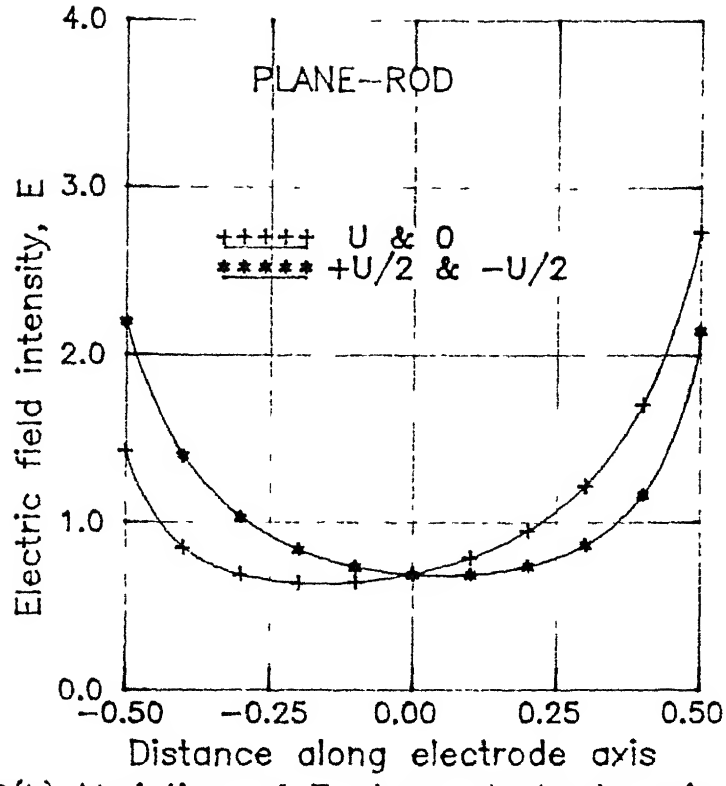

Fig.2.6(k) Variation of E along electrode axis for Plane–Rod electrode.

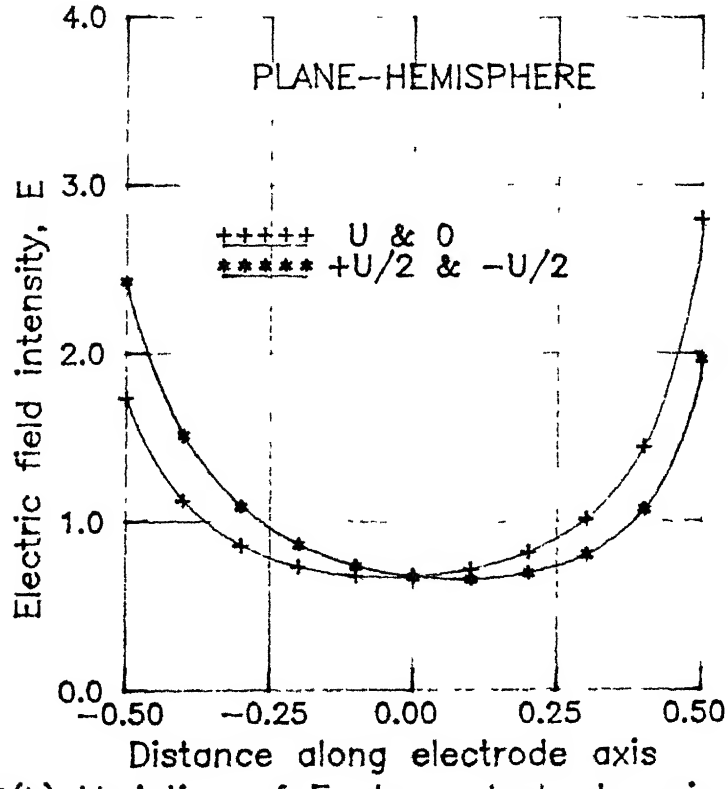

Fig.2.6(L) Variation of E along electrode axis for Plane–Hemisphere electrode.

2.5.4.4 Effect of applied voltage on the degree of uniformity, η

The factor of uniformity , η is calculated for each case of electrode pair and both mode of applied voltage It is given in Table 2 2 It can be observed from this table that for the same gap distance, plane-plane electrode has the maximum value of η compared to all other electrode arrangements The plane-plane electrode of the particular shape considered here does not comprise a uniform field (η = 1) as described by some workers [2 3] The field between a pair of electrode is more uniform (greater value of η) when applied with symmetrical voltage of +U/2 & -U/2 than when the applied voltage is asymmetric, U & 0, in all cases Although the radius of curvature of sphere-sphere, rod-rod and hemisphere-hemisphere electrodes is the same, the rod-rod have greater value of η, for both symmetrically and asymmetrically applied voltages

In case of unequal spheres, the value of η remains the same even if the positions of small and large spheres are interchanged in case of symmetrically applied voltage But if the voltage is asymmetric, the electrode arrangement in which the larger sphere is the HV electrode, has higher value of η

For all other unsymmetrical electrode arrangements, such as sphere-plane, rod-plane, hemisphere-plane, plane-sphere, plane-rod and plane-hemisphere etc , the value of η remains unchanged if the electrodes are interchanged in their positions, in case of symmetrically applied voltage But in case of asymmetrically applied voltage, plane-sphere has higher value of η than sphere-plane. Similar is the case for plane-hemisphere and hemisphere-plane and plane-rod and rod-plane also

Table 2.2 : The degree of uniformity, η

	η	
Electrode configuration	Symmetrical voltage	Asymmetrical voltage
Plane-plane	0 491	0 331
Sphere-sphere	0 444	0 313
Rod-rod	0 448	0 341
Hemisphere-hemisphere	0 431	0 292
Unequal spheres dia up=1, lo=0 9	0 407	0 314
Unequal spheres dia up=0 9, lo=1	0 407	0 284
Sphere-plane	0 421	0 298
Rod-plane	0 457	0 351
Hemisphere-plane	0 413	0 322
Plane-sphere	0 421	0 397
Plane-rod	0 457	0 366
Plane-hemisphere	0 413	0 358

While comparing sphere-plane, rod-plane and hemisphere-plane, the rod-plane has higher value of η than the other two, in both the cases of applied voltage But while comparing plane-sphere, plane-rod and plane-hemisphere, plane-rod has higher value of η compared to the other two in case of symmetrically applied voltage In case of asymmetrically applied voltage, plane-sphere has higher value of η compared to plane-rod and plane-hemisphere electrode

The following can be concluded from these computational results -

(1) Plane-plane electrode system has more uniform field

(2) For the same radius of curvature, rod-rod electrode comprises more uniform field than sphere-sphere or hemisphere- hemisphere electrode

(3) If symmetrical voltage is applied , the interchange of position of unsymmetrical electrodes does not change the value of η

(4) In case of asymmetrically applied voltage, the field is more uniform if the HV electrode has larger radius of curvature, in case of unsymmetrical electrode systems

(5) For any electrode pair, the field is more nonuniform (lower η) for asymmetrically applied voltage than for symmetrically applied voltage

2 5.5 Conclusion

The CSM is an effective tool to estimate the distribution of the equipotential lines, field intensity E and the degree of uniformity η Application of this method found to be most appropriate to study the effect of grounding of one of the electrodes on the distribution of field which was not possible analytically This enables the degree of uniformity, η to be suitably adopted as a parameter for any investigation The study performed with the help of CSM on electrodes of regular shapes in this work, can be easily extended to electrodes of any shape It may be useful in the design of GIS and space borne systems more confidently

REFERENCES

2 1 A S Pillai and R Hackam,"Electric field and potential distribution for unequal spheres using symmetric and unsymmetric applied voltages", IEEE Trans on Elect Insul vol EI-18, 1983, pp 477-484

2 2 T Shioiri, I Ohshima, M Honda, H Okumura, H Takahasi, H Yoshida, "Impulse voltage field emission characteristics and breakdown dependency upon field strength in vacuum gaps", IEEE Trans on PAS, vol PAS-101, pp 4178-4184, 1982

2 3 K Tsuruta, "Prebreakdown field emission current and breakdown mechanism of a small vacuum gap", IEEE Trans on Electrical Insulation, vol EI-18, pp 204-208, 1983

2 4 B Mazurek, and J D Cross, "An energy explanation of the area effect in electrical breakdown in vacuum", IEEE Trans on Electrical Insulation, vol EI-22, pp 341-346, 1987

2 5 H Toya, T Hayashi, M Yorita and Y Murai, "Numerical modeling to evaluate the withstand voltage of a HV vacuum interrupter", IEEE Trans on Electrical Insulation, vol EI-24, pp 21-30, 1989

2 6 D Linhjell, L Lundgard and G Berg, "Streamer propagation under impulse voltage in long plane-point oil gaps", IEEE Trans on Dielectrics and Elect Insul vol 1,No 3, pp 447-458, 1994

2 7 R Arora and W Mosch, "High voltage insulation engineering", Wiley Eastern Ltd , India, 1995

2 8 M D R Beasley, J H Pickles, G dAmico, L Bretta, M Fanelli, G Giuseppetti, A diMonaco, G Gallet, J P Gregoire and

M Morin, "Comparative study of three methods for computing electric fields", Proc of IEE, vol 126, pp 126-134, 1979

2 9 G W Carter and S C Loh, "The calculation of electric field in a sphere gap by means of dipolar coordinates", Proc of IEE, vol 106 C, pp 108-111, 1959

2 10 P K Mukherjee and C K Roy, "Computation of fields in and around insulators by fictitious point charges", IEEE Trans on Elect Insul vol EI-13, 1978, pp 24-31

2 11 H Singer, H Steinbigler and P Weiss, "A charge simulation method for the calculation of high voltage fields", IEEE Trans vol PAS-93, 1974, pp 1660-1668

2 12 J M Mattingley and H M Ryan, "Potential and potential-gradient distributions for standard and practical electrode systems", Proc of IEE, vol 118, pp 720-732, 1971

2 13 M A G Khan and R Arora, "Application of charge simulation method (CSM) for the estimation of field between HV and grounded electrodes", Proc of 3rd workshop and conference on EHV technology, Bangalore, India, 1995

3.2 High voltage ac supply

A variable high voltage supply was obtained from a 100 kV, 50 kVA, single phase, ac power frequency (50 Hz), partial discharge free test transformer (Fig 3 1) The output terminal of the transformer was connected to an 1100 pF, 100 kV, PD free capacitor with the help of a 7 5 cm diameter alluminium pipe The high voltage terminals of both the transformer and the capacitor were provided with large alluminium domes for stress control

The high voltage terminal of the capacitor was connected to the test object with the help of a flexible steel conduit of 2 5 cm diameter In order to provide a support this conduit was passed through a bell shaped fixture suspended from the roof with the help of a toughened glass insulator string This was done to control the electric field at the sharp bends of the high voltage conductor and thus prevent any PD

3.3 Impulse Generator

A four stage 500 kV impulse generator was used for impulse voltage tests (Fig 3 2) The specifications are given in Table 3 1 The output of the impulse generator was connected to a capacitive voltage divider having ratio of 750 1 The rating of the HV capacitor was 1 5 nF, 600 kV The impulse generator could be triggered with the help of a Trigatron circuit, which produced pulse of 10 kV at an interval of 1 to 30 seconds (adjustable)

Table 3 1 : Specification of Impulse generator

Sl No	Specification	Value
1	Max charging voltage	500 kV
2	Max noload output voltage	450 kV
3	Rated energy	4 4 kJ
4	No of stages	4
5	Input voltage	440 volts, 3 ϕ
6	Capacitor per stage	35 nF x 4, 125 kV
7	Waveshape of li	1 2/50 μs
8	Waveshape of si	250/2500 μs, 190/1900 μs
9	Make	TUR, Germany

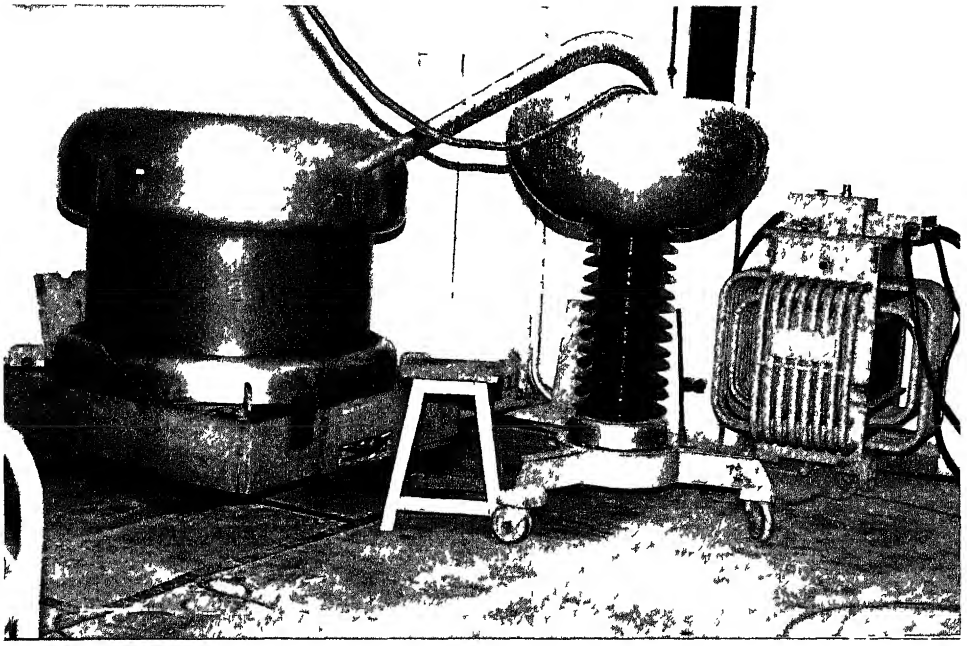

Fig.3.1 HV testing transformer and capacitor, 100 kV, 50 kVA.

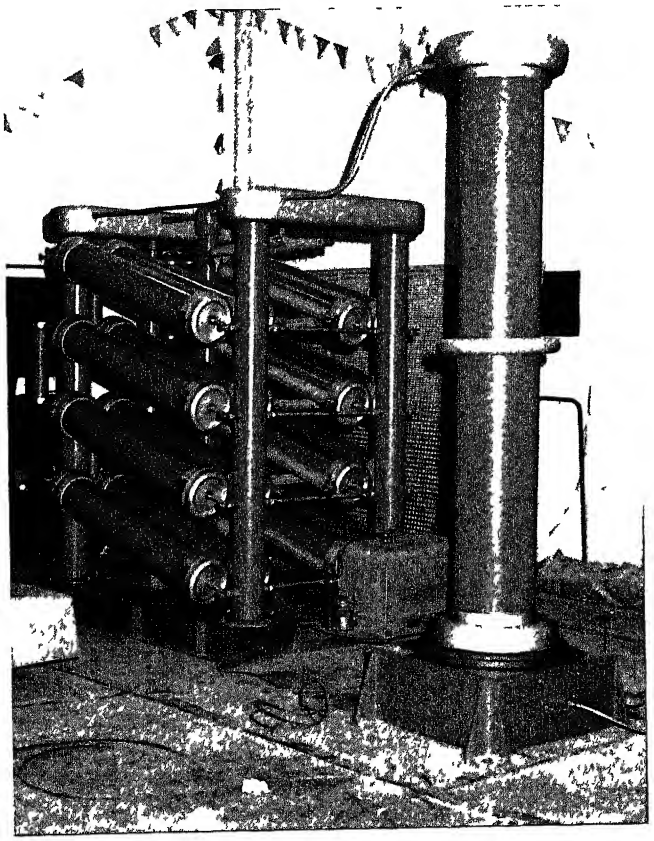

Fig.3.2 Impulse generator with measuring capacitor, 500kV, 4.4 kJ.

3 4 Oscilloscope

A digital storage oscilloscope of KIKUSUI made, (model No COR5502U) was used to measure the impulse voltage and the prebreakdown current It was connected with a PC through RS-232 serial interface and the recorded data was transferred to the PC for further analysis and storage A digital plotter was connected with the oscilloscope to obtain the hard copy of the waveform recorded by the oscilloscope (Fig 3 3)

3 5 Current viewing resistor

Two shunt resistors, one of 0 5 Ω and another of 1 0 Ω were used to measure the current with the help of the oscilloscope The first one was a so called "squirrel cage" measurement shunt described in [3 1], made by connecting 24 nos of resistors in parallel, each of 12 Ω value, as shown in Fig 3 4 The assembly was enclosed in a stainless steel container which provided shielding against any external electromagnetic interference One end of the shunt was connected to the stainless steel container which was grounded The other end was connected to the oscilloscope with the help of a coaxial cable, approximately 6 meters long The other resistor was a Nichrome wire resistor A two meter long wire was wound on a bakelite bobbin in antiparallel fashion, as shown in Fig 3 4

3.6 Vacuum pumping system

Vacuum can be produced by a number of methods Some of them are as follows

(a) It can be produced by mechanical displacement of gases from an enclosed space by means of pistons and cylinder, rotating vanes

Table 3.2 . Specification of oscilloscope

Model COR5502U

Digital storage mode

Max sampling rate	100 MS/s, 2 channels
Vertical axis resolution	8 bits, 25 points/cm
Memory capacity	Acquisition, 4 kWx2 Save memory, 4 kWx2
Effective storage	Single event, 28 6 MHz,
Frequency	repetitive mode, 100 MHz
Equivalent sampling	Max 20 GS/s
Pre trigger	0/1/5/9 div
View time	Off/1 s
Roll mode	0 2-5 s/div
Interpolation function	Linear/curve
Magnification factor	Horizontal x100

Real mode

Sensitivity & bandwidth	1,2 mV, DC - 20 MHz 5 mV-5V, DC - 100 MHz
X-Y operation	DC - 2 MHz
Sweep time	NORM 20 ns - 0 5 s/div MAG Max 2 ns
Sweep magnification	x5, x10, x50

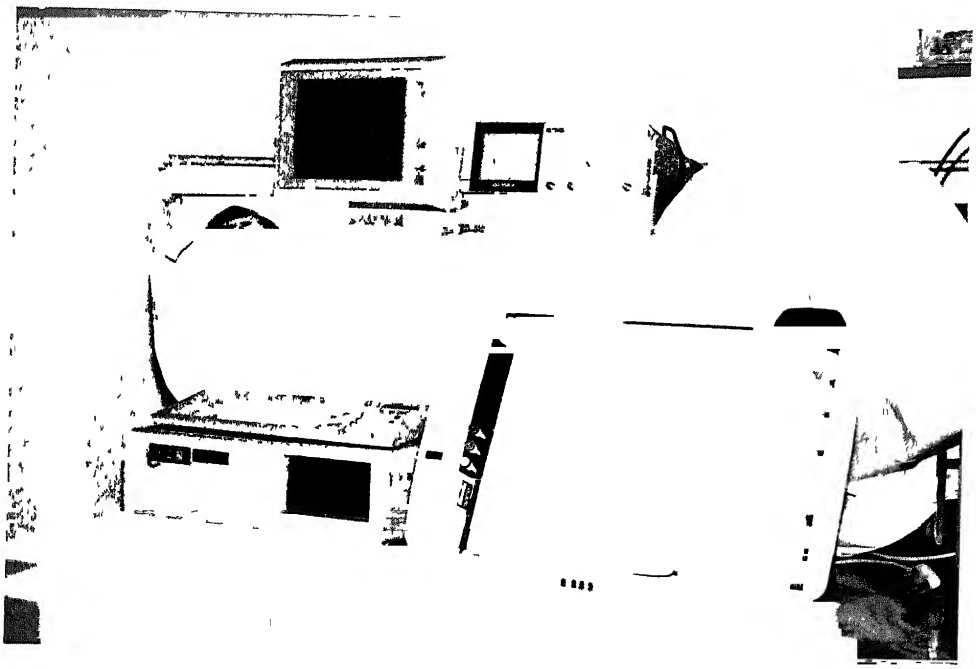

Fig.3.3 Digital oscilloscope interfaced with PC and digital plotter.

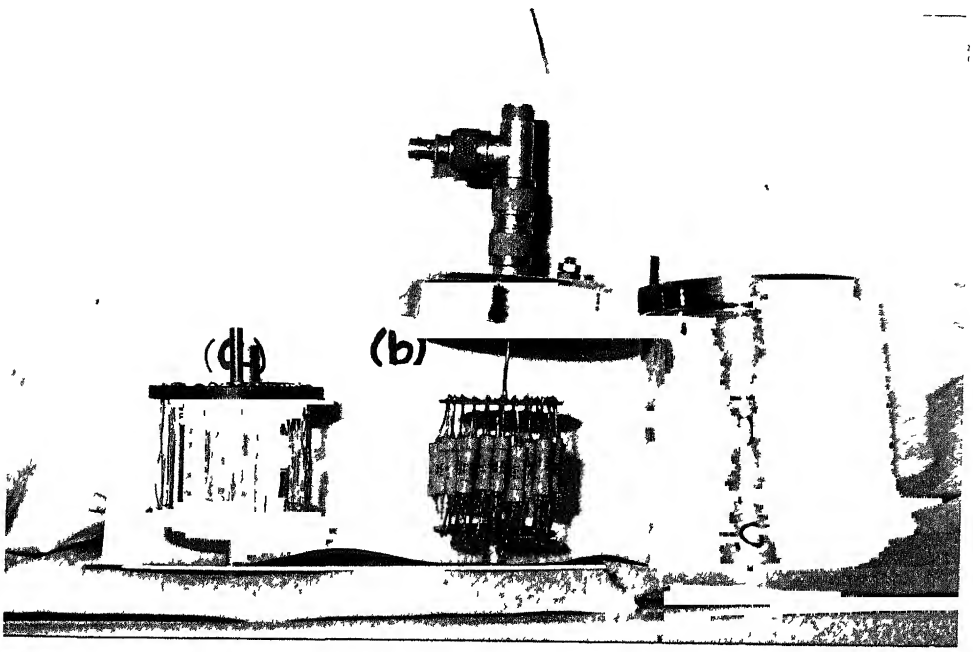

Fig.3.4 Current viewing resistor with container, (a) wire wound (b) Squirrel cage.

etc

(b) It can also be produced simply by condensing and freezing the gas in the enclosed vessel Normally this requires very low temperatures (cryogenic pumping)

(c) Vacuum can also be created by chemical reactions with the gas, which produces solid residues, thereby removing the gas from the space (chemical pumping or gettering)

The creation of vacuum involves two processes The first being the removal of gases originally contained in the volume of the work chamber The second is the competition between the capacity of the pump and the production of gas, not originally in the gas phase, but stemming from leaks, real or virtual, the latter being the gas desorbed from the walls and contents of the vacuum chamber

To produce a very high vacuum in a chamber, the evacuation process must start at atmospheric pressure Due to the enormous range of gas densities involved, a single pumping device is in-efficient for the complete evacuation process Usually a sequence of at least two different devices are required A coarse vacuum is produced either by mechanical means or by cryosorption, while the higher degree of vacuum is developed either by a vapour jet pump (called diffusion pump), cryopump, turbomolecular pump, or by an ion-gettering pump [3 2]

The instruments used to measure the degree of vacuum must also span a very wide range of gas densities At least two different vacuum gauges are used in most vacuum systems At low vacuum, gauges based on force measurements can be used At a high degree of vacuum, the pressure force becomes so small that direct force measurement becomes impractical and indirect ways must be applied One of the common methods involves ionizing of the gas and measurement of the intensity

of the ion current, which depend upon the amount of gas present.

The pumping system used in the present work had two different pumping devices For low vacuum a two stage rotary vane pump was used To produce high vacuum, a three stage diffusion pump backed by this rotary pump was used [3 3] The specifications of the pumping system are given in Table 3 3

3 6.1 The rotary vane pump

Rotary pumps are useful for producing vacuum of the order of 10^{-3} Torr In each stage of this pump, there were two sliding vanes placed on the rotor The vanes were pushed towards the stator wall by springs as shown in Fig 3 5(a) Oil was used to seal the end surfaces of the vanes and along the entire length of the vanes, as well as the ends of the rotor The rotor was run by a single phase motor As the rotor is rotated in the direction shown in figure, air is being pressed by the vanes and pumped out to the atmosphere Two single stage rotary pump were used in cascade as shown in Fig 3 5(b)

The presence of oil in the pump produces the possibility of migration or backstreaming into the vacuum chamber in case of sudden power failure A solenoid operated valve was used to check this The construction and working principle of this valve is illustrated in Fig 3 6 and explained in the following.

The solenoid was supplied through the same switch of the rotary pump so that as soon as the pump was on, the solenoid was also energized at the same moment When actuated, the solenoid attracts the plunger with which valve 1 is attached thereby the air inlet port was closed The valve 2 is opened with the help of gravitational force and allowed air to be sucked from the vacuum chamber to the rotary pump

Table 3.3 . Specification of vacuum pumping system

Direct drive rotary vacuum pump·

Model	ED - 12
Displacement	200 Lit/min
Ultimate vacuum	10^{-3} Torr
No of stages	2
Motor rating	1/2 HP
Pump r p m	1440
Oil charge	2 Lits
Inlet coupling	25 mm
Oil recommended	Molecular distilled oil

Diffusion Pump.

Model	Difpak OD-114
Air speed	150 Lit/sec
No of Stages	3
Type of jet	Fractionating
Critical backing pressure	0 1 mBar
Heater rating	500W, 230V ac
Recommended oil	D C 704 Silicon fluid
Cooling water supply	1 5 Lit/min
High vacuum valve	114 mm
Ultimate vacuum	10^{-6}Torr

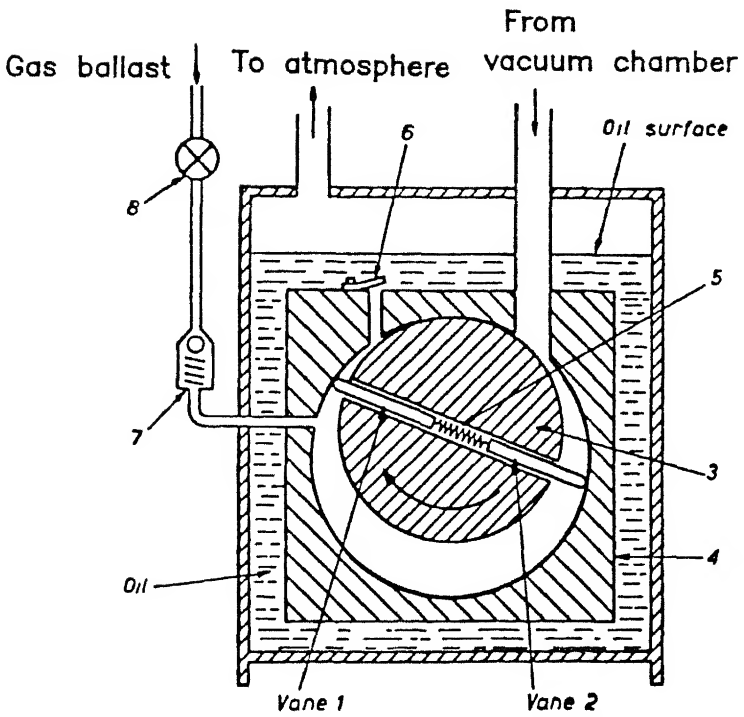

1 & 2 Vane
3 Rotor
4 Stator
5 Spring
6 Flap valve
7 Spring loaded valve
8 Valve

(a) Single stage.

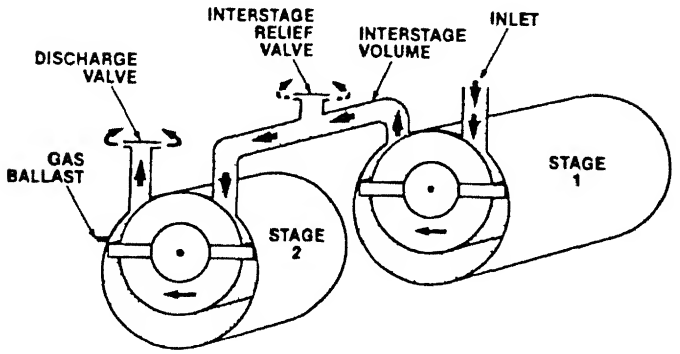

(b) Two single stage cascaded.

Fig.3.5 Working principle of rotary pump.

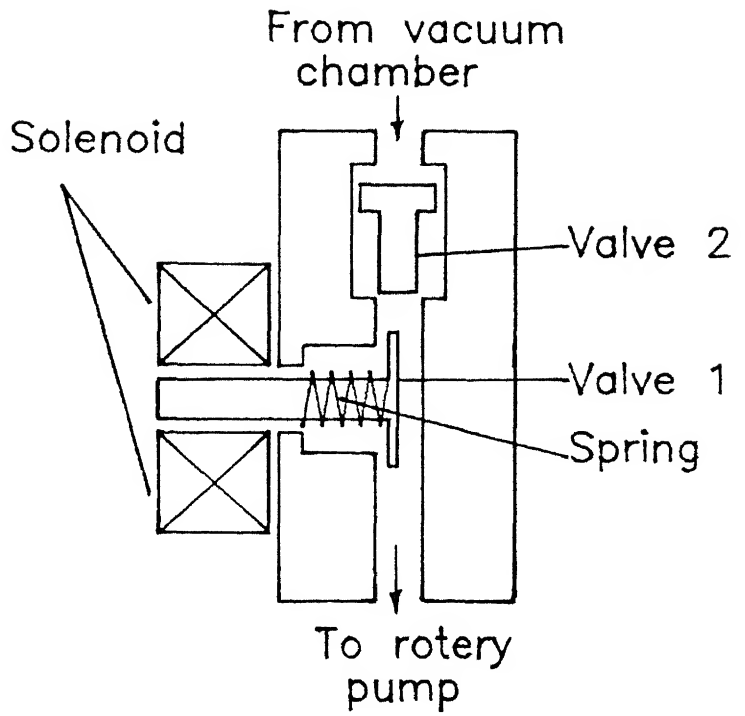

Fig.3.6 Working principle of solenoid operated valve to minimise backstreaming of oil.

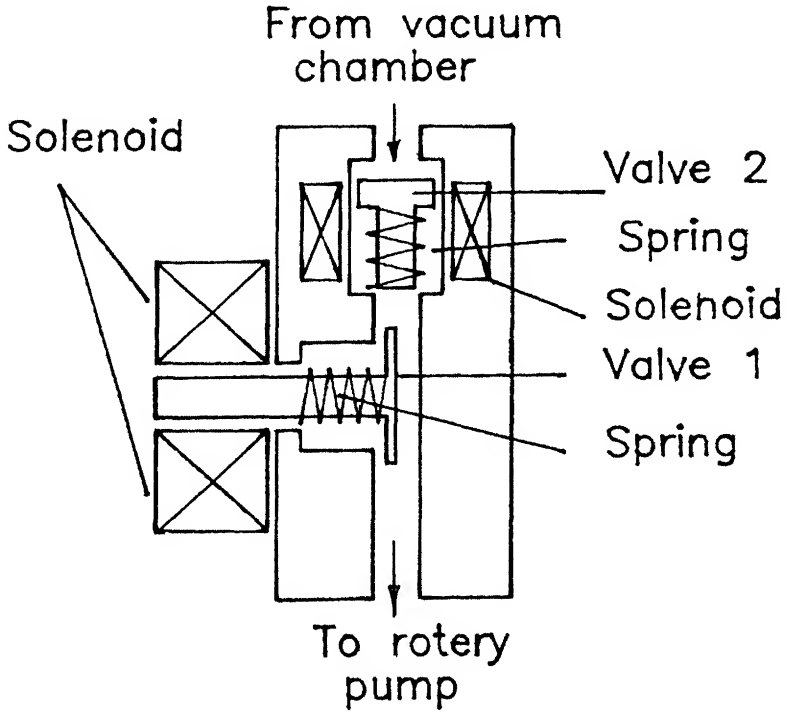

Fig.3.7 Proposed modification of solenoid operated valve to minimise backstreaming of oil.

In case of a sudden power failure, the solenoid is de-energized and releases valve 1, which was spring loaded As soon as valve 1 is opened, air from atmosphere rushes into the pump and pushes valve 2 upward which closes the vacuum chamber Thereby the pressure at the inlet and at the outlet of the pump became the same, i,e, equal to the atmospheric pressure In this way the possibility of migration of oil from the rotary pump to the vacuum chamber was minimized

However this mechanism was found not to work properly Several times it happened that at the event of a sudden power failure, valve 2 did not close the vacuum chamber properly thereby admitting air into it from atmosphere To overcome this problem, an improved mechanism was designed as illustrated in g 3 7 However it could not be implemented as it requires modification of the chassis of the rotary pump which was not possible in our part

3.6 2 Diffusion pump

Diffusion pumps (DP) are vapour jet pumps used for pumping rarefied gases in the high vacuum range of pressures These pumps cannot discharge directly into the atmosphere The rotary pump was used to reduce the pressure in the vacuum system within the operating range of 0 05 Torr

The working principle of this pump is illustrated in Fig 3 8 The vapour (of rich grade silicon oil) is produced in the boiler and is expanded through the nozzle achieving a very high velocity, typically 1000 ft/s The high velocity jet entrains the air molecules that enter due to their usual thermal motion The gas and the vapour are separated in the condenser The air molecules are pumped away by the mechanical pump and the oil condensate returns to the boiler The

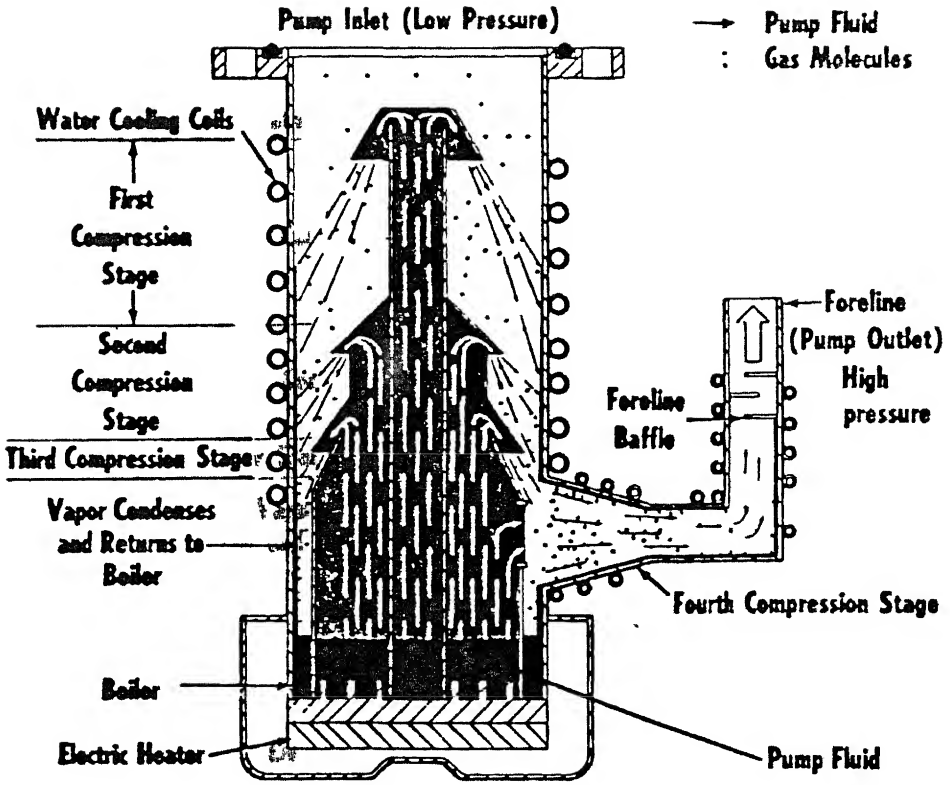

Fig.3.8 Working principle of diffusion pump.

arrows in the figure represent pumping fluid molecules, and the black dots, the pumped air molecules As the vapour jet is directed downward, it is difficult for the molecules in region P to cross the vapour jet in upward direction against the vapour stream Once a molecule has entered the vapour stream from above, the collisions with vapour molecules will impart into a downward motion

The performance of the pump is dependent upon the rate at which vapour is produced in the boiler, which further depends upon the heat produced by the heater Therefore different pressure levels can be achieved by controlling the heater temperature which in turn can be controlled by varying the heater voltage

3.6 3 Measurement of pressure

Two pressure gauges were used to measure the pressure at two different pressure levels At low vacuum, i,e upto 10^{-3} Torr, a Pirani pressure gauge was used At high vacuum, i e 10^{-6} Torr, a Penning gauge was used [3 4] Their operating principles are discussed below

Pirani gauge : The gauge head consists of a resistive filament energized by a regulated 2 volt dc supply Any change of pressure in the vacuum chamber brings about a rise or fall in the number of the gas (air) molecules and hence a rise or fall of thermal conductivity of the gas surrounding the filament The filament is made of a material having high temperature coefficient of resistance Thus a little change in pressure causes a considerable change in the resistance of the filament This change is sensed and measured with the help of a wheatstone bridge arrangement, as shown in the circuit

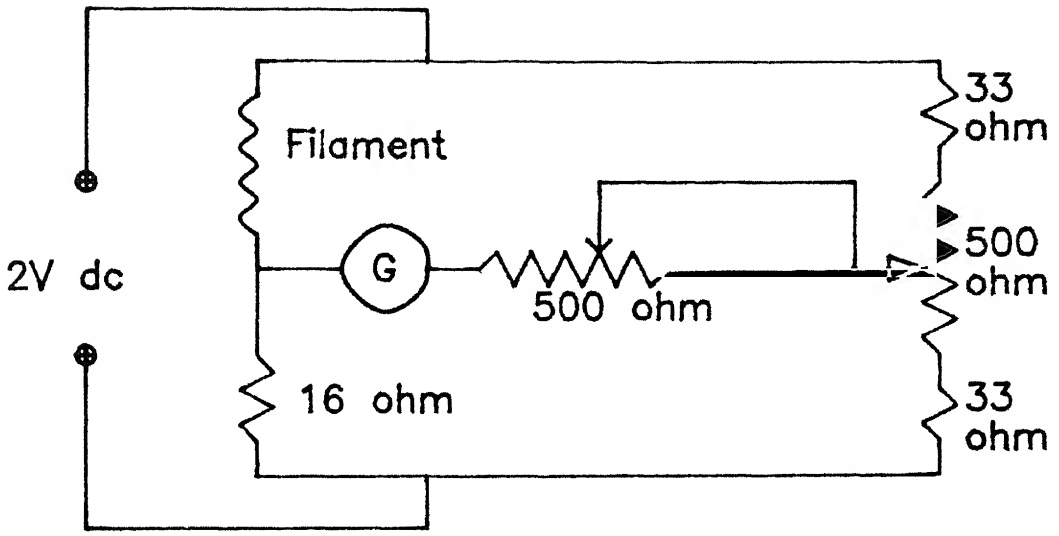

Fig.3.9 Circuit diagram of Pirani gauge.

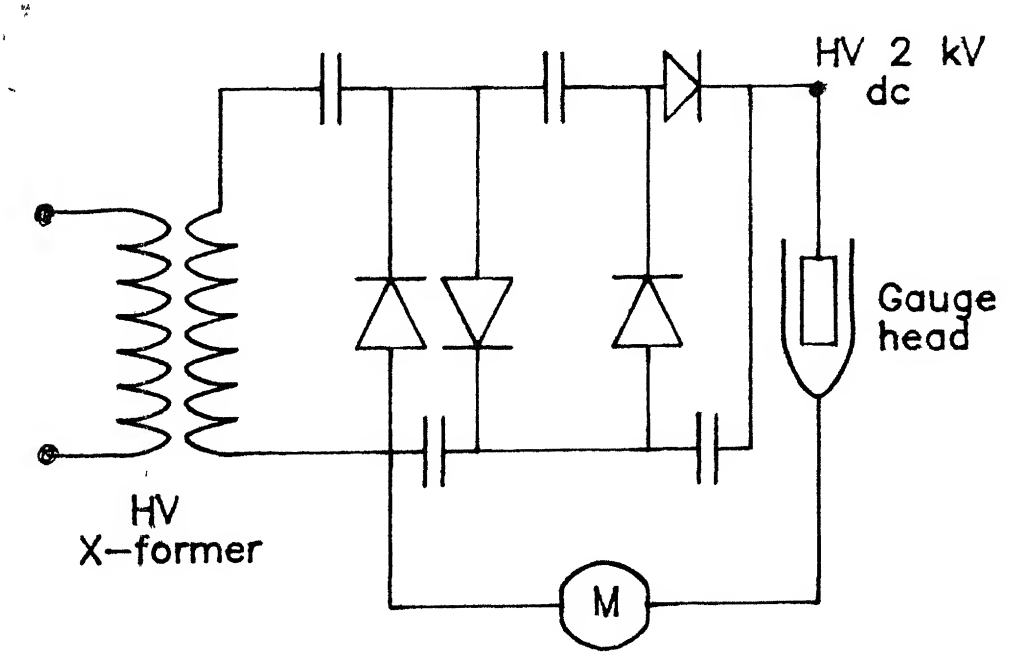

Diode : DR150, C : 0.1×10^{-6}F, 2 kV

Fig.3.10 Circuit diagram of Penning gauge.

diagram (Fig 3 9) The galvanometer is so scaled that it directly reads the pressure in mbar

This gauge has a disadvantage that it can not read pressure instantaneously There is a time lag between the change in pressure and the pressure display by the meter Another problem was that the meter dial display had first graduation at 0 5 mbar So pressure higher than 0 5 mbar (but below atmospheric pressure) could not be read

Penning gauge The gauge head consists of a rectangular wire loop, made of stainless steel as anode The anode is surrounded by a cylindrical cathode of stainless steel, which also forms the gauge head body A constant dc supply of 2 kV is maintained across the anode and the cathode (Fig 3 10) A magnetic field is introduced at an angle of 90° to the plane of the electrodes by using a permanent magnet The electron emitted from the cathode are deflected by the magnetic field and travel in a helical path before reaching the anode Thus even under low pressures, the emitted electrons have a high probability of collision with the gas molecules The secondary electrons produced by impact ionisation produce a cascading effect and the rate of ionisation increases Eventually the electrons are captured by the anode and an equilibrium is reached when the number of electrons produced is the sum of positive ion current to the cathode and the negative electron current to the anode This current is measured by a milliammeter which is scaled to read pressure directly in mbar.

3.7 Modifications of vacuum pumping system for high voltage use

During experiments with high voltage, it was realized that the pumping system was not designed for HV applications The solenoid of the rotary pump and the heater of the diffusion pump were damaged several times when breakdown used to take place in the vacuum chamber Hence modifications of these two parts were necessary to prevent any further damage to the equipment during working with high voltage

3.7.1 Modification of solenoid

The solenoid designed to operate at 230 V was found not insulated adequately for high voltage applications It got damaged by the event of breakdown when the high voltage applied across the electrodes was 40 kV Due to breakdown, high current flows to the earth plate through the body of the pump As the solenoid was mounted directly on the body of the pump, a portion of the breakdown current might have reached the coil of the solenoid producing large induced voltage across it and caused damage

The solenoid coil was refabricated with some modifications as shown in Fig 3 11 The bobbin was made of 2 mm thick bakelite sheet and a very fine superenamel copper wire (AWG No 40) was wound on it to provide sufficient number of turns (8000 turns) Interlayer insulation was provided with thin plastic sheets which could withstand 9 kV The complete winding was covered with three layers of this plastic sheet The terminals were taken out carefully by using teflon insulated copper wires Finally the complete assembly was dipped into insulating varnish The full load current of the solenoid was measured to be 90 mA Two 100 mA rating fuses were used in both the line and neutral for overload protection This modification improved the

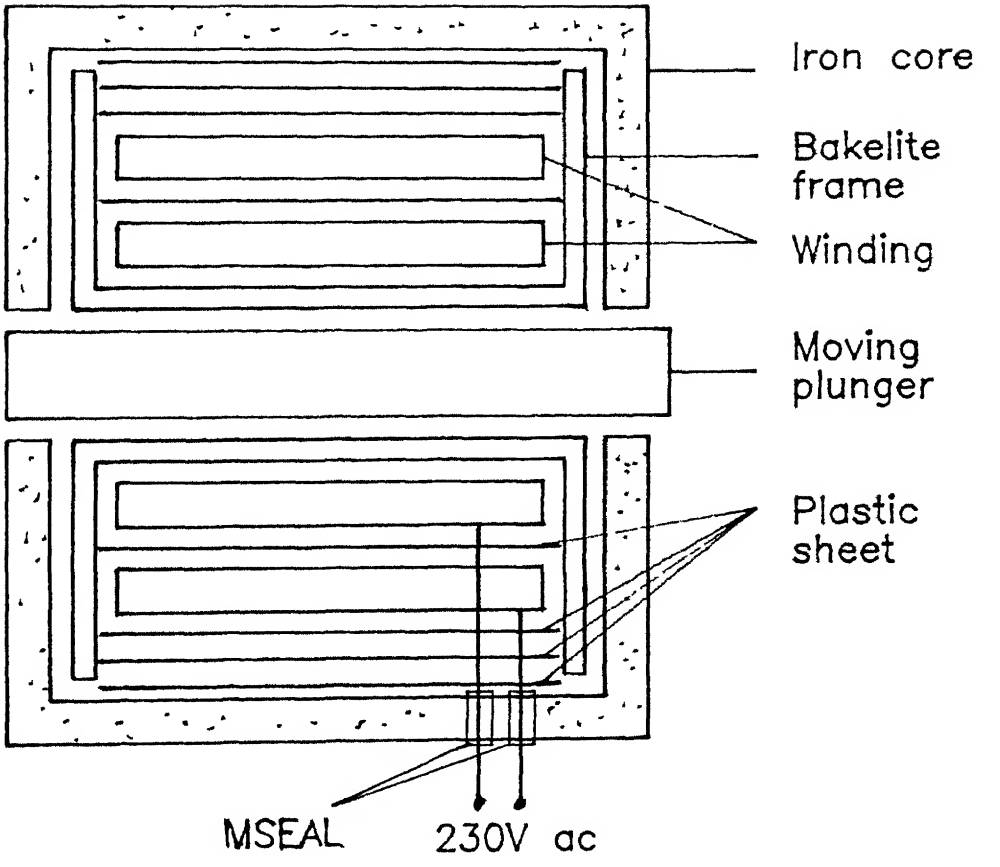

Fig.3.11 Cutaway view of modified solenoid.

performance of the solenoid and prevented any further damage to it

3.7.2 Modification of heating arrangement of diffusion pump

While performing experiments, the heater of the diffusion pump was damaged several times at the event of breakdown in the vacuum chamber Sometimes, even a flashover was seen between the pump body and the earthing plate through the pump body, heater etc The original heater was not properly sealed against such flashovers A new heater had to be therefore designed to withstand such flashovers which is shown in Fig 3 12

Nichrome ribbon having resistance of 16 ohms per meter was wound on a hexagonal mica frame of 2 mm thickness Total length of the wire was 8 meters which gave approximately 125 ohms of resistance The size of the ribbon was 26 AWG which can carry a current of 4 A This mica frame, containing Nichrome ribbon winding, was placed between two circular mica sheets of 1 mm thickness The whole assembly was placed inside an aluminium case, consisting of two circular discs which provided adequate shielding against flashovers The terminals were taken out through 3 mm diameter brass bolts, insulated from the aluminium case by using MSEAL, a commercially available insulating bonding material

To supply power to the heater, an isolating transformer was designed and fabricated as shown in Fig 3 13 The transformer has equal turns on both primary and secondary but the windings are placed on two different limbs of the core which are physically separated from each other by a distance of about 5 cm Thereby any possibility of back flash to/from the supply mains was prevented The primary of the isolating transformer was energized by an autotransformer having

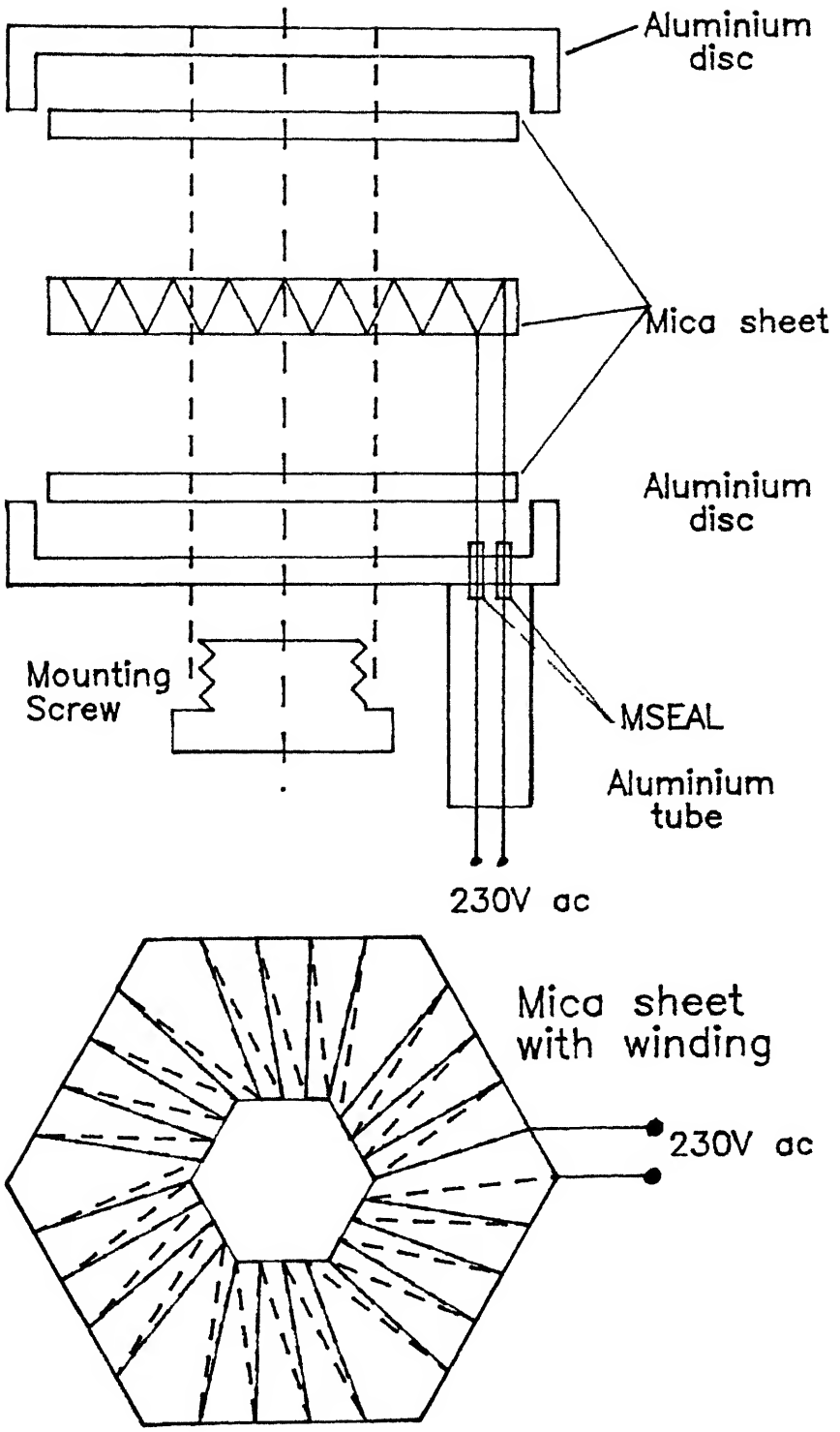

Fig.3.12 Different parts of the heater, 230 V, 500 W.

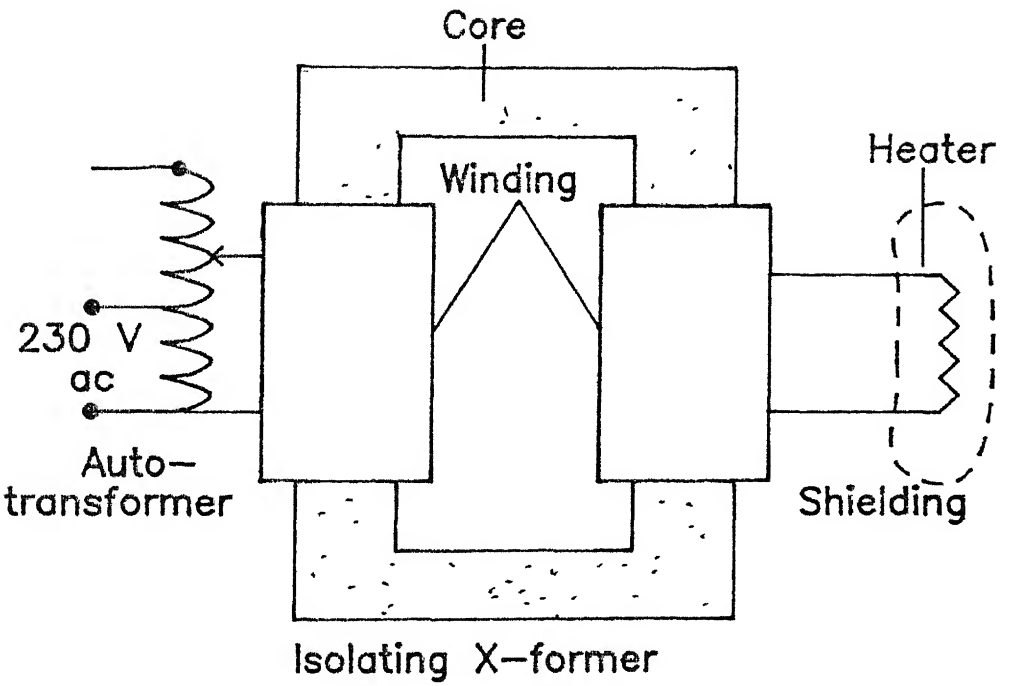

Fig.3.13 Modified heating arrangement for DP.

variable output voltage to regulate the supply voltage of the heater It was observed that at about 180 V, the ultimate pressure obtained in the vacuum chamber was 10^{-3} Torr To obtain pressures of 10^{-4}, 10^{-5} and 10^{-6} Torr, the supply voltage required was approximately 200, 220 and 250 V respectively

3 8 Design and fabrication of vacuum chamber

An attempt was made to use the vacuum cum pressure vessel available in the laboratory with the new vacuum pumping system procured specifically But a vacuum level less than 10^{-2} Torr could not be achieved in this vessel After considerable struggle, it was realized that the operating principle of the diffusion pump was such that the connection between the vessel and the pump should have diameter more than 5 cm , while that of the existing vessel was only 8 mm Moreover, a more effective evacuation was possible in a shorter time if the vessel could be mounted directly on the pump by replacing its top cover Commercially available vessel, made of stainless steel cylinder [3 5, 3 6], was not suitable because it was desired to observe what is going on inside the vessel during the experiments. Hence a new vacuum chamber suitable for producing vacuum of the order of 10^{-6} Torr was needed to be designed and fabricated

Different parts of the vacuum chamber fabricated has been shown in Fig 3 14 High quality PYREX glass tube was used for the chamber [3 7, 3 8] Two chambers were fabricated, one of 40 cm height and other was of 60 cm high The inner diameter of both the glass tubes was 128 mm and the wall thickness was 3 mm Two similar end flanges were made from 25 mm thick Acrylic sheet These flanges were joined with the 40 cm long glass tube with the help of "ARRALDITE", a

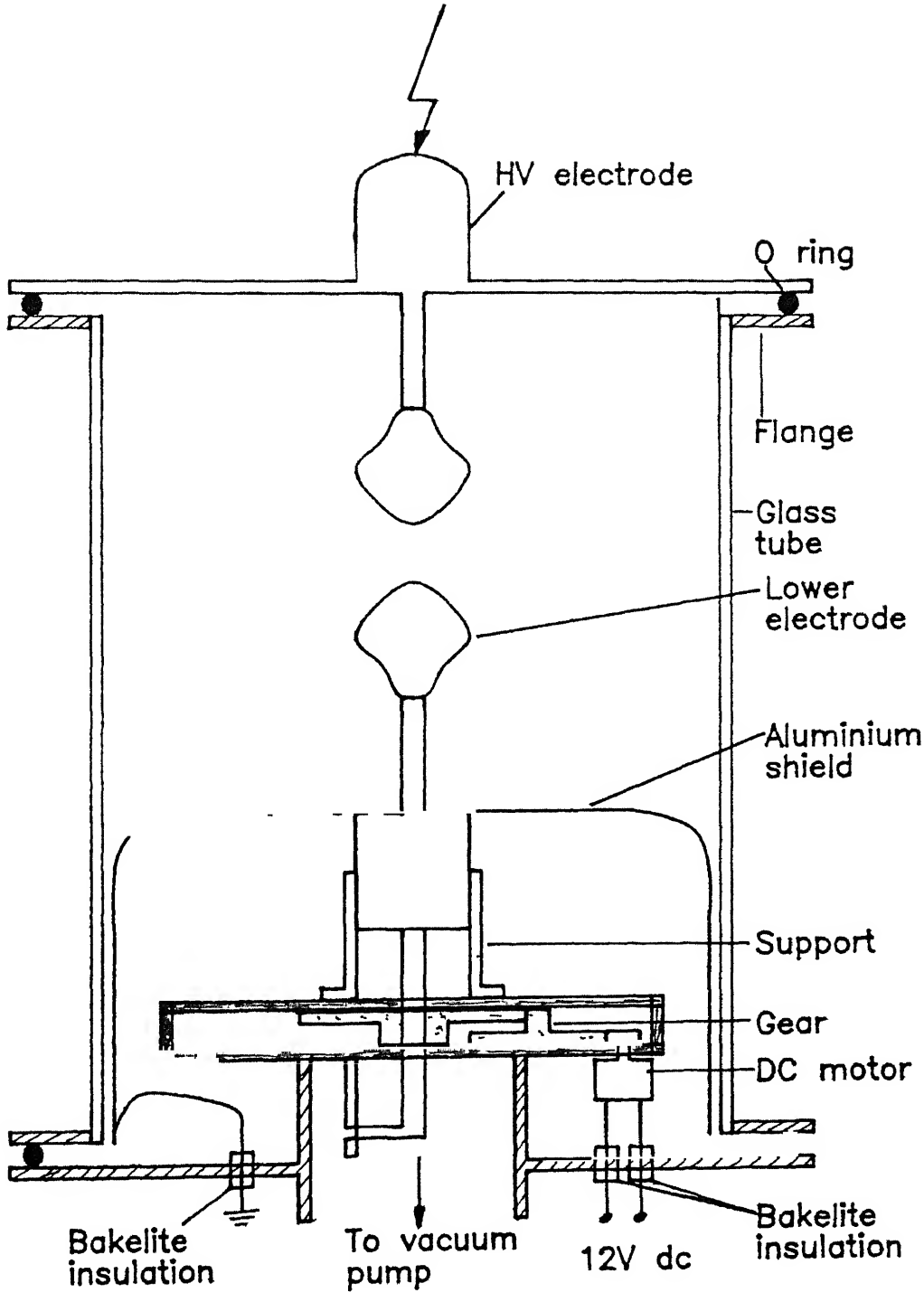

Fig.3.14 Vacuum chamber with gap adjustment device.

commercially available all purpose epoxy resin glue It took about 24 hours to set the glue properly

The vacuum chamber needed frequent cleaning with acetone during experiments It was noticed that acetone reacted with Acrylic flanges deteriorating its surface smoothness Therefore another vacuum chamber was fabricated with the 60 cm long glass tube The flanges for this chamber were made from 12 mm thick Alluminium sheet and joined with the glass tube in a similar way by using "ARRALDITE"

The top cover for the vessel was made out of 6 mm thick Brass plate A cylindrical stem, made of 25 mm diameter Brass rod, was fixed at the center of the top cover There were internal threads made at both the ends of the stem to fix the HV connection on the top of the vessel and the upper electrode inside the vessel All the ends of the stem and the edges of the top cover were given suitable shape to control the electric stress

The bottom cover was made in a similar fashion but at the center it had an opening of 10 cm diameter at which a brass tube was fixed The other end of the brass tube was fixed to the top cover of the diffusion pump Thus the vessel was directly mounted on the pump with an opening of 10 cm diameter which was adequate for required operation of the pumping system to produce high vacuum

At the junction of the end flanges and the cover plates on both the sides, two Neoprene "O" rings were placed which provide seal against any possible leakage of vacuum High grade silicon vacuum grease was applied on the "O" rings before placing them in position

The vacuum chamber was tested after fabrication for high voltage application and found to work without any surface discharge on the glass tube upto 80 kV (ac, rms)

3.9 Design and fabrication of gap adjustment mechanism

In order to maintain the conditions inside the vessel fairly clean, it was inconvenient and time consuming to open the vessel and adjust the interelectrode gap every time Moreover it took about 3 hours of continuous operation of the pump to achieve the desired level of vacuum It was necessary therefore to design a gap adjustment device [3 8] with the help of which the interelectrode gap could be adjusted from outside the vessel without opening it and disturbing the vacuum condition inside

This mechanism is shown in Fig 3 14 A 12v dc motor (conventionally used in tape recorders) was used as a drive The supply leads of the motors were taken out through two insulated leads through the lower end plate of the vacuum vessel By reversing the polarity of the supply voltage, the motor could be run in reverse direction Thus lowering or raising of the lower electrode was possible without opening the vessel To reduce the speed and to increase the torque, a gear train having speed ratio of 60.1 was used with the motor At the center of the last gear which has the lowest speed, inner thread (TPI = 24) was made through which a long screw (length 15 cm) was fitted As the motor runs, the gear rotates and the screw moves upward or downward The whole assembly was mounted between two parallel circular disks, made of Bakelite sheets. The lower disk was mounted on the brass tube directly Thus the motor and the gear train were insulated from the metal parts

On the top of the central screw, a 5 cm long cylinder made of bakelite was fixed There were inner threads provided at the other end of this cylinder at which the lower electrodes could be mounted This

way the lower electrode was insulated from the metallic body of the assembly

In order to connect the lower electrode to the ground or to a current measuring shunt, an insulated flexible copper lead was fixed on the lower end plate At the beginning, this lead was of 2 mm diameter and connected to ground through a thin wire On applying high voltage, at the event of breakdown, heavy current flow through this connection A considerable portion of this current reached the screw mechanism and the motor got damaged

To overcome this problem, the ground lead was replaced with a 6 mm diameter brass bolt and the entire gear train and the dc motor was enclosed within a cylindrical metallic container connected to ground through a thick flexible copper conductor This modification improved the performance and no such damage to the motor took place afterwards during experimentations

As the evacuating process begins the pressure inside the vessel reduces and due to atmospheric pressure from outside the end plates get pressed firmly against the flanges The Neoprene "O" rings also get compressed As a result the upper electrode position shifts downwards. The lower electrode mounted on insulated fixtures remains fixed in its position Because of this, the gap adjustment was made every time after the evacuation process was completed, otherwise a considerable error in gap distance measurement could have been introduced

A photograph of the entire experimental set up is shown in Fig 3 15

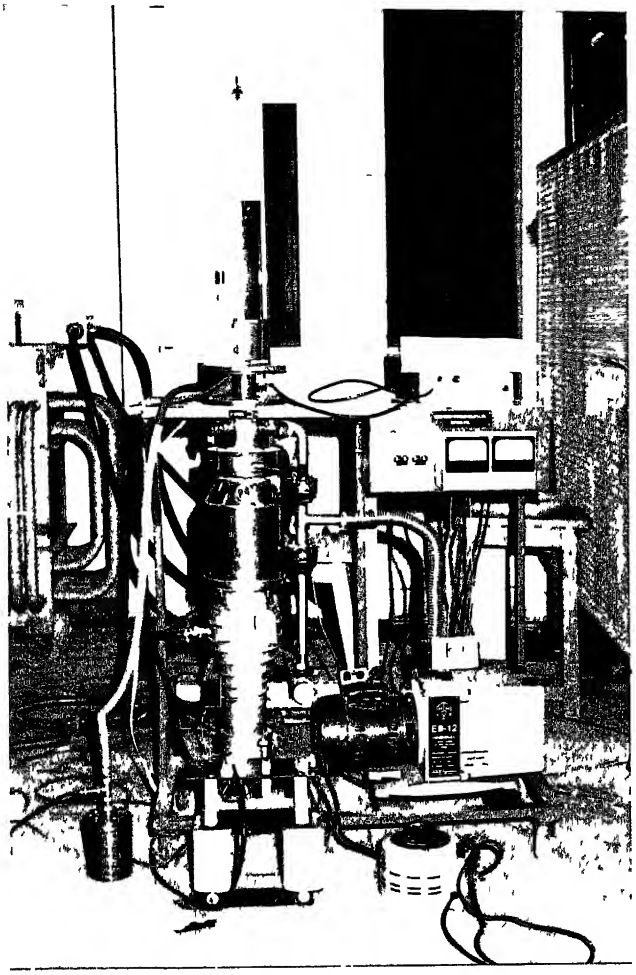

Fig.3.15 Photograph of the entire setup.

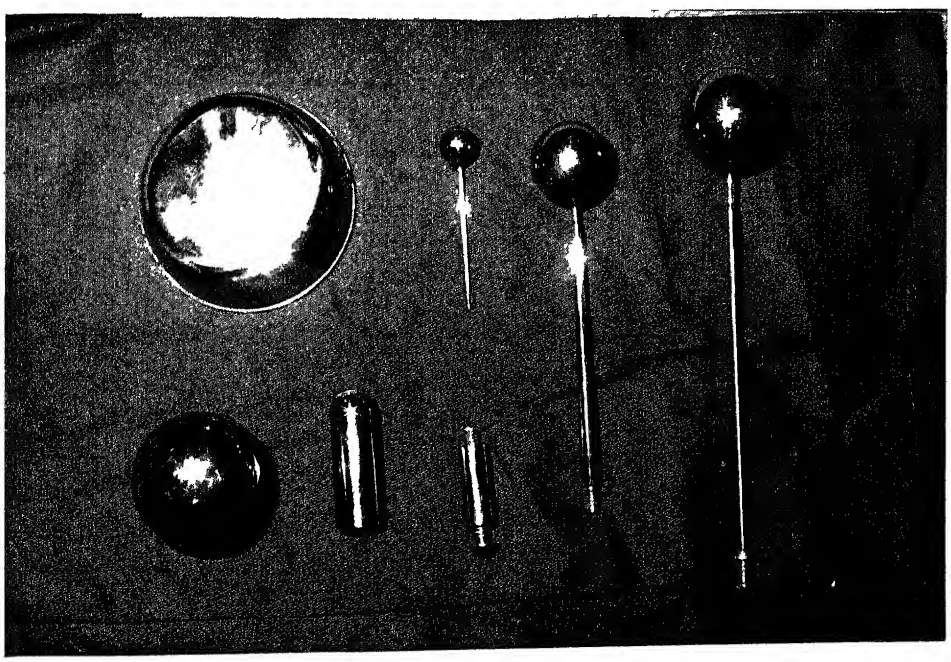

Fig.3.16 Photograph of the electrodes.

3.10 Electrode preparation

The shape and size of the electrodes fabricated (Fig 3 16) for the experiments are as follows -

(a) Spheres of diameters 50, 40, 25, 10 and 5 mm, made of stainless steel

(b) Hemispherical rods of diameter 18 5 mm, overall length 70 mm, made of Brass

(c) Circular planes of overall diameter of 85 mm, edge rounded with a radius of 5 mm, made of stainless steel

The shanks used to hold the electrodes in position were made of brass having diameter of 8 mm and overall length of 10 cm To hold the smaller spheres, shanks of stainless steel having diameter of 2 mm were used Apart from the shanks, extension rods of brass, having length of 10, 8, 5, 3 and 2 cm, diameter of 1 cm, were also used to adjust the longer gap distances All the electrodes, shanks, extension rods and the end plates of the vacuum chamber were polished successively with different grades of sand papers to give mirror finish. Then they were electroplated and buffed (commercially available electroplating and buffing facility were utilized)

3.11 Cleaning of electrodes and vacuum chamber

Before starting the experiments, all parts of the vacuum chamber, electrodes and the shanks were thoroughly washed with liquid soap and distilled water Then they were cleaned with acetone Rubber gloves were used on hands to hold the electrodes and different parts of the vacuum chamber while cleaning and mounting

The surface smoothness of the electrodes were found to deteriorate due to breakdown Hence the process of polishing,

electroplating, buffing and cleaning of the electrodes were repeated for a number of times during the entire course of the experiment Deposition of carbon and carbon compounds were observed on the inner surface of the vacuum chamber because of discharge which was cleaned periodically by using acetone

REFERENCES

3 1 M Barrault, G Bernard, J Maftoul and S Rowe, "Post-arc current measurement down to the ten milliamperes range", IEE/PES winter Meeting, Columbus, 1993

3 2 Marsbed H Hablanian, "High Vacuum Technology", Marcel Dekker, New York, 1990

3 3 "Instruction manual of vacuum pumping system", Hind High Vacuum (P) CO Ltd , Bangalore, India

3 4 "Instruction manual of Pirani-Penning combined pressure gauge", HI-Tech Instruments (P) Ltd , Bangalore, India

3 5 H Toya, N Veno, T Okeda, and Y Murai, "Statistical property of breakdown between metal electrodes in vacuum", IEEE Trans on PAS, vol 100, pp 1932-1939, 1981

3 6 H Pursch, P Siemroth and B Juttner, "On the nature of prebreakdown emission currents in vacuum interrupters", IEEE Trans on Electrical Insulation, vol EI-24, pp 917-920, 1989

3 7 L.G Carpenter, "Vacuum Technology", Adam Hilger Ltd , Bristol, 1983

3 8 K.Tsuruta, "Impulse electrical breakdown fields of short vacuum gaps", IEEE Trans on Electrical Insulation, vol EI-22, pp 77-79, 1987

3 9 G F Weston, "Ultrahigh Vacuum Practice", Butterworths, London, 1985

CHAPTER 4

INVESTIGATION WITH ALTERNATING POWER FREQUENCY VOLTAGE

4 1 Introduction

It is well known that the breakdown strength of any gaseous dielectric depends upon the pressure of the gas besides other parameters like field configuration and condition of the electrode The breakdown mechanism in vacuum is different from that of in air or gas At low gas pressures, electron ionization process becomes inadequate to cause breakdown because the "mean free path" of an electron is very long compared to that at atmospheric pressure Table 4 1 shows a comparative data of the number of molecules present per cm^3 and the mean free path at different pressures [4 1] In a vacuum better than 10^{-4} Torr, less than $3x10^{12}$ molecules per cm^3 are estimated to be present and the mean free path is of the order of meters In such a vacuum, an electron may cross a gap of few cm between two electrodes without any collision Therefore, unlike in gases, in vacuum the initial stage of breakdown cannot be due to the formation of electron avalanche The process of multiplication of charge particles by collision in space between the electrodes is far too insufficient to create avalanches However, if a gas cloud forms in the vacuum, the usual kind of breakdown can take place

Table 4.1 Mean free path at different pressures

	Pressure in Torr			
	760	10^{-3}	10^{-6}	10^{-9}
Mean free path in cm	$6\ 5x10^{-6}$	5	$5x10^{3}$	$5x10^{6}$
No of molecules/cm^3	$2\ 3x10^{19}$	$3x10^{13}$	$3x10^{10}$	$3x10^{7}$

4 2 Investigations at low vacuum

The insulating properties and behavior of low vacuum (pressure around 10^{-3} Torr) is quite different from that of high vacuum (10^{-6} Torr) At low vacuum, the mean free path is in order of few cm At this condition, electrons moving in the volume not only make enough ionizing collisions with the gas molecules but also excite the gas atoms to produce light radiation as they return to their ground state This phenomenon accounts for the characteristic light emission from a discharge At this condition the ion and electron densities are appreciable and almost equal Such a neutral state of high ion and electron density is known as "ambient plasma" [4 2]

At such low pressure of the gas, some rays are emitted from the cathode which are not visible to the naked eyes When these rays hit the wall of the pressure vessel and the gas within, it fluoresces This is known as "Faraday Glow Discharge" Various stages of this discharge arise because of the collision pattern between the charged particles emitted from the cathode and the atoms of the gas After receiving energy from the external source, the excited atoms come down to their ground states by successive transition through intermediate stages of lower energy and in the process electromagnetic radiations are emitted which carry away the excitation energy

The conductivity of the gas at this state becomes maximum and

the glow becomes voltage dependent The entire phenomena are pressure dependent and different glow phenomenon were observed at different values of applied voltage and pressure

Recently investigations are going on to establish the basis for treating problems in the areas of high voltage insulation and to develop pulsed power systems to be operated at low earth orbit environment (LEO) that make use of space vacuum as the insulating medium LEO environment is not a perfect vacuum but is actually a low density gas or plasma containing charged particles, ions and electrons, which causes problems in exposed spacecraft components [4 3]

4.2.1 Experimental setup

The circuit diagram of the set up is shown in Fig 4 1 Power frequency ac voltage was supplied by a 5 kV, 50 mA high voltage transformer having an automatic tripping device which disconnects the power supply immediately as the current on the secondary side exceeds 50 mA(rms) In our experiment, this condition was considered to be a breakdown In order to measure the current, a current viewing resistor (CVR) was connected to the lower electrode as shown in the figure

4.2.2 Adjustmentment of pressure

Only the rotary pump was enough to create low vacuum The pressure in the chamber could be adjusted by adjusting the (a) gas inlet valve, (b) roughing valve (c) both After creating a certain level of vacuum in the chamber, all these valves were kept closed Even then an increase in pressure was observed This is due to leakage through the "O" rings placed at different joints of the vacuum

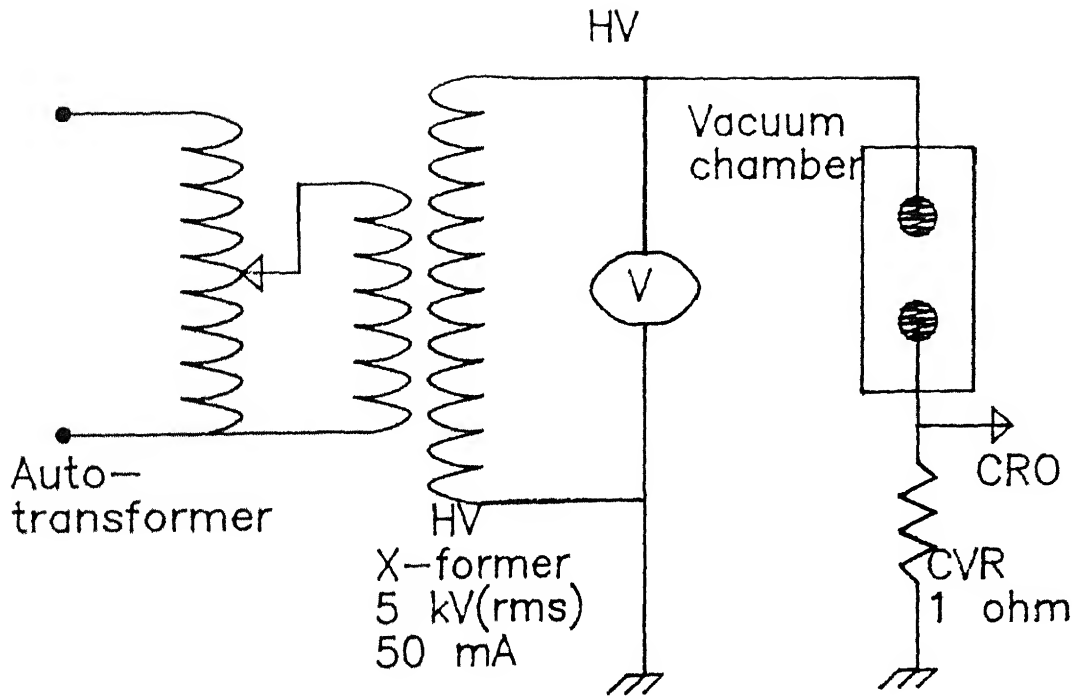

Fig.4.1 Circuit diagram of the set up used for investigation at low vacuum with ac voltage.

pipeline Therefore to obtain a constant pressure level in the chamber, the pump had to be run continuously In order to maintain a particular pressure, the roughing valve was adjusted very cautiously so that inlet through the leakage equaled the outlet through the roughing valve The pressure could be read by a Pirani pressure gauge The meter was calibrated in mbar Reading was taken in mbar and converted to Torr by multiplying with a factor of 0 76 The meter was calibrated from 0 5 mbar to 0 001 mbar However a minimum pressure of 0 005 mbar $\cong$ 3 8x10^{-3} Torr could be achieved in the vacuum chamber by running the rotary pump only

4.2 3 Observations

Voltage was applied from the secondary side of the test transformer and increased slowly by adjusting the variac on the primary Voltage was measured on the secondary side by (a) a moving coil voltmeter for voltage less than 1 kV, (b) an electrostatic voltmeter for voltage more than 1 kV

As the voltage was applied, no current could be measured in the beginning On increasing the voltage gradually a stage reached when the glow appeared The waveshape of current was recorded by the oscilloscope at four different stages, viz, (a) at the starting of the glow, (b) at an advanced stage, (c) at the inception of PD, and (d) at breakdown On further increasing the voltage, the glow became more prominent. Magnitude of current measured increased with the increase of voltage and sharp bright spots were observed which correspond to the sharp spikes on the current waveshape As the voltage was increased further, these sharp spikes increased in number, the glow become more and more bright until breakdown occurred However all

these phenomena occurred with different types of glow and colour at different levels of pressure described in the following A video recording was also made

These experiments were performed with a pair of equal spheres of diameter of 50 mm Electrodes of other shapes and sizes were also investigated, but no appreciable difference on the glow phenomenon was observed due to the change of shape of the electrodes

Case I . Pressure between 0 38 and 0 30 Torr

On applying the voltage no current could be measured before the appearance of the glow On increasing the voltage to 390 volt (ac,peak), glow appeared all of a sudden and the current was measured The current waveshape was a distorted, 50 Hz sine wave (Fig 4 2(a)) The glow could be seen just around the surface of the electrodes, shanks and the two end plates (Fig 4 2(b)) An attempt to increase the voltage caused breakdown The colour of the glow observed was bright violet

Case II : Pressure between $30x10^{-2}$ and $7.6x10^{-2}$ Torr

On increasing the voltage slowly, glow appeared at about 500 volt (ac,peak) As soon as the glow appeared, the voltage came down by 20 - 30 volts The colour of the glow was pink On increasing the voltage, the glow became more bright and extended all over the chamber (Fig 4 3(b)) On further increasing the voltage, bright luminous PD incepted on the lower end plate, which shifted from one spot to other These also caused radio interference, as sensed by a FM radio receiver The number and frequency of appearance of these bright spots were increased on increasing the voltage, causing more noise in the

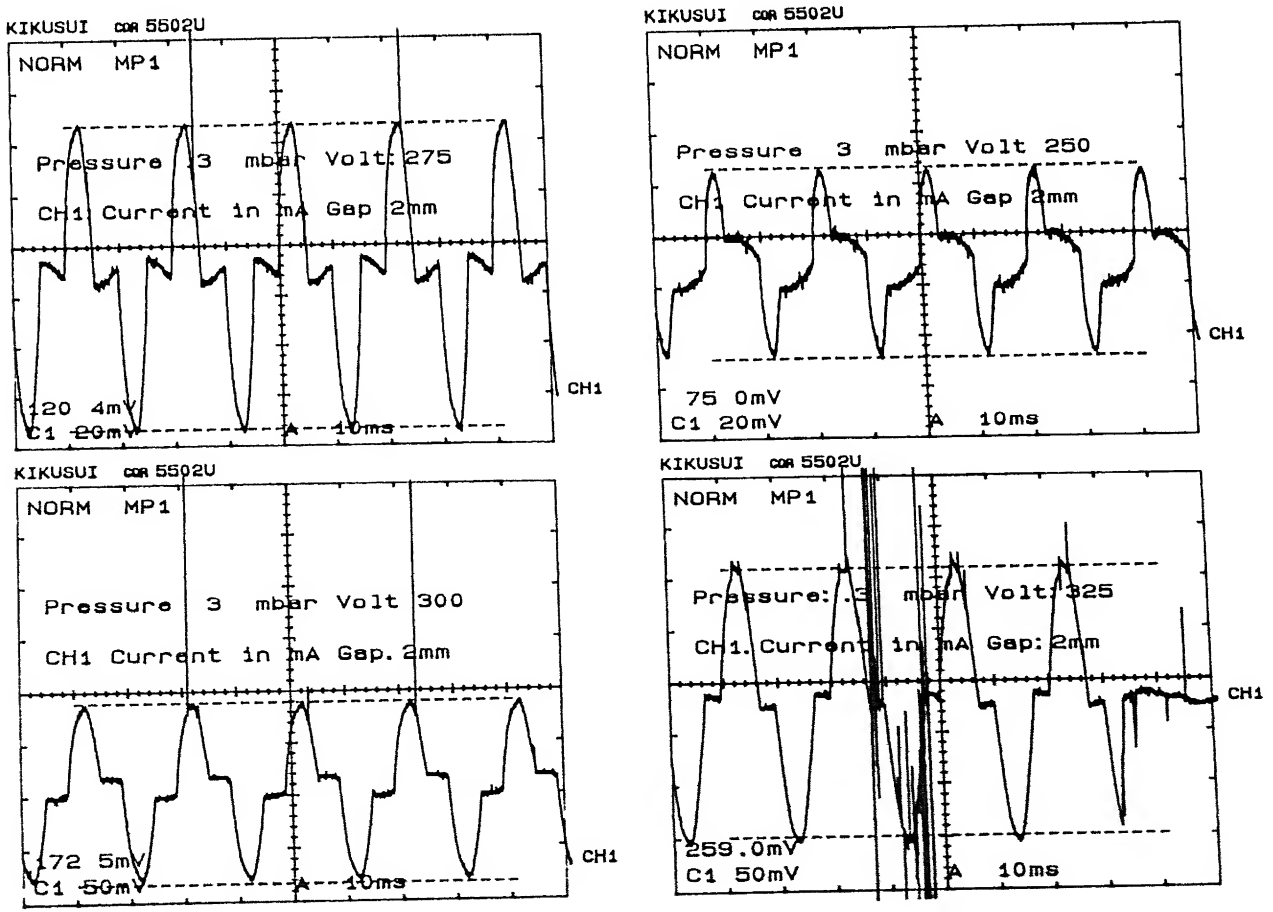

Fig.4.2(a) Oscillogram showing current waveshape for case I

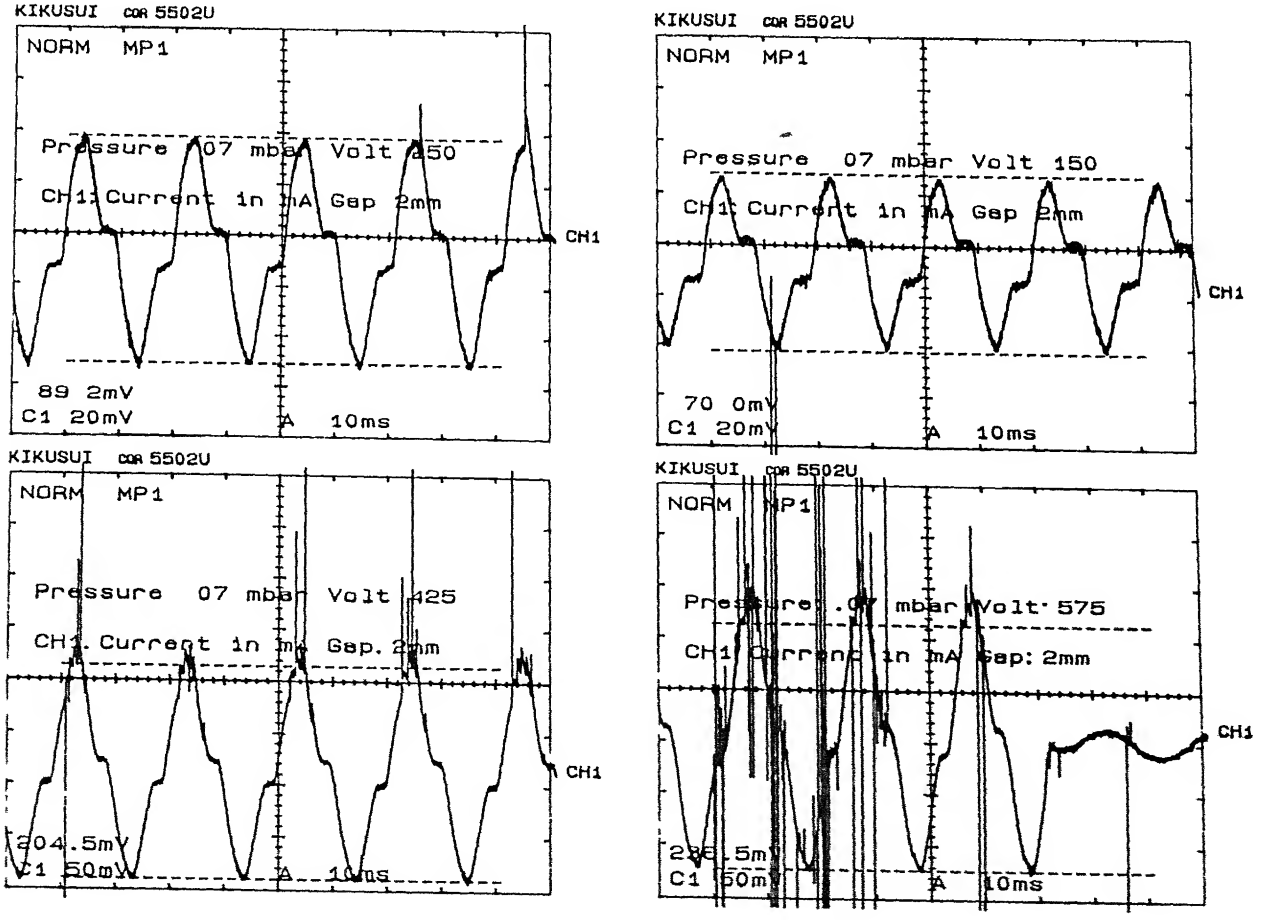

Fig.4.3(a) Oscillogram showing current waveshape for case II

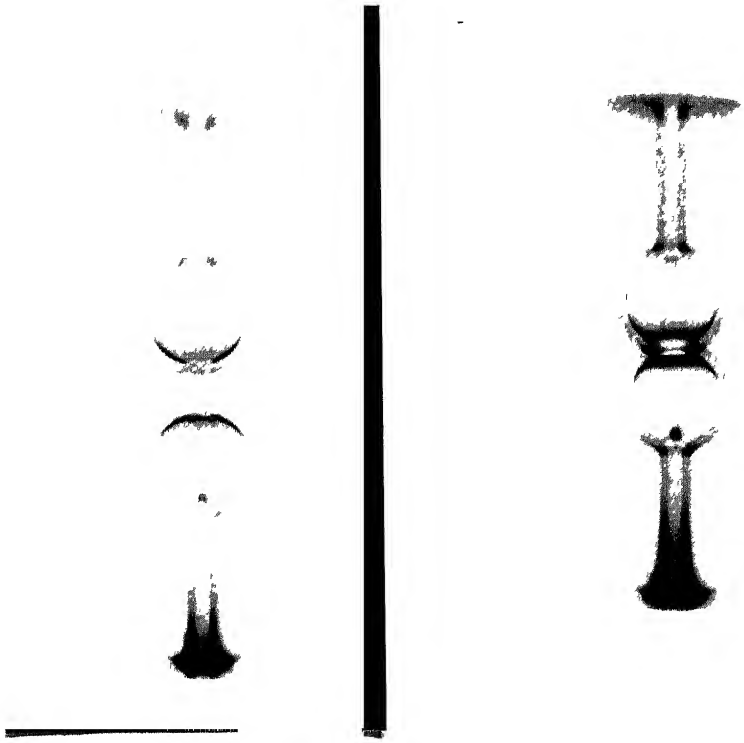

Fig.4.2(b) Photographs showing glow for case I

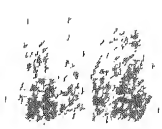

Fig.4.3(b) Photographs showing glow for case II

radio receiver Sharp spikes were observed superimposed on the current waveshape which increased in number towards breakdown (Fig 4 3(a)) Two dark bands could be seen in the chamber, one above the lower end plate and another below the upper end plate

Case III : Pressure between 7 6x10^{-2} and 7.6x10^{-3} Torr

At this pressure range, the inception of glow took place at a lower voltage compared to the breakdown voltage In other words, the glow could be observed in a wider range of applied voltage The intensity of glow was brighter than that in earlier cases (Fig 4 4) Once the glow incepted, on reducing the voltage, the intensity reduced, and two wide dark bands became clearly visible near the two end plates On increasing voltage, these bands narrows down and the glow became prominent, colour of the glow observed was bright pink

Case IV : Pressure between 7 6x10^{-3} and 3 8x10^{-3} Torr

In this pressure range, the colour of the glow changed towards a mixture of white and pink, as the pressure was reduced Glow appeared on all of a sudden as the voltage was increased slowly and breakdown occurred at a voltage closer to the voltage at which the glow was incepted, that is, the range of voltage in which the glow could be observed was small. The dark bands were comparatively less dark At pressure 3 8x10^{-3} Torr, the colour became almost white and the bands disappeared (Fig.4 5(b)) This was the lowest pressure which could be achieved by running the rotary pump alone The breakdown voltage increased rapidly with further decrease in the pressure, i e , with the increase of vacuum

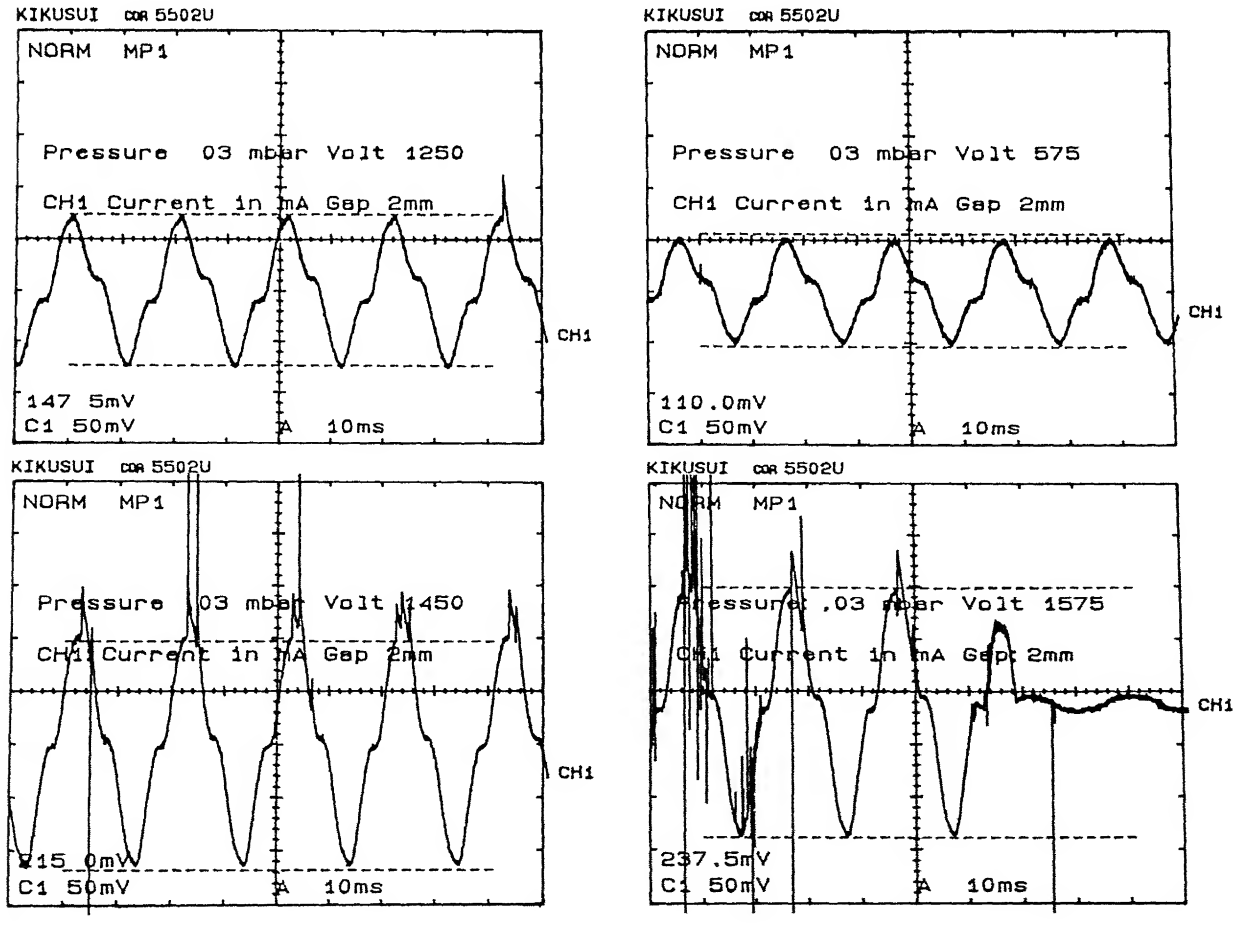

Fig.4.4(a) Oscillogram showing current waveshape for case III

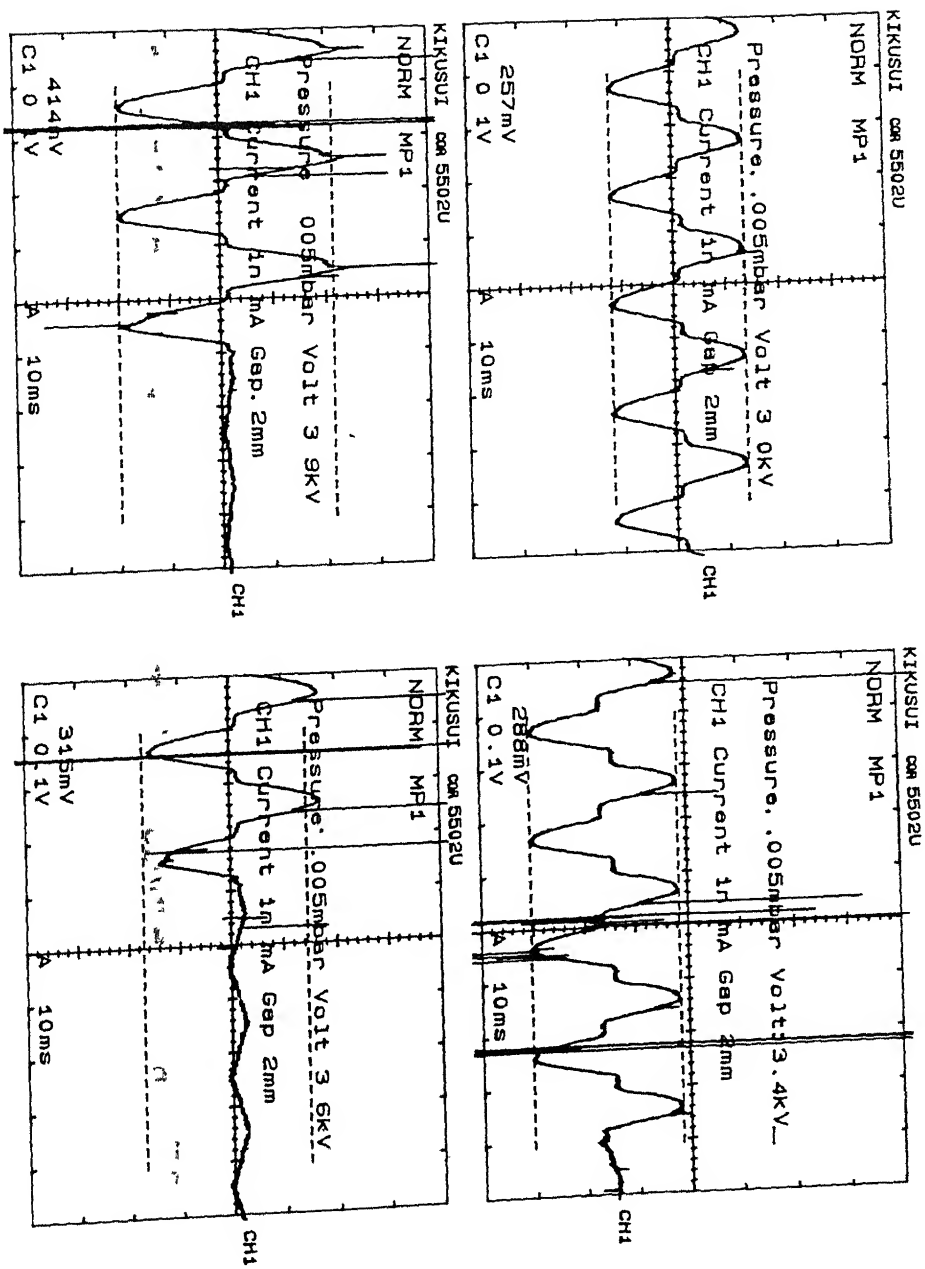

Fig.4.5(a) Oscillogram showing current waveshape for case IV

Fig.4.4(b) Photographs showing glow for case III

Fig.4.5(b) Photographs showing glow for case IV

4 2.4 Measurement of conduction current with increasing voltage

The variation of conduction current as a function of applied voltage at different pressures is shown in Fig 4 6 The first measurement was performed at a pressure of 0 34 Torr (curve A) As the pressure decreased to 31 Torr, both the glow inception and breakdown voltage decreased (curve B) But both these voltages started increasing as the pressure was continued to be decreased (curves C,D,E etc) It could be observed that the current increased sharply with applied voltage at comparatively higher pressures and the glow inception voltage was nearly equal to the breakdown voltage (curves A-E) at these pressures But at lower pressure the conduction current increased slowly with the applied voltage and the breakdown voltage was much greater than the glow inception voltage (curves H to P). Towards the end of the low vacuum range, i e , at the transition from low vacuum to high vacuum, both the glow inception and breakdown voltages increased sharply as the pressure was decreased (curves O and P in Fig 4.6)

Although these experiments were performed at a fixed gap distance of 2 mm, gap distance could be changed upto 10 mm No appreciable difference in breakdown voltage were observed on changing the gap distance This is because, the electrical conductivity of the gas under these conditions becomes so high that a very small voltage was adequate to set up a current in the gap which was practically independent of gap length

The glow could be observed over a wider range of voltage for pressure range between 3 $1x10^{-2}$ and 3 $8x10^{-3}$ Torr At pressure above and below this range, the glow could be observed over a narrow range of voltage. In other word, the glow inception voltage and the

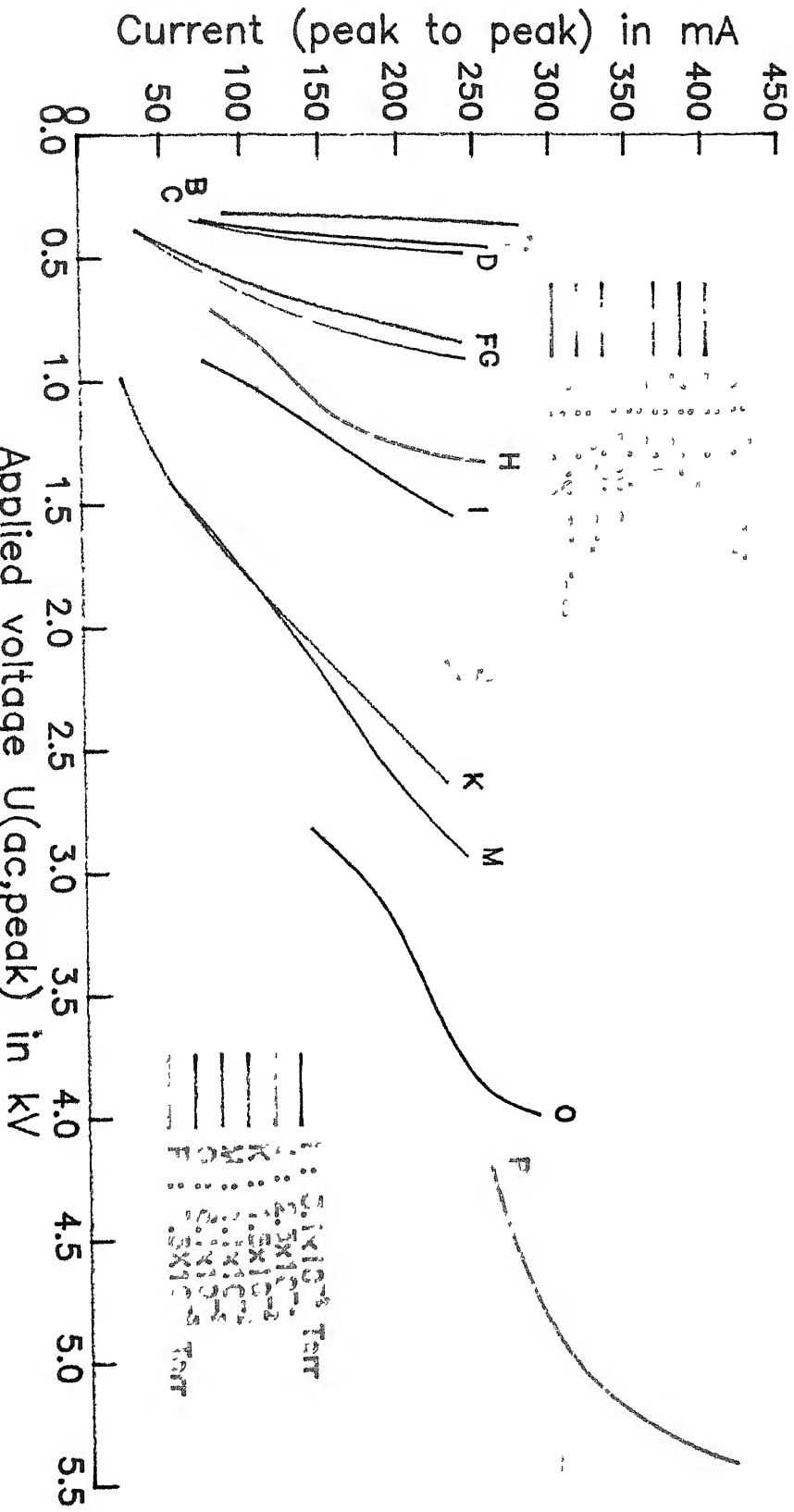

Fig.4.6 Variation of conduction current as a function of applied voltage at different pressures within low vacuum.

breakdown voltage were almost the same under this condition

4 2.5 pd versus Breakdown voltage

The breakdown voltage was measured at different pressures ranging from just below atmospheric pressure to 0 005 mbar ≅ 3 8x10^{-3} Torr The gap distance was kept constant at 2 mm Total four pairs of spheres of diameters 25, 30, 40 and 50 mm were used for the investigation The results obtained have been plotted taking pd (pressure in Torr x Gap distance in mm) on X-axis and breakdown voltage U_b (ac,peak) in kV on Y-axis as shown in Fig 4 7

It can be seen from this plot that at a pressure, just below atmospheric, the breakdown voltage increases sharply with the increase in pd As the pressure decreases, the breakdown voltage also decreases but remains almost constant at about 450 volts in the pd range of 0 25 to 1 3 Torr-mm. At lesser pressures, pd less than 0 25 Torr-mm, the breakdown voltage again increases rapidly

This is because at low pressure, the density of the molecules decreases, consequently the probability of an electron making collisions with the molecules goes down as it travels in the gap of the electrodes. Since each collision results in loss of energy, a lower electric field intensity, hence a lower voltage suffices to provide electrons the kinetic energy required for ionization by collision to achieve a breakdown When the minimum of the breakdown voltage is reached and the pressure still continues to decrease, the density of gas becomes so low that relatively fewer collisions occur Under such conditions, an electron may not necessarily ionize a molecule on colliding with it, even if the kinetic energy of the electron is more than the energy required for ionization The

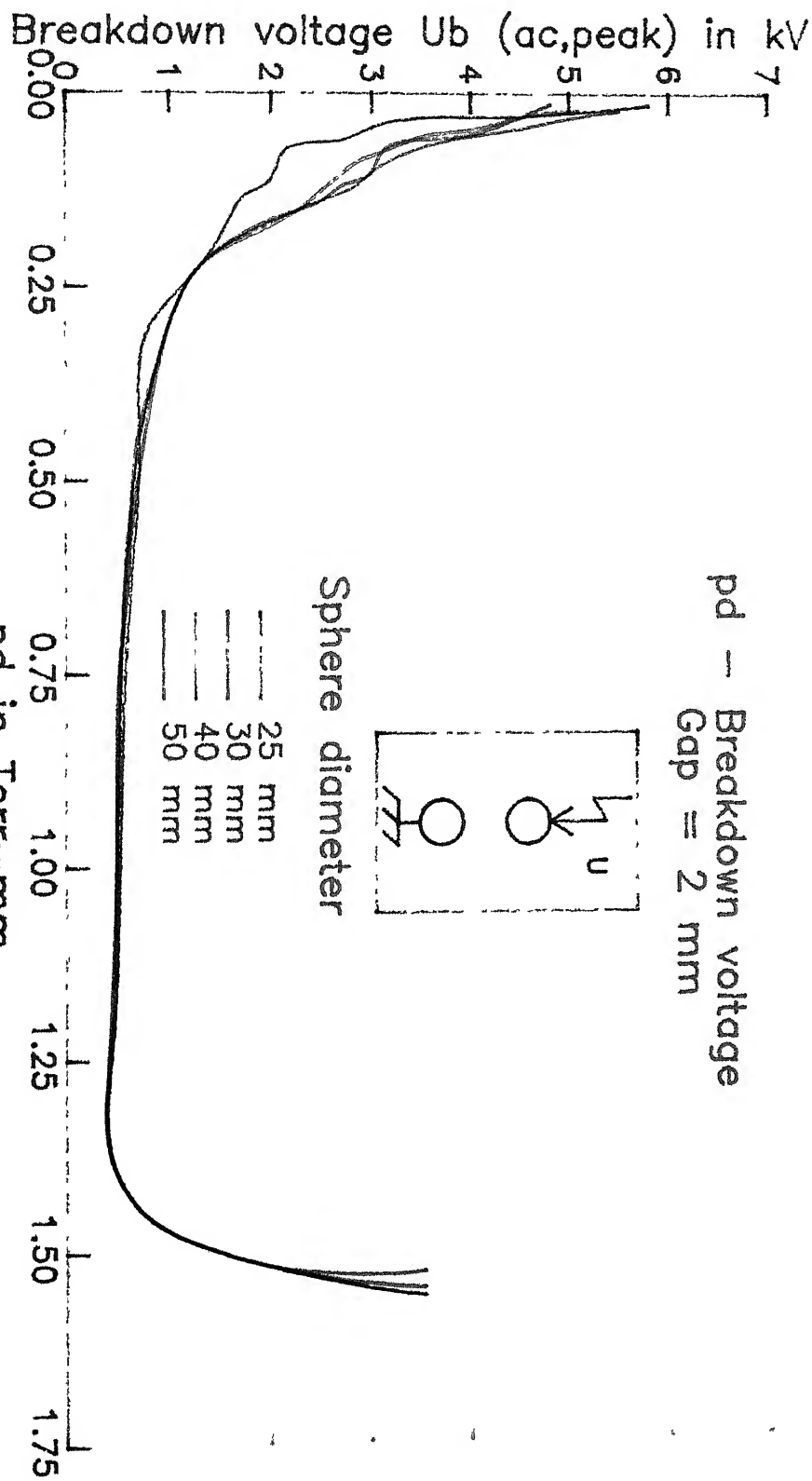

Fig.4.7 Variation of breakdown voltage with pd

breakdown can occur only if the probability of ionization becomes greater by increasing the field intensity, i e by increasing the applied voltage

4 3 Investigation at high vacuum

The insulating property and the behavior of high vacuum as electrical insulation is different from those of low vacuum The breakdown strength is much higher and this property is extensively utilized in high voltage apparatus Large amount of research already has been done on high vacuum Although considerable amount of experimental work has been performed investigating the breakdown strength of vacuum, no attempt has yet been made to investigate the breakdown strength of vacuum with respect to the degree of uniformity of the field. In this work an attempt has been made to establish a relationship between the degree of uniformity, η and breakdown strength at different pressures and gap distances

4.3.1 Electrodes used for investigation

It was desired to investigate the breakdown strength for a particular gap distance but having different degree of uniformity at different levels of vacuum Therefore a number of electrodes having different shapes and sizes were prepared Total five different pairs of electrodes were chosen for this investigation They are -

a) SPSP50 Sphere-Sphere, diameter 50 mm

b) SP50PL Sphere-Plane, sphere diameter 50mm, plane diameter of 85 mm, edge rounded with a radius of 5 mm

c) SP25PL : Sphere-Plane, sphere diameter 25 mm, plane dimension as above.

d) RODPL Rod-Plane, tip diameter of rod 18 5 mm, plane dimension as above

e) PLPL PLane-PLane, dimension as above

The dimension and materials of the shanks used to hold the electrodes in position and the method of electrode preparation for experiment is discussed in Chapter 3

4 3 2 Experimental procedure

The circuit diagram of the set up is shown in Fig 4 8 Voltage was applied from the secondary side of the test transformer Although the voltage rating of the transformer was 100 kV, only upto 50 kV could be supplied This is because at the event of breakdown at higher voltages, very high current flows in the primary circuit, which caused frequent tripping of the circuit breaker in the substation Moreover it was also noticed that, at the event of breakdown at higher voltages (more than 40 kV), sparking took place between different metallic parts of the vacuum pump, which caused damage of some components, as discussed in Chapter 3

Due to these constraints, the maximum gap distance was limited to 3 mm only The gap distance was adjusted at an interval of 0 5 mm The experiments were performed at three different pressures, viz, 10^{-3}, 10^{-4} and 10^{-5} mbar, by adjusting the heater voltage of the diffusion pump (Chapter 3) The dial of the pressure gauge was directly graduated in mbar, so readings were taken in mbar and then it was converted to Torr by multiplying with a factor 0 76

4.3.3 Experimental results

The breakdown voltages were measured at different gap distances

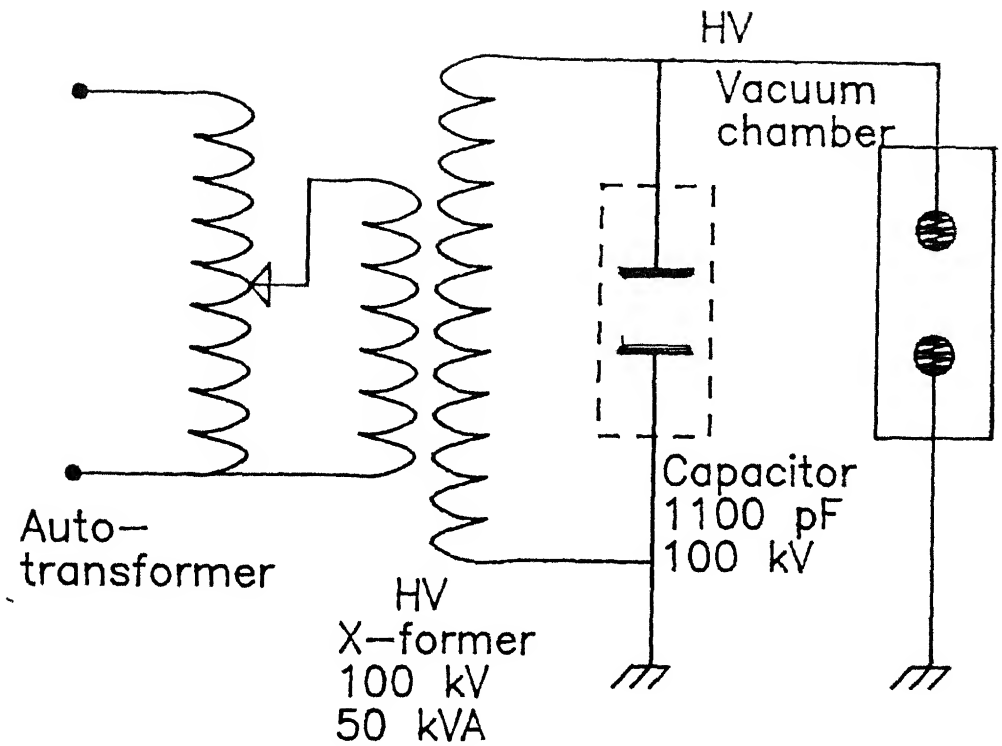

Fig.4.8 Circuit diagram of the setup used for investigation at high vacuum with ac voltage.

under different levels of vacuum It was observed that even if the pressure and gap distance were kept constant, different readings of breakdown voltage were obtained, when voltage was applied successively Minimum four and maximum seven readings were taken for a particular gap and pressure setting In some cases, sparking was observed in the space between the electrodes when the voltage was increased gradually which did not cause breakdown On increasing the voltage further, breakdown occurred at a higher voltage A typical plot of the distribution of sparking voltage along with the breakdown voltage is shown in Fig 4 9 for RODPL and SPSP50 electrodes

The measured results were plotted to obtain four sets of curves for each electrode pair, viz, (i) Breakdown voltage U_b versus gap distance, (ii) Breakdown strength E_{bmax} versus gap distance, (iii) Breakdown voltage U_b versus pressure, and (iv) Breakdown strength E_{bmax} versus pressure. The graphs are shown in Fig 4 10(a-d), 4 11(a-d), 4 12(a-d), 4 13(a-d) and 4 14(a-d) for SPSP50, PLPL, SP50PL, SP25PL and RODPL respectively

From these figures, it can be seen that the breakdown voltage increases whereas the breakdown strength decreases with the increase in gap distance in high vacuum. Both the U_b and E_{bmax} increase as the vacuum level is increased from low vacuum to high vacuum upto 10^{-4} Torr beyond which no appreciable increase was measured Rather U_b and E_{bmax} decreased slightly after attaining the maximum value in the pressure range of $5x10^{-4}$ to 10^{-4} Torr The breakdown strength is high in case of smaller gap distances compared to that for longer gaps

Different discharge phenomena were observed in the gap for each electrode system In almost all cases, sparking was observed somewhere in the gap before breakdown which was bluish in colour and was

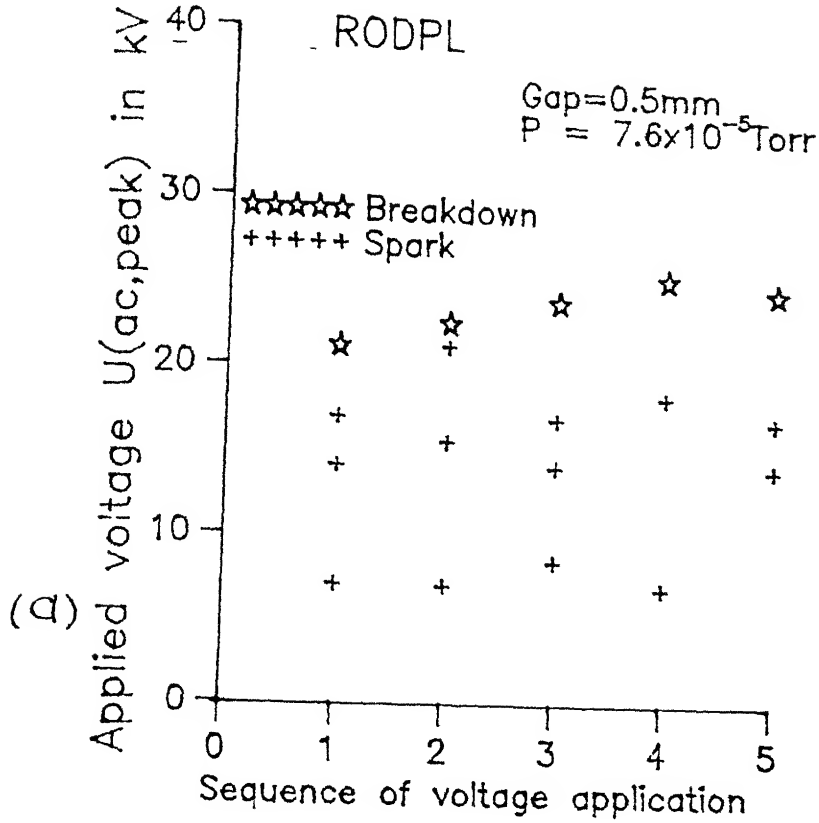

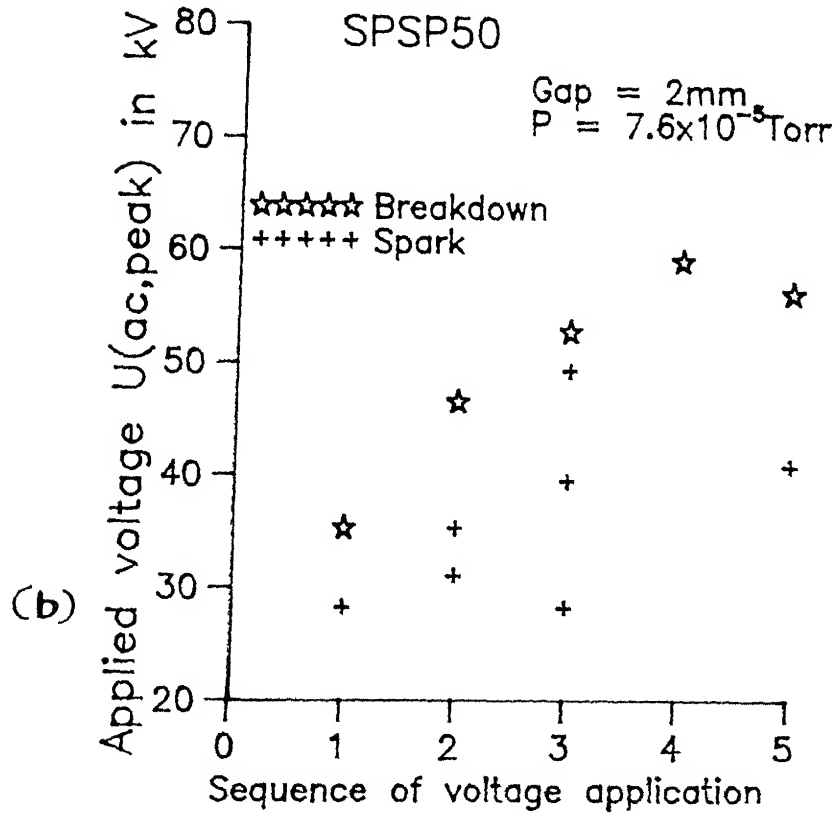

Fig.4.9 Distribution of sparking and breakdown voltage; (a)RODPL (b) SPSP50 electrode.

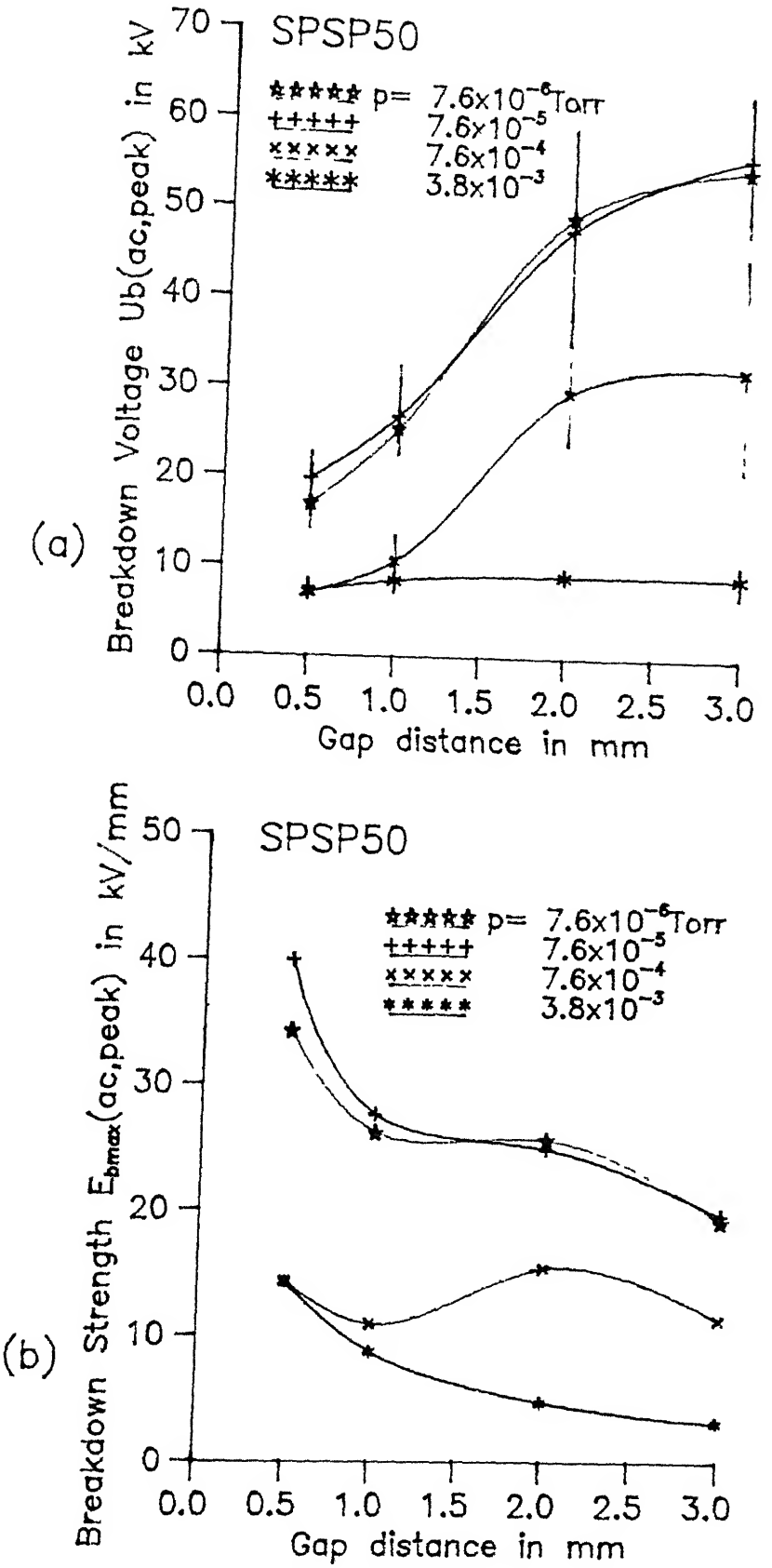

Fig.4.10 Variation of breakdown (a) voltage (b) strength with gap distance.

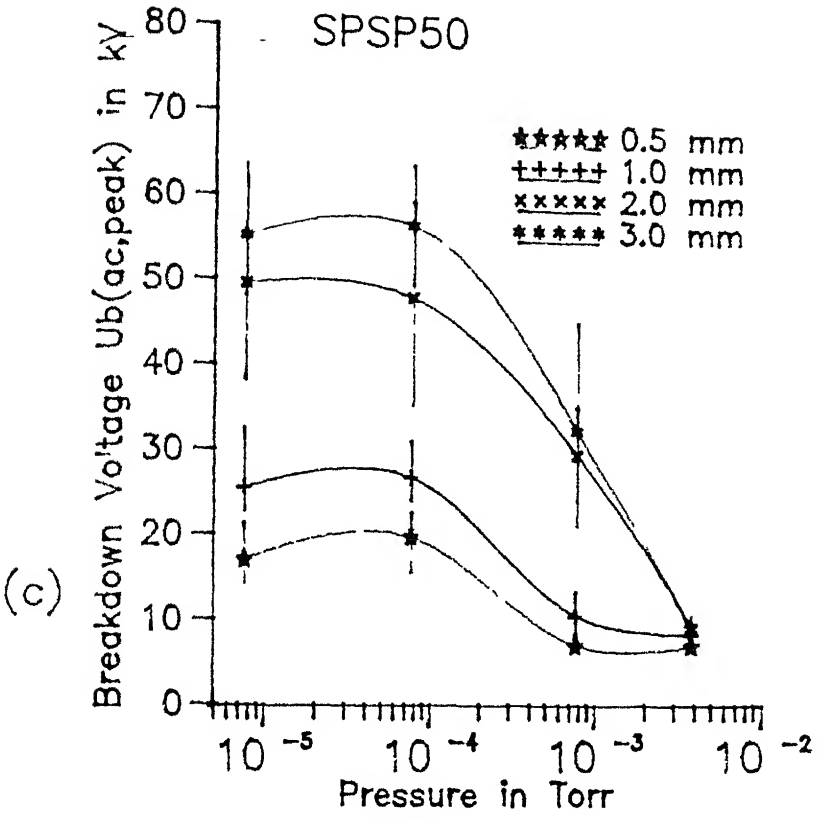

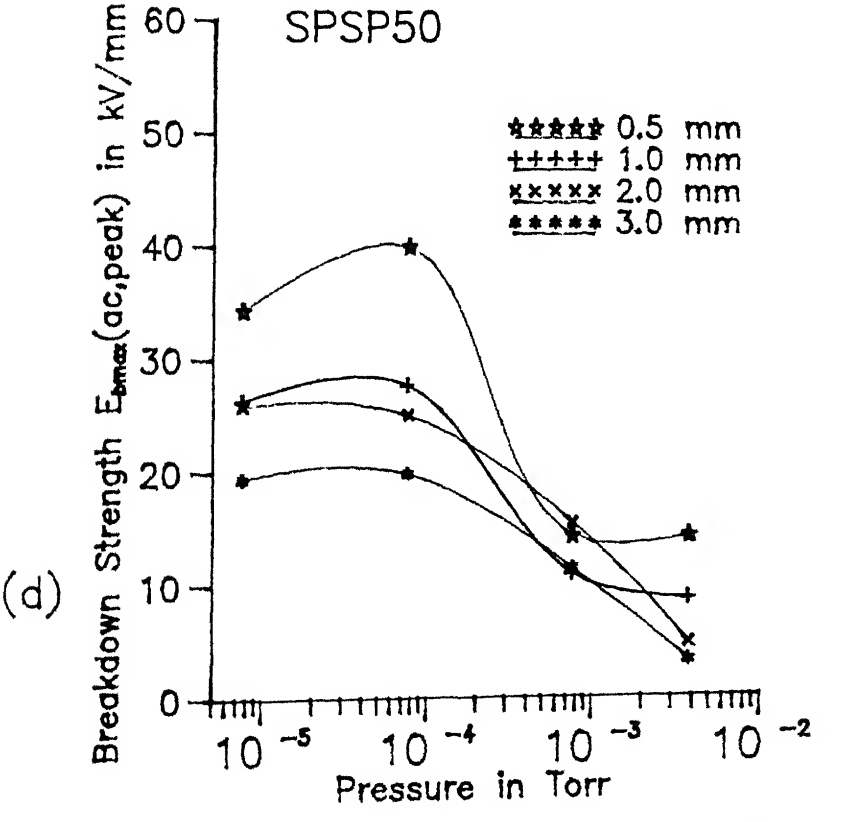

Fig.4.10 Variation of breakdown (c) voltage (d) strength with pressure for different gap distances

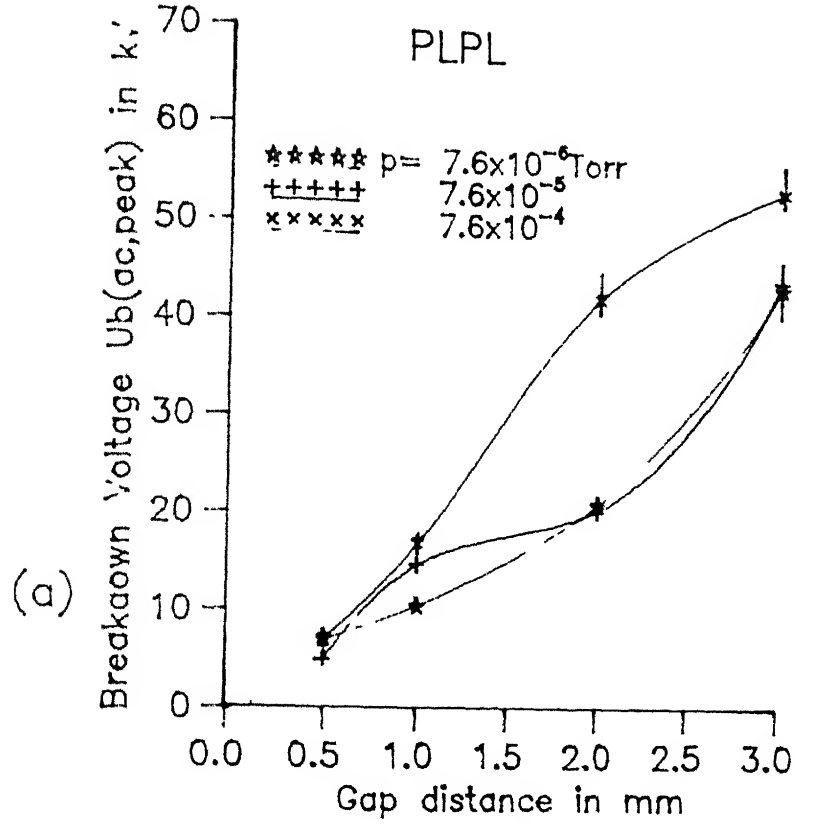

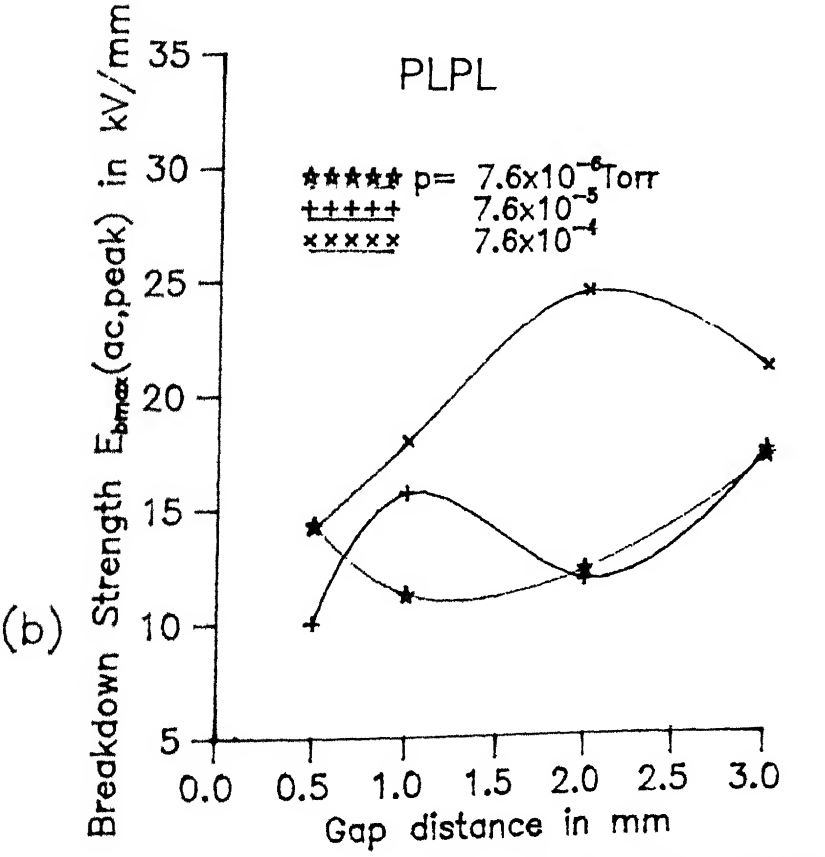

Fig.4.11 Variation of breakdown (a) voltage (b) strength with gap distance.

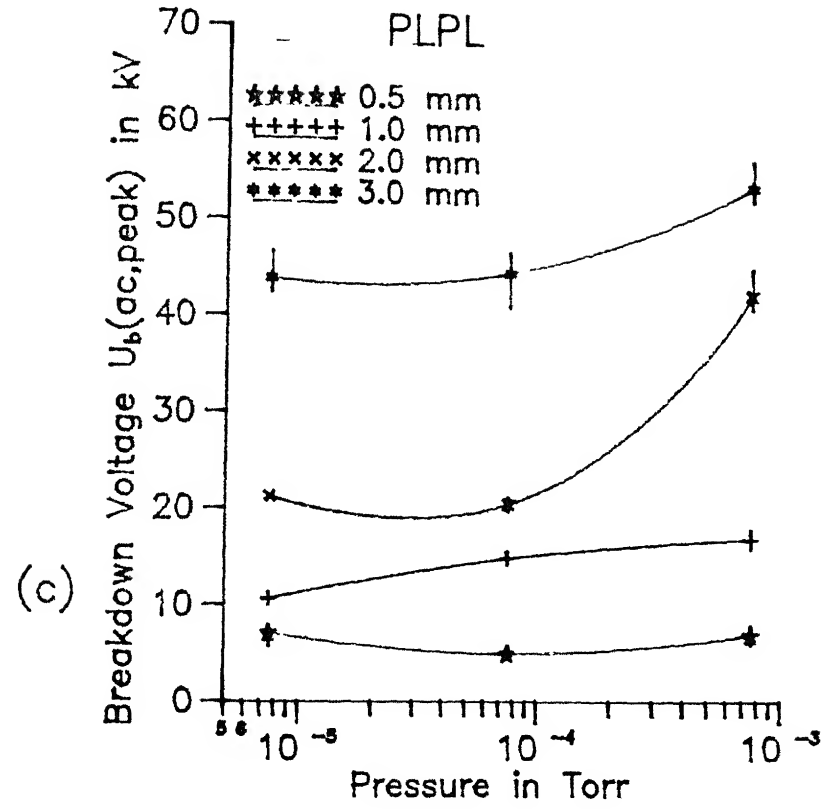

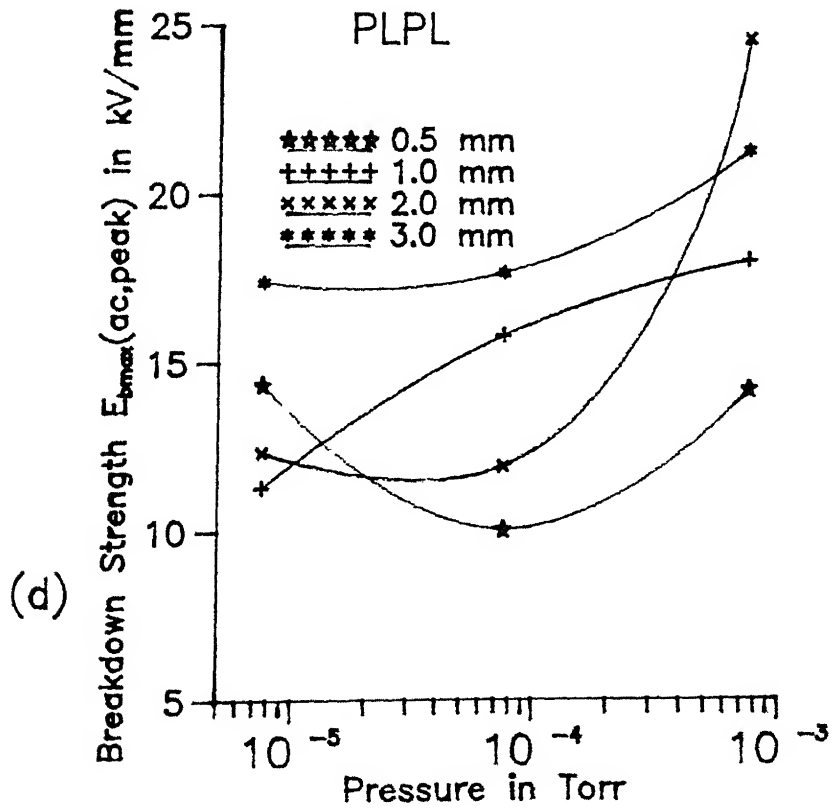

Fig.4.11 Variation of breakdown (c) voltage (d) strength with pressure for different gap distances.

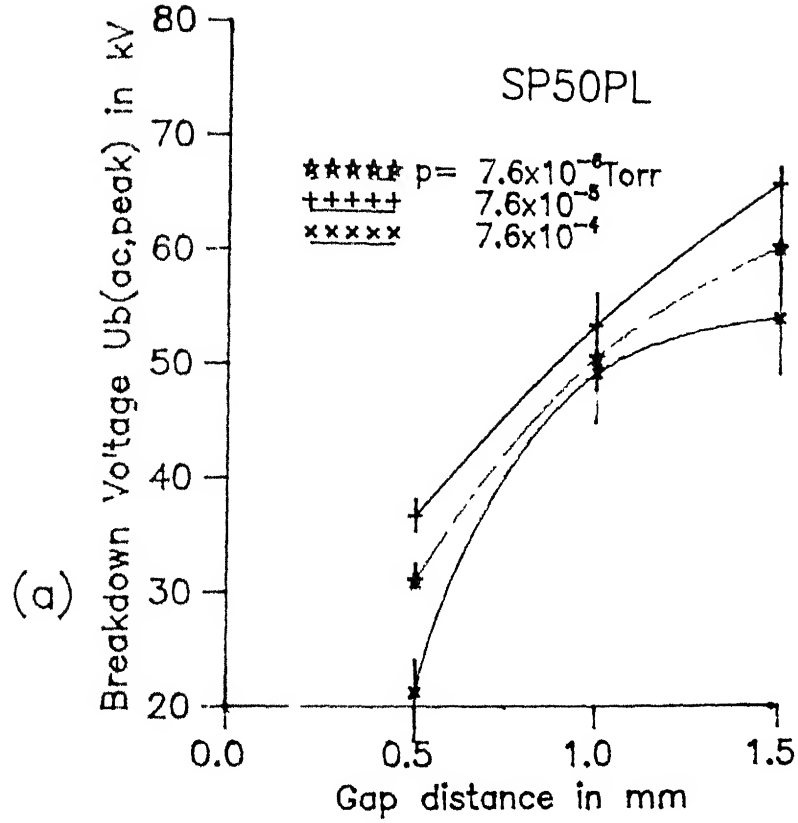

(a)

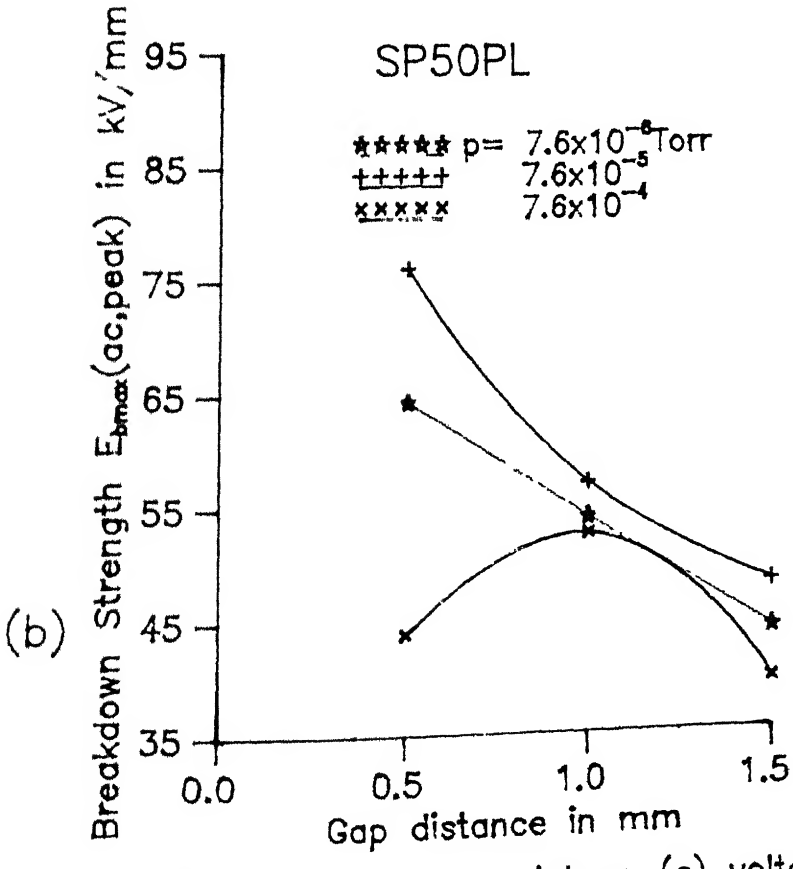

(b)

Fig.4.12 Variation of breakdown (a) voltage (b) strength with gap distance.

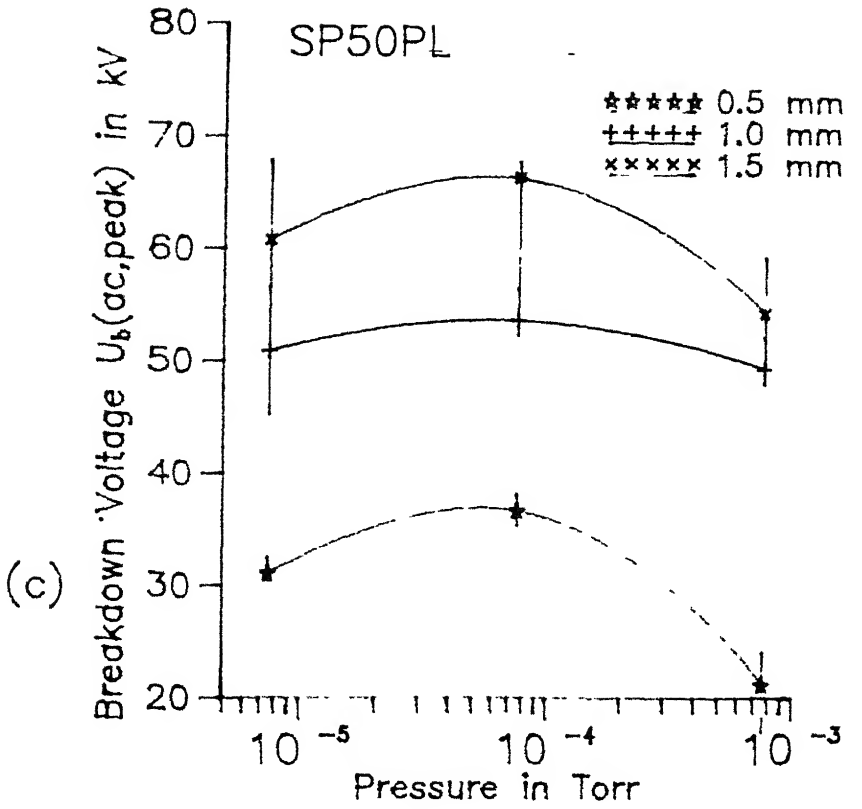

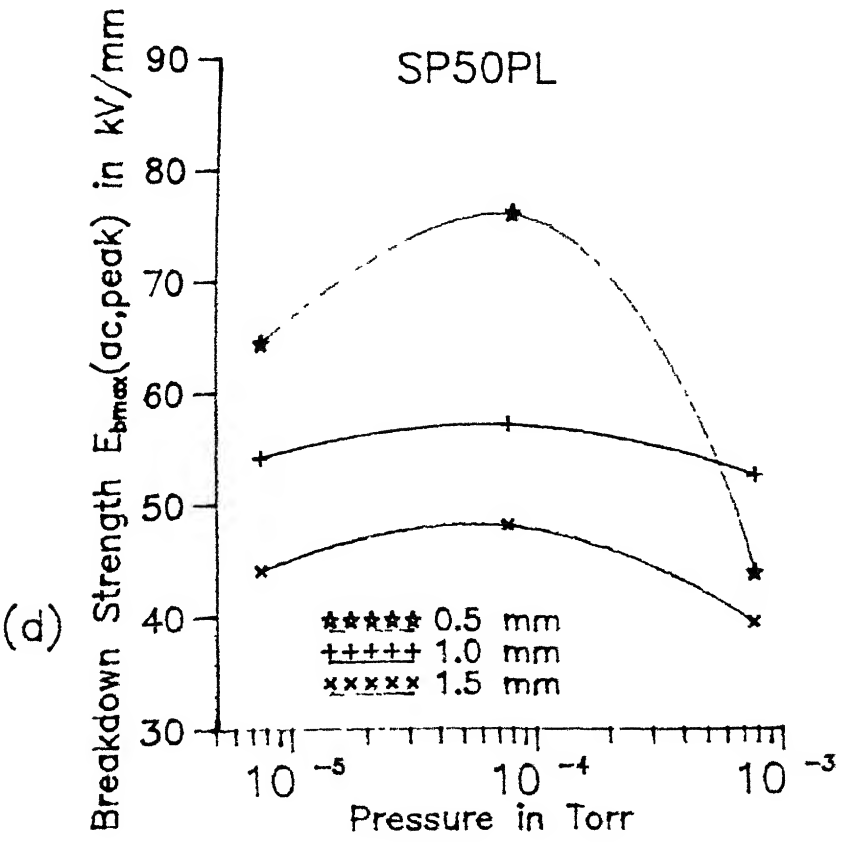

Fig.4.12 Variation of breakdown (c) voltage (d) strength with pressure for different gap distances.

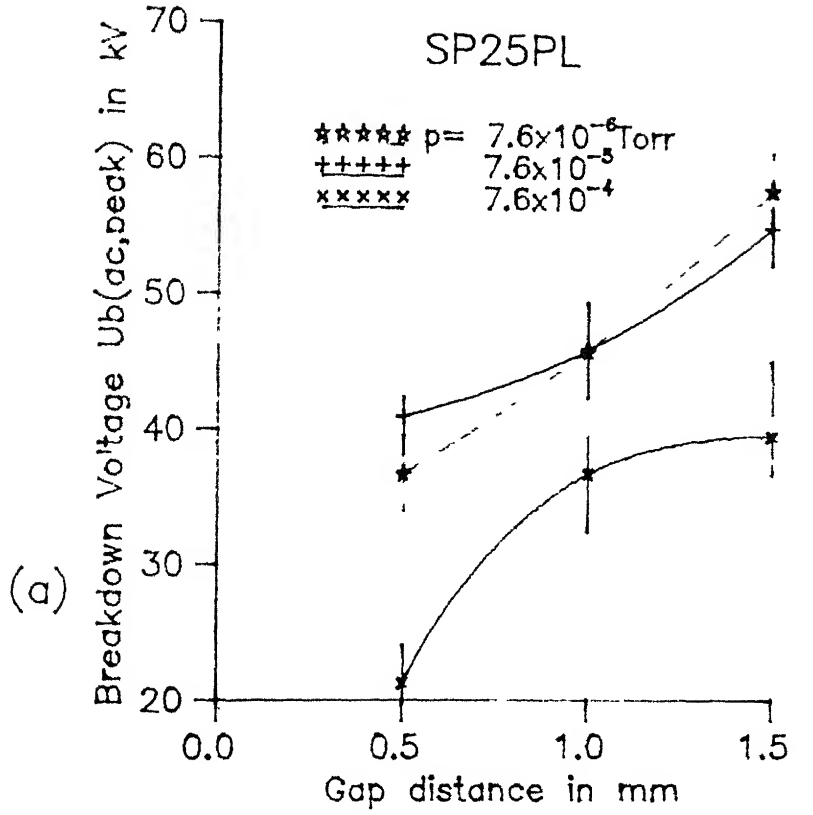

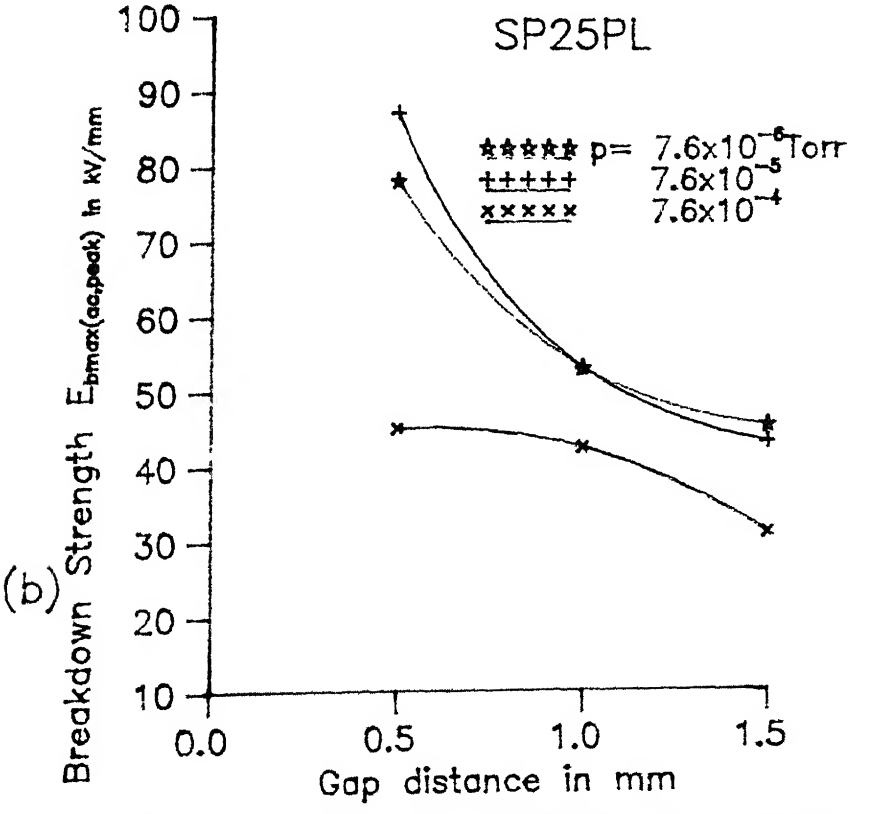

Fig.4.13 Variation of breakdown (a) voltage (b) strength with gap distance.

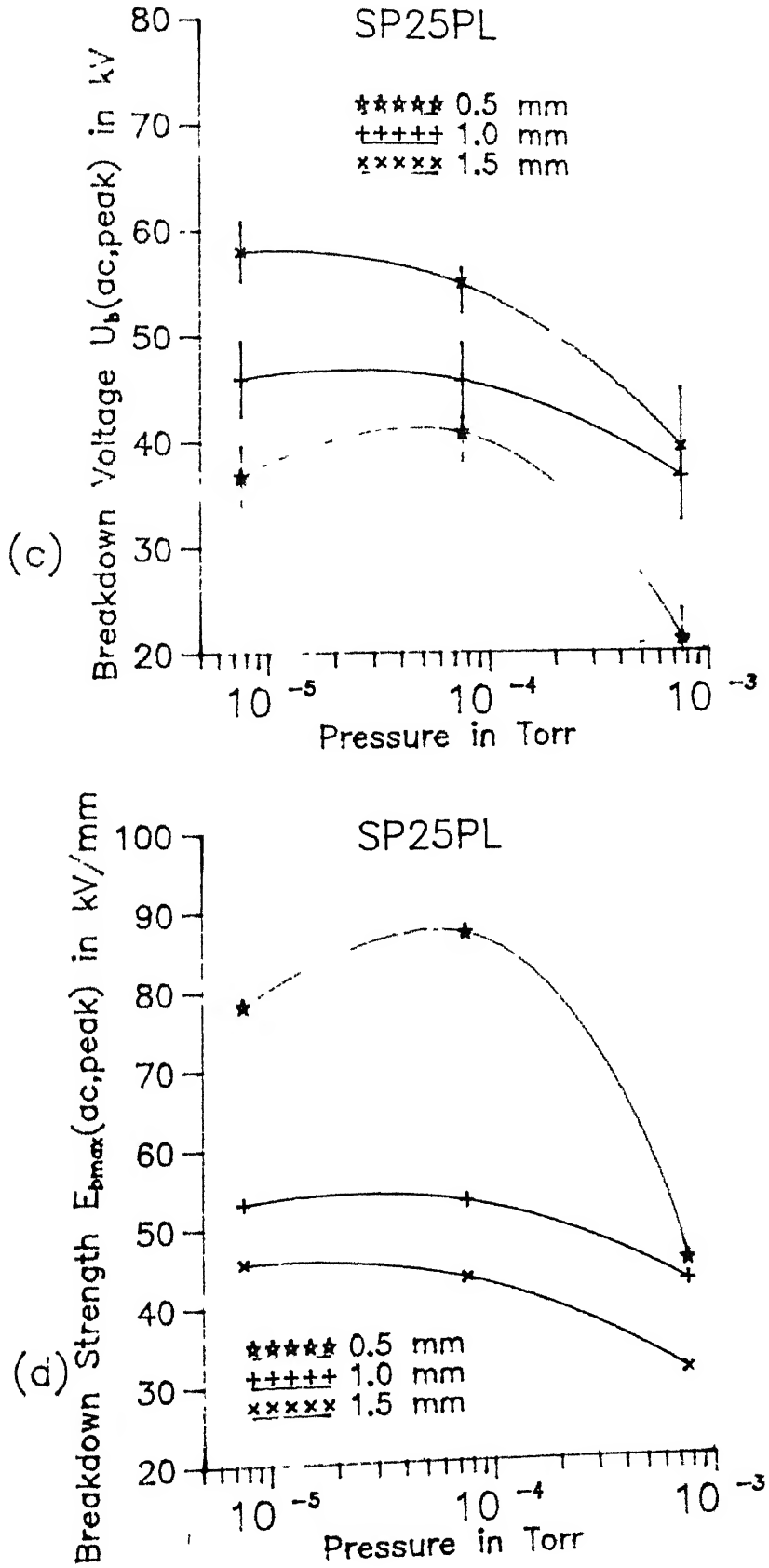

Fig.4.13 Variation of breakdown (c) voltage (d) strength with pressure for different gap distances.

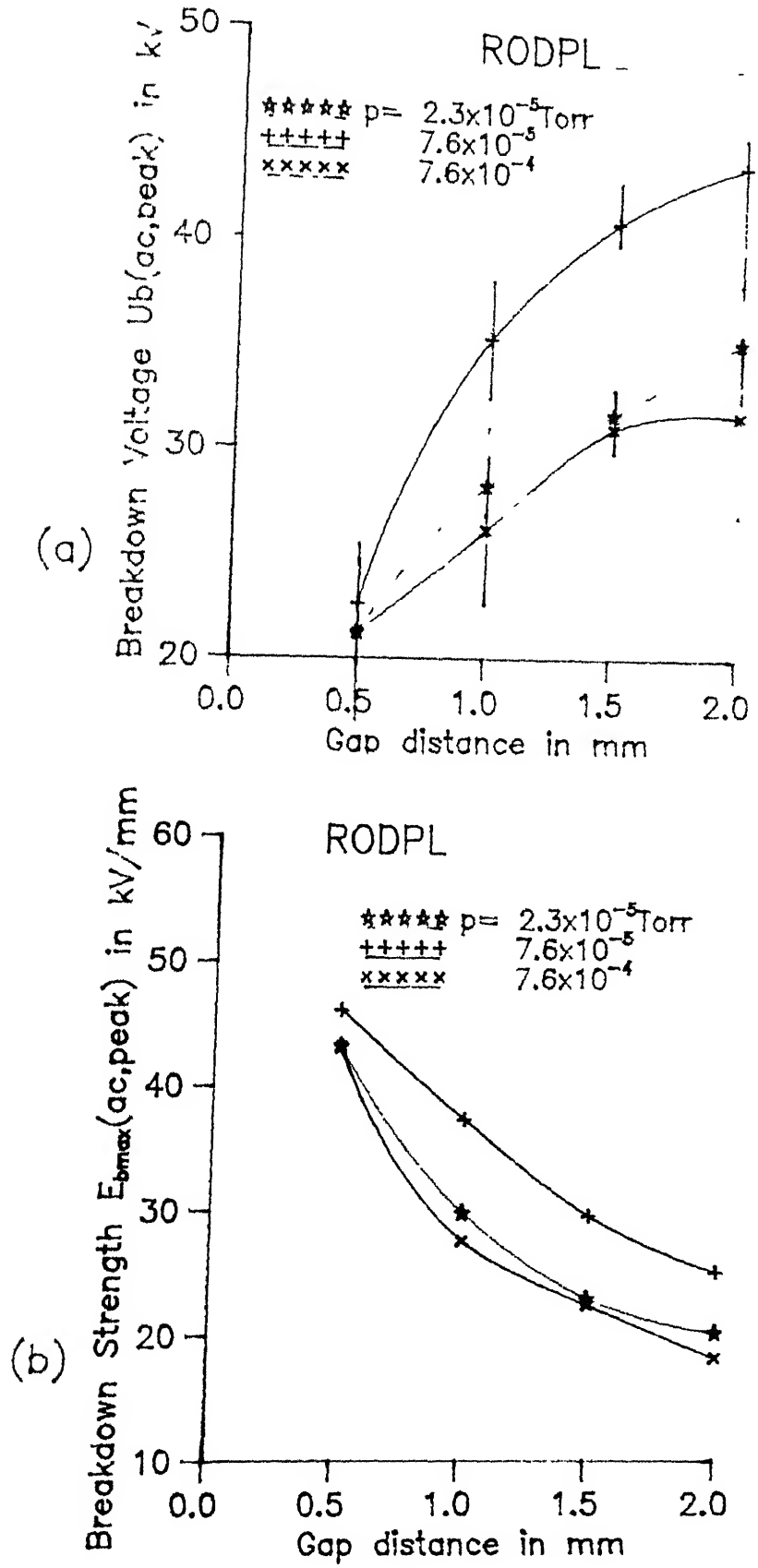

Fig.4.14 Variation of breakdown (a) voltage (b) strength with gap distance.

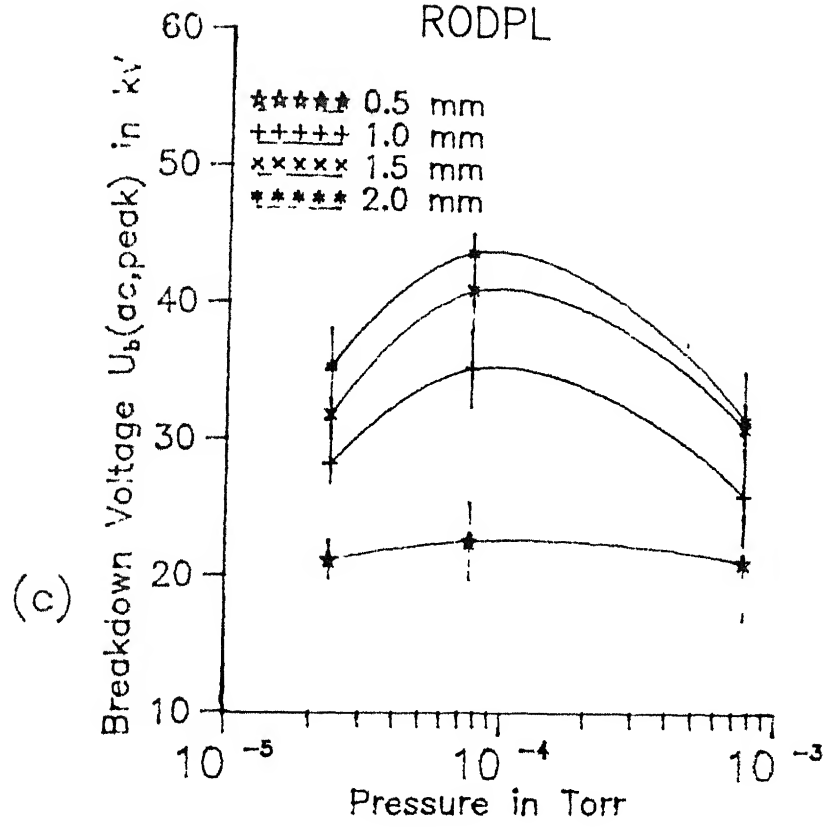

(c)

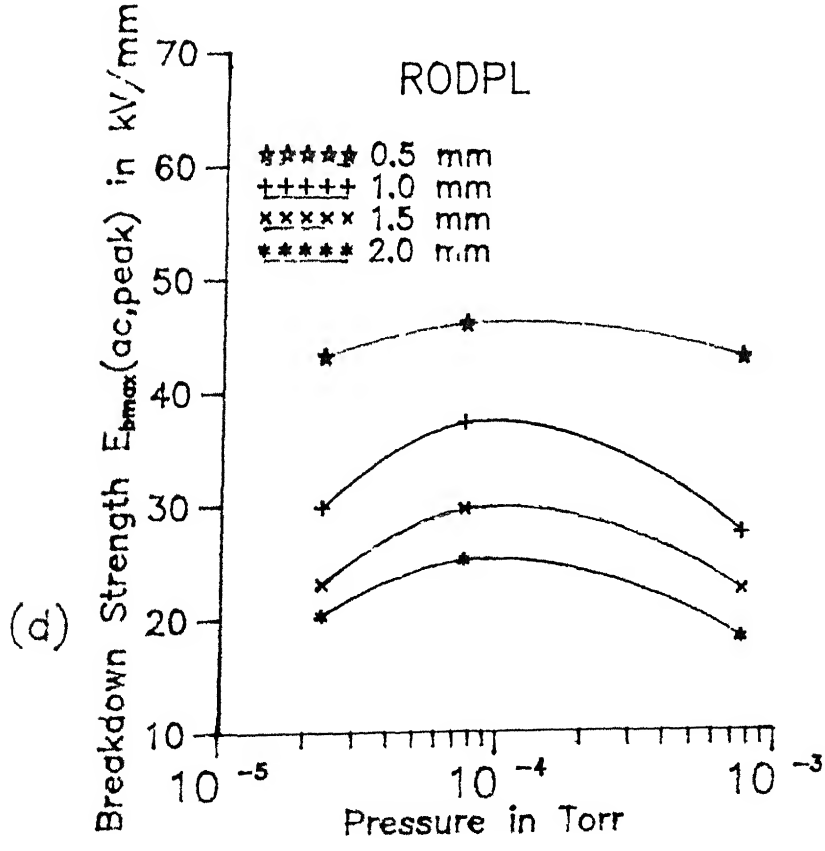

(d)

Fig.4.14 Variation of breakdown (c) voltage (d) strength with pressure for different gap distances.

concentrated at some particular points in the space But breakdown occurred with blue discharge bridging the gap In case of SPSP50, during breakdown, discharge was mostly concentrated along the shortest distance between the electrodes and covering a portion of the space surrounding the main breakdown channel as shown in the sketch (Fig 4 15) In case of PLPL, the discharge was scattered along the gap and spread over the electrode surface and was also extended towards the edges But with SP25PL and SP50PL, the main breakdown channel in the center was surrounded by a conical extension towards the plane electrodes For RODPL, some different phenomena was observed The discharge was in the shortest gap with an extension over the surface of the rod and its extension

At longer gap distances, for which the breakdown voltage was also high, the discharge was expanded more in the volume surrounding the gap and sometimes it was extended upto the wall of the glass vessel, specially in case of PLPL and RODPL At this stage it was noticed that, first a milky-white discharge originated in the space between the electrode and the glass vessel which was followed by a bluish discharge at the central zone and breakdown occurred eventually. Under this condition breakdown voltage did not increase even if the gap distance was increased

4.4 Comparison of breakdown strength of different electrode pairs

The shape and sizes of the electrodes used for the experiments were chosen such that for a particular gap distance, different degree of uniformity, η could be obtained For a particular electrode system, η varies with gap distance The variation of η with gap distance for all the electrodes has been estimated with the help of CSM (Chapter

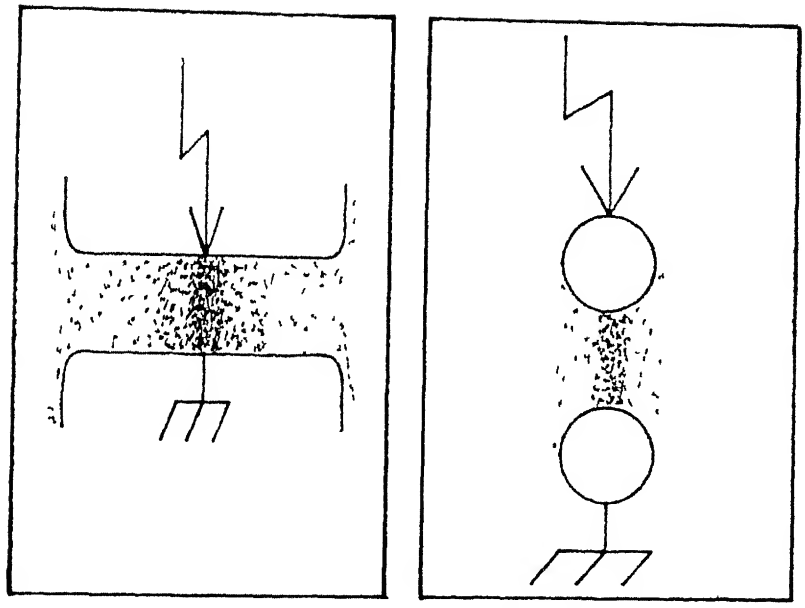

PLPL

SPSP50

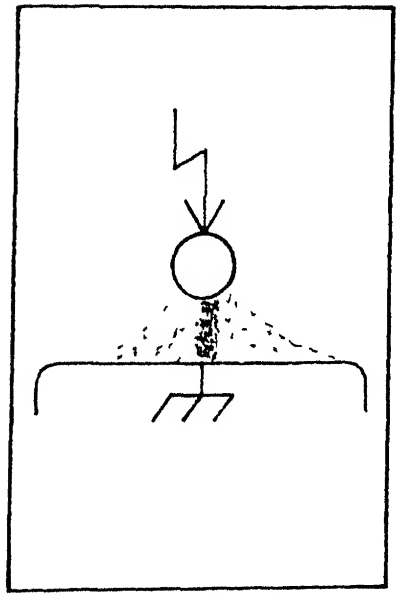

SP50PL

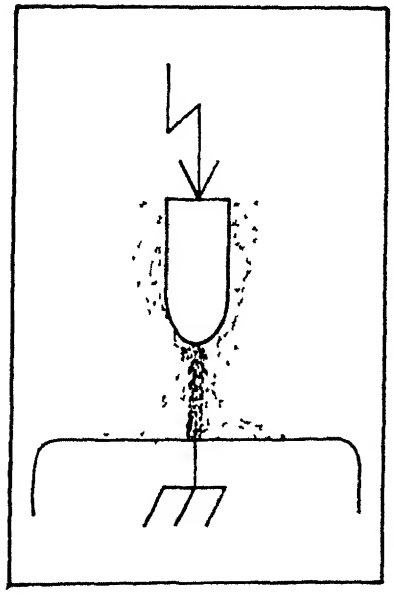

RODPL

Fig.4.15 Discharge following breakdown at high vacuum for different electrodes.

2) The variation of breakdown voltage and breakdown strength along with the variation of η with gap distance have been shown in Fig 4 16 to 4 20 for SPSP50, RODPL, SP50PL, SP25PL and PLPL electrodes respectively It can be seen from all these figures that E_{bmax} has a decreasing trend with decreasing values of η except in the case of PLPL electrode The decreasing trend of E_{bmax} is observed to saturate as the gap distance is increasing, i,e, the value of η is decreasing The values of E_{bmax} and η for a particular gap distance could be obtained from these figures

These types of curves have immense practical importance because a practical system may have different shapes and sizes of electrodes leading to different values of η although the gap distance may be same Therefore the breakdown strength at different parts of the system may be different

Because of different constraints of the set up, the gap distance could not be increased more than 3 mm during the experiment Therefore, the investigation was limited within weakly nonuniform field with values of η closer to unity For such a small gap distance, different factors such as surface roughness, inaccuracy of setting gap distances etc became more dominant and affect the breakdown strength more than the effect of η In case of PLPL, the gas molecules desorbed from the electrode surfaces could not diffuse in the volume of the vacuum chamber Therefore they could not be evacuated by the diffusion pump which caused local pressure rise in the gap between the electrodes This is responsible for lowest measured breakdown voltage and breakdown strength for PLPL electrode A better understanding of variation of E_{bmax} with respect to η could have been obtained if the investigation could be performed over a wide range of η starting from

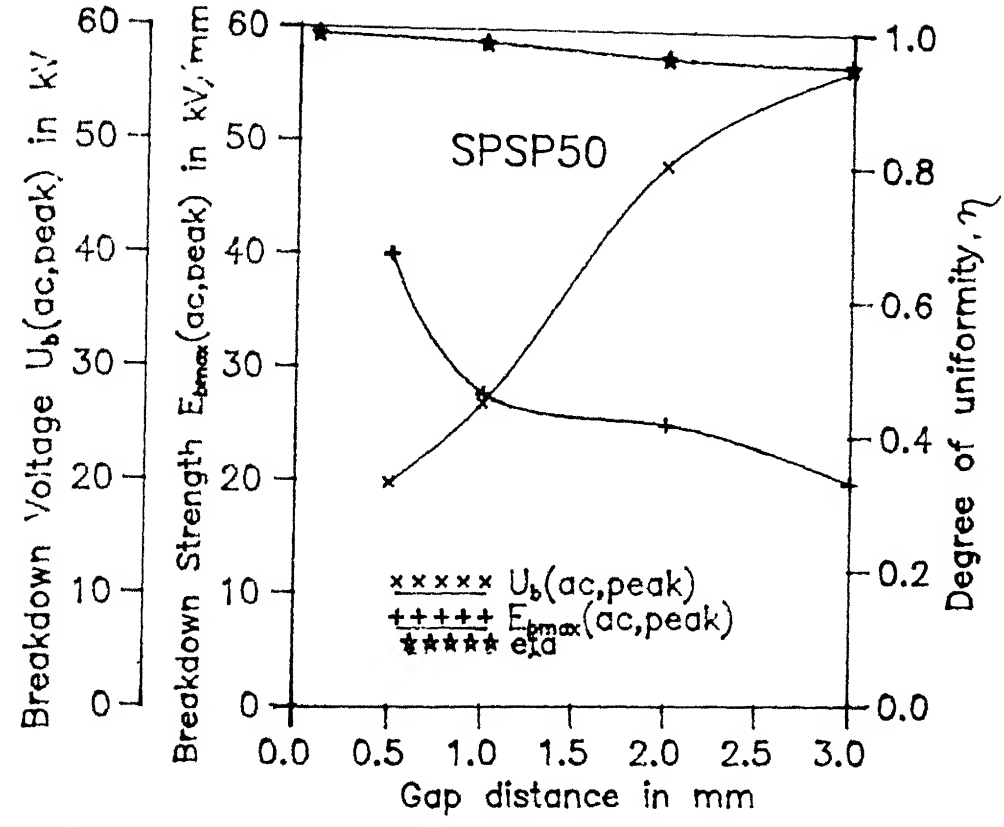

Fig.4.16 Variation of U_b, E_{bmax} and degree of uniformity with gap distance at 7.5×10^{-5} Torr

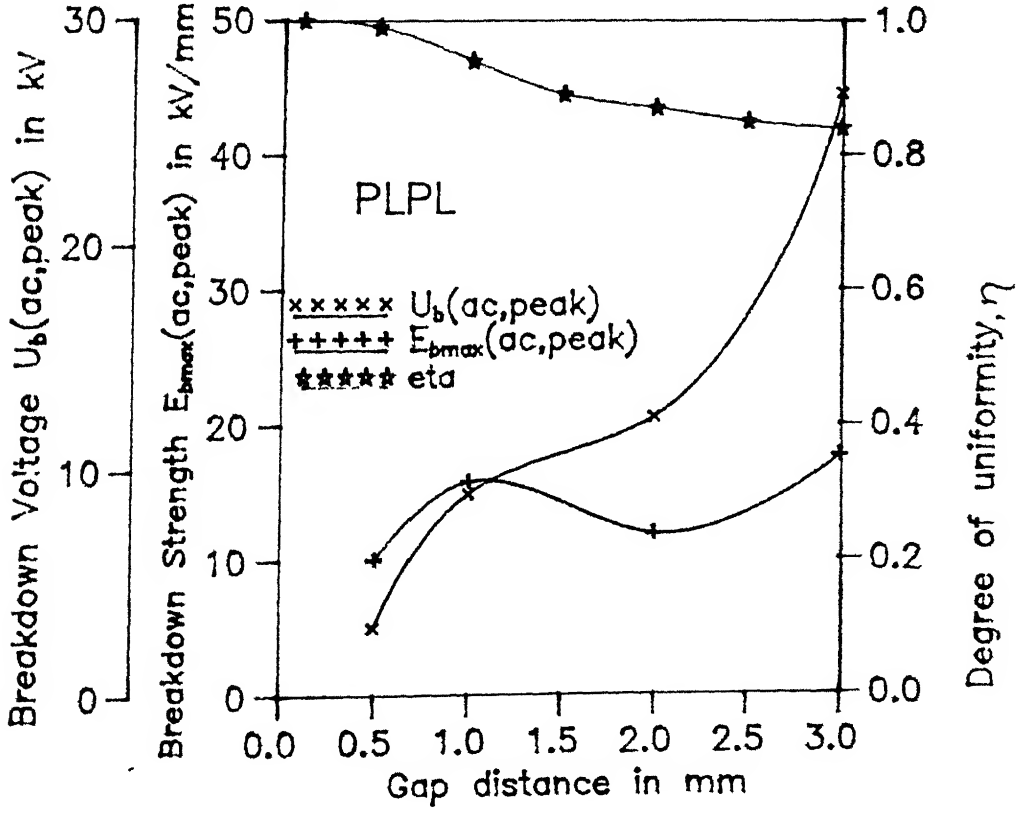

Fig.4.17 Variation of U_b, E_{bmax} and degree of uniformity with gap distance at 7.5×10^{-3} Torr

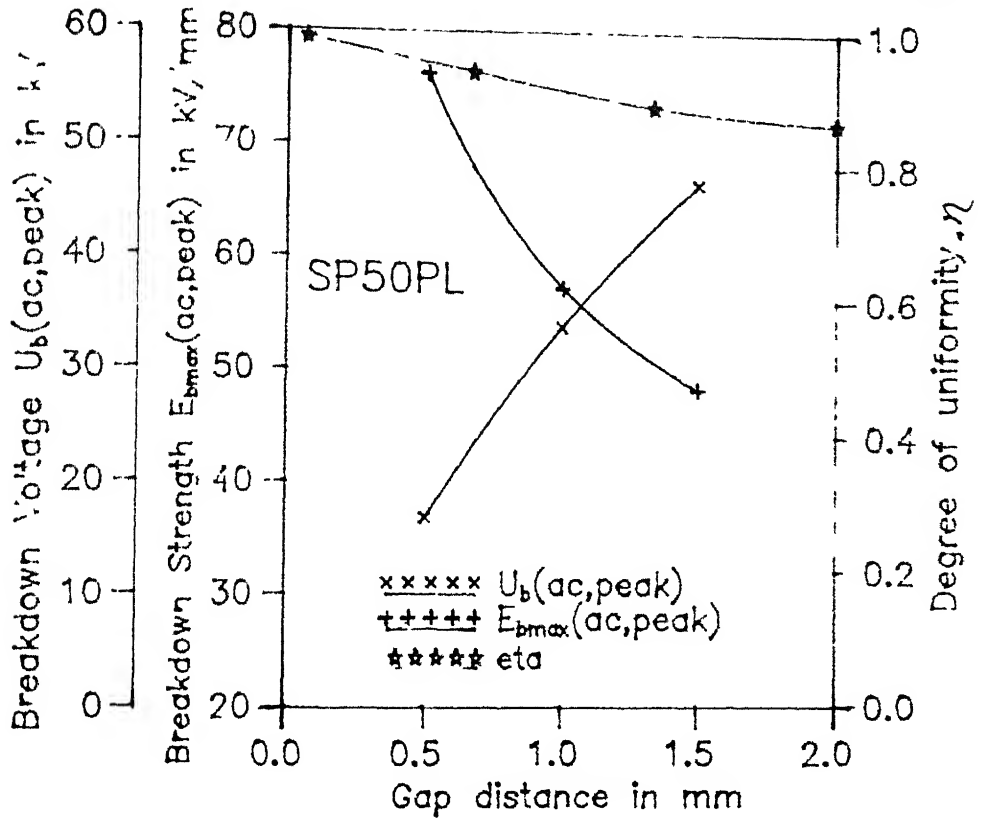

Fig.4.18 Variation of U_b, E_{bmax} and degree of uniformity with gap distance at 7.5×10^{-5} Torr

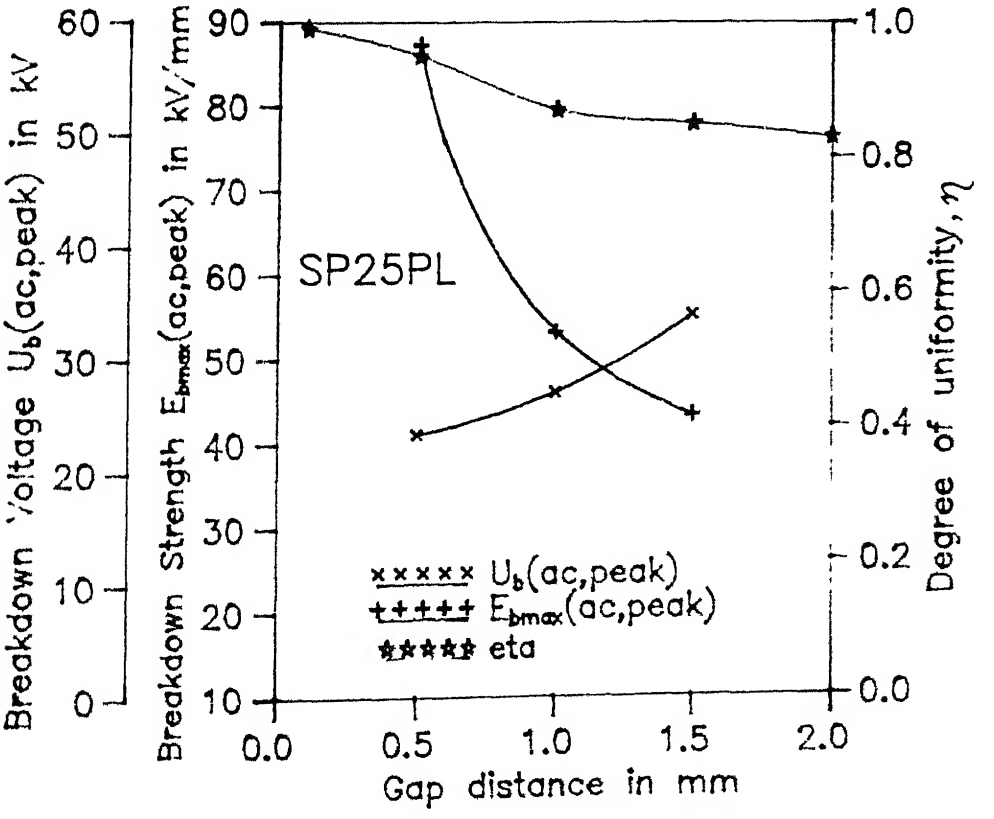

Fig.4.19 Variation of U_b, E_{bmax} and degree of uniformity with gap distance at 7.5×10^{-5} Torr

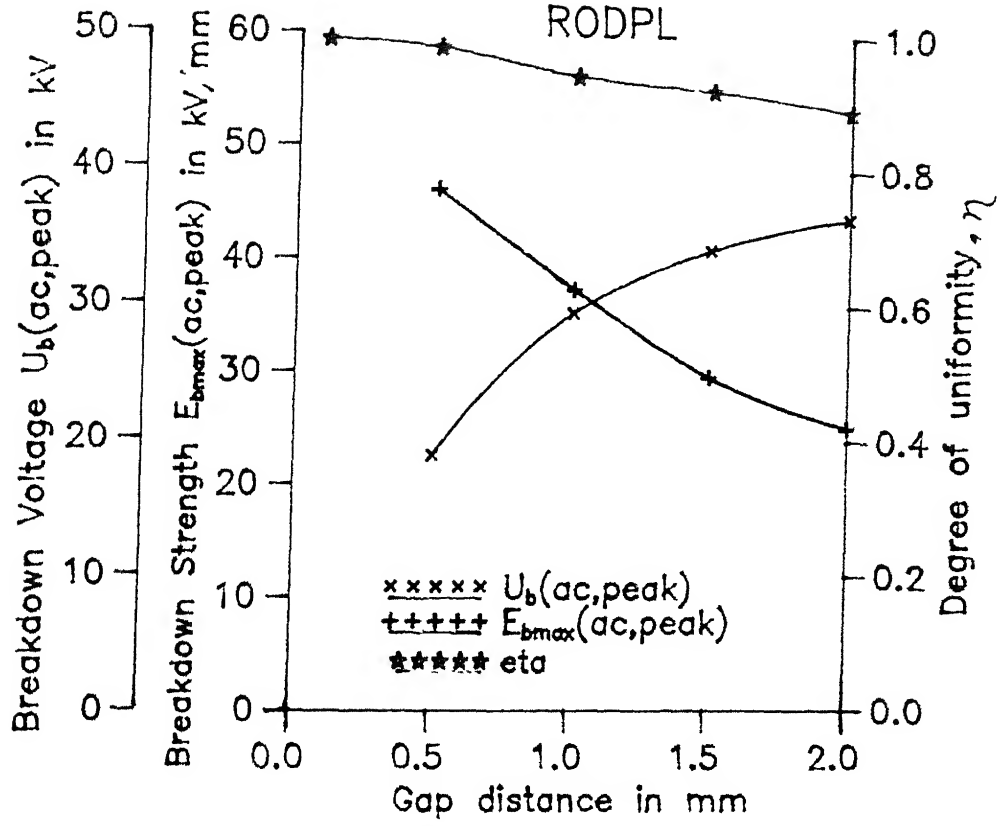

Fig.4.20 Variation of U_b, E_{bmax} and degree of uniformity with gap distance at 7.6×10^{-5} Torr.

extremely nonuniform field changing over to weakly nonuniform field configuration

REFERENCES

4 1 Marsbed H Hablanian, "High vacuum technology", Marcel Dekker, New York, 1990

4 2 G F Weston, "Glow Discharge Display", Mills and Boon limited, London, 1972

4 3 P L Rustan, Jr , "SDIO space insulation technologies", Conference record of IEEE International symposium on electrical insulation", Baltimore, USA, 1992

CHAPTER 5

INVESTIGATION WITH LIGHTNING IMPULSE VOLTAGE

5.1 Introduction

The importance of the investigation of the behaviour of vacuum with impulse voltage arises because in practice vacuum power switches and circuit breakers may get subjected to lightning and switching transients Vacuum devices are also used to operate under pulsed high voltage as in Klystrons and x-ray tubes which are subjected to high voltage transients

5.2 Experimental setup

The circuit diagram of the setup is shown in Fig 5 1. A four stage 500 kV, 4 4 kJ impulse generator was used to generate standard lightning impulse of both positive and negative polarity The generator output was connected to the high voltage electrode of the test vessel in parallel with the measuring capacitor A current viewing resistor (CVR) of 0 5 ohm was connected in series with the lower electrode to measure the prebreakdown and breakdown currents The voltage and current waves could be seen on the oscilloscope The voltage signal was taken from the secondary of a capacitive voltage divider having ratio of 750 1 The voltage signal was fed to the oscilloscope through a 10 1 probe Therefore, the magnitude of the impulse voltage could be obtained directly in kV by multiplying the

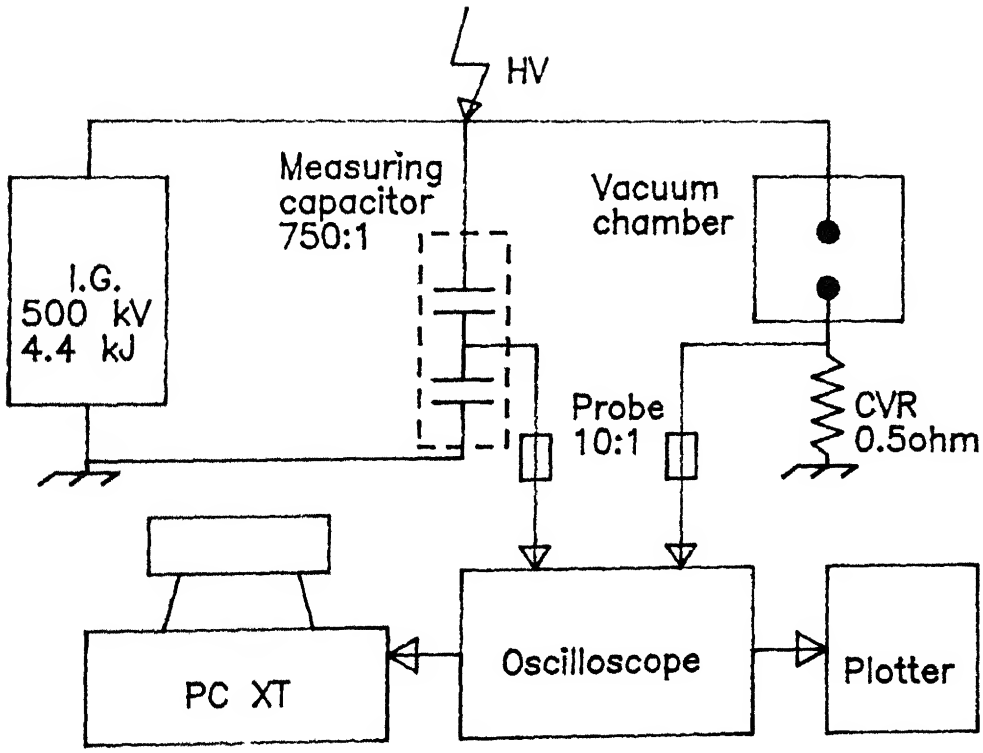

Fig.5.1 Circuit diagram of the setup used for investigation with lightning impulse.

oscilloscope reading with a factor Of 0 75

5.3 Experimental procedure

Breakdown characteristics of three different electrode pairs SPSP50, SP50PL and RODPL were investigated The same electrode pairs were also investigated under alternating power frequency voltage Identical procedure for electrode preparation and cleaning were adopted The gap distance in this case could be varied from 2 to 30 mm The investigations were performed at two pressure levels i,e, $7\ 6x10^{-4}$ and $7\ 6x10^{-6}$ Torr The adjustment of pressure was done according to the procedure discussed in Chapter 3

After the desired level of pressure was obtained, the impulse voltage was applied The magnitude of the applied voltage was increased slowly till first breakdown occurred The magnitude of this impulse voltage was kept constant and the pulses were applied at an interval of 30 seconds Total 20 shots of a particular voltage level were applied and the number of shots for which breakdown occurred was counted. The percentage breakdown voltage for a particular gap was obtained by dividing the number of shots at which breakdown occurred with the total number of shots applied Then the voltage was increased slightly and the above procedure was repeated till 50% breakdown voltage, U_{b50} was obtained The voltage and current waveforms were recorded by the oscilloscope and a print out could be taken as and when desired

5.4 Determination of 50% breakdown voltage, U_{b50}

As discussed above, a particular level of voltage was applied at an interval of 30 seconds but all of them did not cause breakdown It

was observed that initially a few first breakdown occurred at a comparatively lower voltage which soon ceased to take place The pattern of the occurrence of breakdown was more distributed on increasing the voltage level

A typical graph of such distribution of breakdown and withstand characteristics is shown in Fig 5 2(a) for SPSP50 electrode for a gap distance of 10 mm It could be seen that the first breakdown occurred at a voltage of 122 kV On raising the voltage applied to 145 kV, out of 20 shots, breakdown occurred for six Next voltage level applied was 172 kV, for which eight breakdown out of 20 pulses occurred Ultimately, on applying a voltage level of 196 kV it was found to be the 50% breakdown voltage, U_{b50} The same procedure was adopted in case of all other electrodes and gap distances

5.5 Occurrence of partial breakdown

At the beginning of the experiment, sharp spikes were observed on the wave tails of both the voltage and the current oscillograms A typical oscillogram is shown in Fig 5 3 The spikes were found to occur at the same instant of time for both current and voltage which is presumed to be a partial or incomplete breakdown commonly known as partial discharge (PD) This certainly does not mean a total failure of the gap. After the application of a few successive pulses, these spikes were found to disappear However, when the vacuum chamber was opened to mount a new set of electrodes and the experiment was repeated, the same phenomenon was observed again

The possible cause of partial discharges is the presence of microparticle within the vessel. Silicon grease was applied on the "O" rings of the vacuum chamber every time when it was re-mounted with new

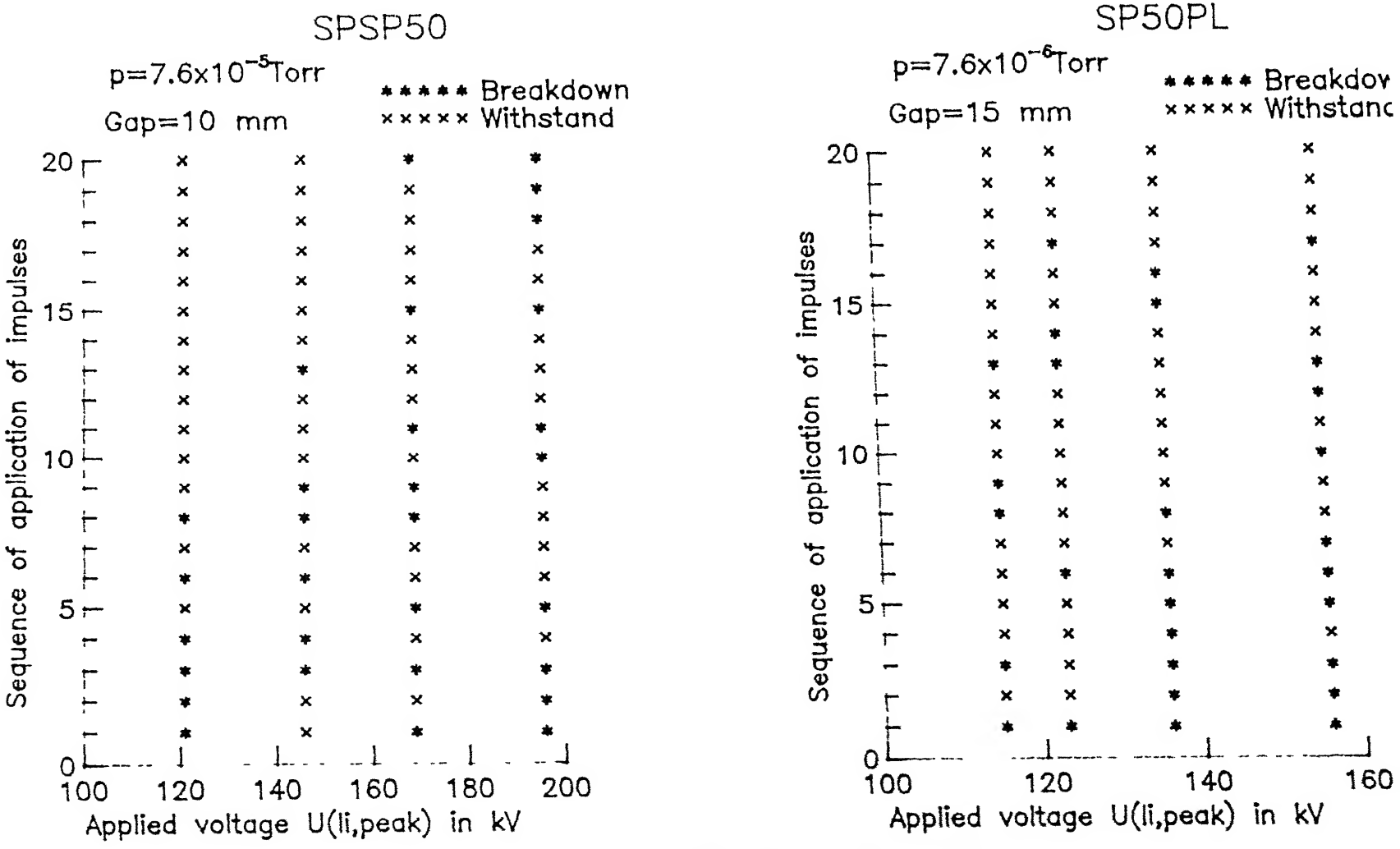

Fig.5.2 Distribution of breakdown and withstand voltage for (a) SPSP50 (b) SP50PL electrode.

set of electrodes which would give rise to organic compound vapour deposited on the electrode surfaces The effects of these foreign particles as adsorbates on the electrode surfaces is more predominant initially as later, after few pulses applied, these may get desorbed and get removed away by the continuous evacuation process

5 6 Time required for breakdown

Every time an impulse wave was applied, it was recorded by the oscilloscope irrespective of whether a breakdown took place or not From the oscillograms of the impulses when a breakdown took place, interesting observation regarding the so called "formative time" for breakdown could be made

The phenomenon of time required for breakdown by an impulse wave is a statistical process. The inconsistency in this time also has been observed in vacuum for weakly nonuniform field

5.6.1 The phenomenon of statistical time lag as observed in vacuum

It could be observed that breakdown took place at different instances after the peak of the impulse even if the applied voltage magnitude was the same on a particular gap A typical oscillogram is shown in Fig.5.4 for SP50PL electrode for a gap of 10 mm and a pressure of 7.6×10^{-4} Torr. Shot number 15 to 18 are shown It can be seen that the applied voltage magnitude is kept constant at 52 5 kV, in spite of which the breakdown occurred after 16 56, 5 9, 11 46 and 4.8 μs respectively in these figures Similar phenomenon was observed for other electrode pairs and at pressures However the range of this statistical time lag became smaller for longer gap distances where higher breakdown voltage were needed

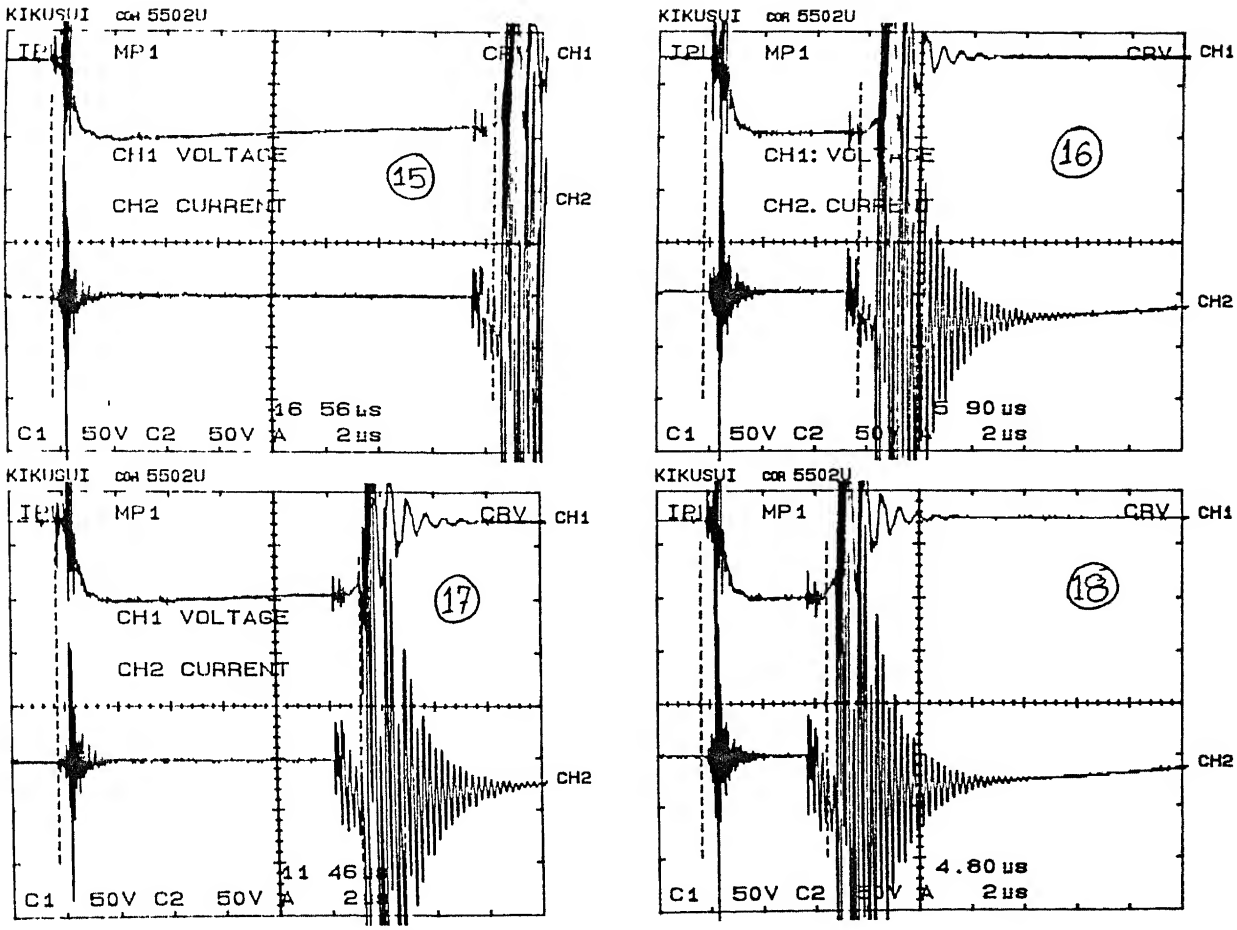

Fig.5.4 Oscillogram showing different time required for the formation of breakdown for the same magnitude of applied lightning impulse.

The time lag between the peak of the impulse and the instant when the voltage collapsed was also measured to be different for different magnitudes of applied voltages at a particular gap distance and pressure for an electrode pair Longer time was required after the peak of the impulse to cause breakdown when the applied voltage was lower When the applied voltage was increased, it took lesser time for breakdown Typical oscillograms showing different time required for the formation of breakdown are shown in Fig 5 5 for RODPL electrode for a gap distance of 5 mm at 7 6x10^{-4} Torr The oscillogram I shows breakdown which occurred at 40 kV, required 15 μs for the formation of breakdown In oscillogram II the breakdown voltage is increased to 41 25 kV and the corresponding time delay is measured to be 11 μs In Oscillogram III, the voltage is further increased to 50 25 kV which reduced this time to 4 4 μs In the last oscillogram, the breakdown voltage is 56 63 kV, which is nearly 100% breakdown voltage and the corresponding time delay is just 3 μs only

The statistical time delay is plotted as a function of breakdown voltage for SP50PL electrode for different gap settings and at a pressure Of 7 6x10^{-6} Torr as shown in Fig 5 6 It can be seen from this figure that the time required for the formation of breakdown reduces on increasing the magnitude of the applied impulse voltage i,e, effectively the rate of rise of the impulse voltage In other words it can be said that the statistical time lag is a function of the rate of rise of the applied voltage

5 6.2 Time required to bridge the gap distance for breakdown

It can be observed from the voltage oscillograms taken for different gap distances that the time required for the voltage from the instant of the beginning of breakdown to its value to zero is

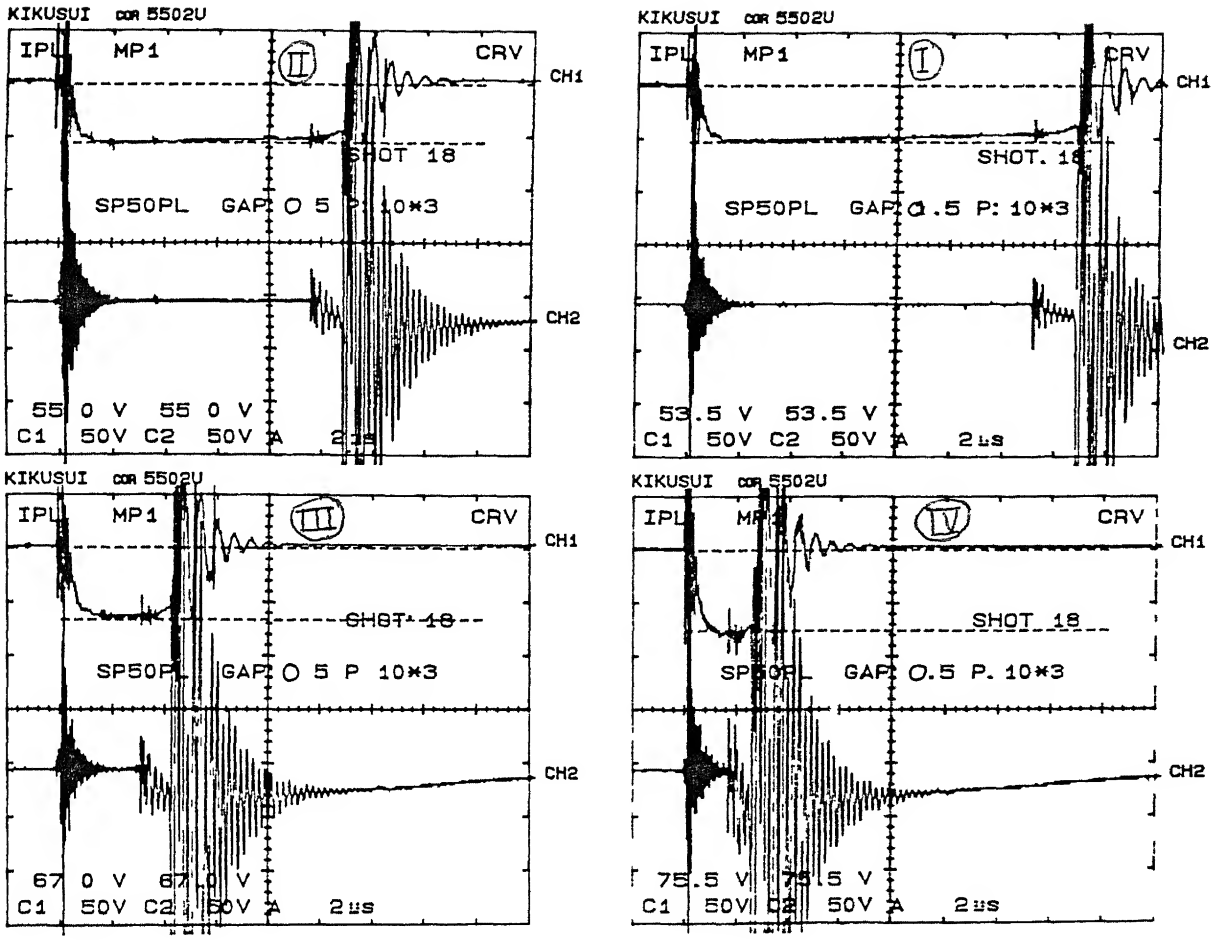

Fig.5.5 Oscillograms showing lower time required for the formation of breakdown at higher magnitude of applied lightning impulse.

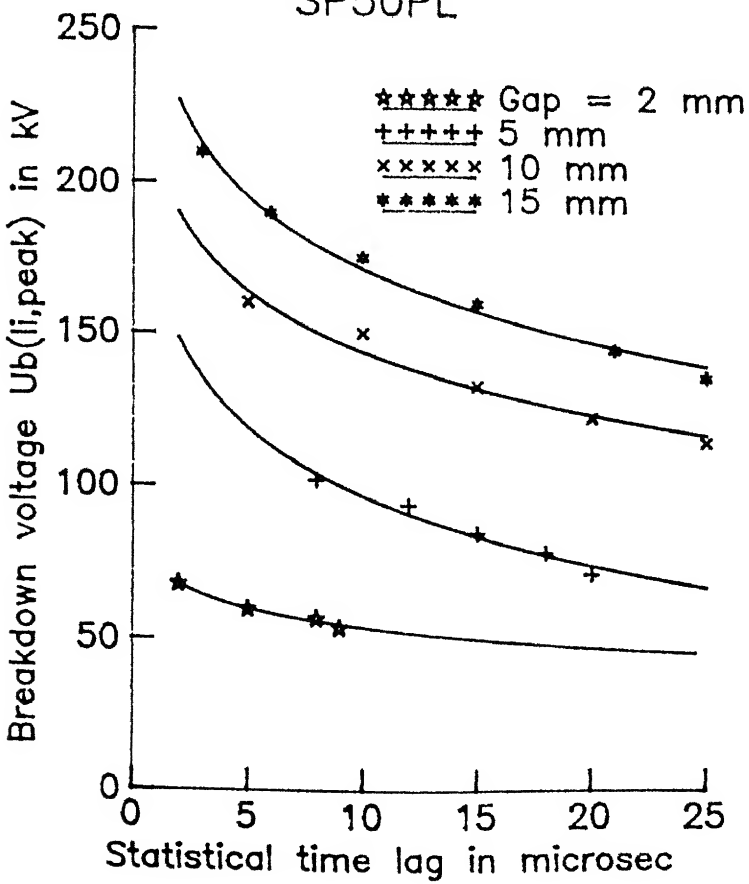

Fig.5.6 Statistical time lag vs breakdown voltage at high vacuum under li for Sphere–Plane electrode.

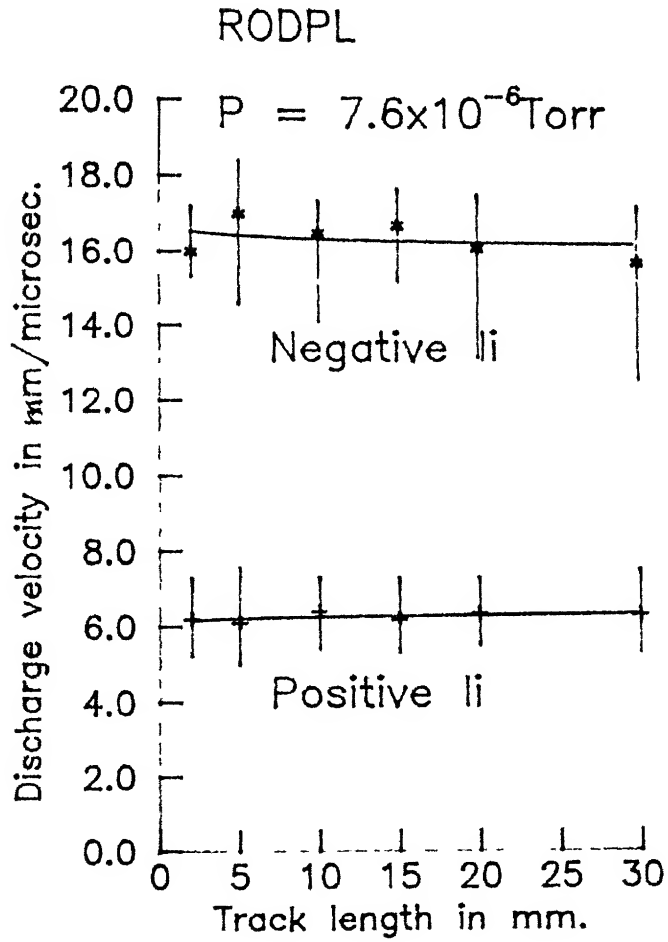

Fig.5.7 Velocity of the discharge at high vacuum under li for Rod–Plane electrode.

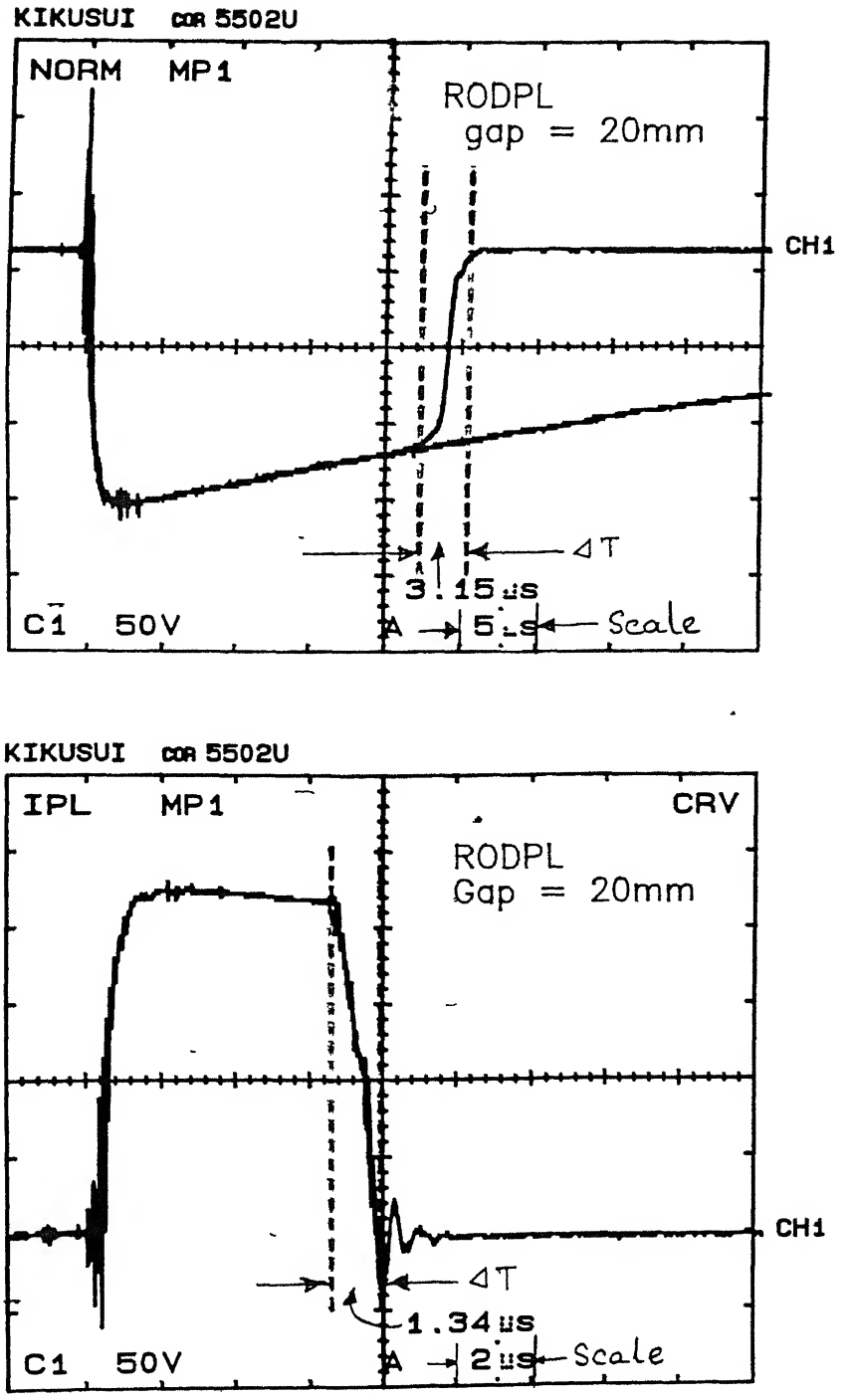

Fig.5.8 Oscillograms showing more time required by negative impulse than positive impulse to bridge the same gap distance during breakdown.

different for different gap distances and the magnitude of applied voltages Actually this is the time required for the discharge in the event of breakdown to travel through the gap distance between the electrodes The velocity of this discharge was obtained by dividing the gap distance with the time This is referred as leader propagation velocity in the literature [5 1] The variation of discharge velocity as a function of gap distance is shown in Fig 5 7 for RODPL electrode at 7 6x10^{-6} Torr for both positive and negative impulses It can be seen from this figure that in case of positive li, the discharge moves faster than in case of negative polarity Oscillograms taken at the event of breakdown under similar conditions for positive and negative polarity impulse as shown in Fig 5 8 also reveal this phenomena

5 7 Investigations at low vacuum

Only rotary pump was used to produce low vacuum of the order of 7 6x10^{-4} Torr In this pressure range the breakdown strength of vacuum is very low as investigated (Chapter 4) in case of experiments with alternating power frequency voltage Since the minimum voltage which could be obtained from the impulse generator was 40 kV, investigation on small gap distances was not possible Hence the gap distance was varied from 5 to 30 mm in this case

After the pressure and the gap distance were set, the lowest voltage was applied at the beginning which did not cause breakdown Then the voltage magnitude was increased gradually till first breakdown occurred Bluish glow discharge along the central zone of the gap distance between the electrodes was observed following the breakdown at small gaps For longer gap distances, such a glow discharge was observed to extend more in the volume of the vacuum

extended all over the vacuum chamber from the upper end plate to the lower end plate The colour of the glow in this condition was light pink On further increasing the gap distance, the glow became pink and the entire vacuum chamber behaved as a mass instead of breakdown occurring at the gap between the two electrodes At this stage the breakdown voltage did not increase on increasing the gap distance Therefore the investigations were limited to the gap distance of 30 mm

The breakdown voltage, U_{b50} was measured for different gap distances for SPSP50, SP50PL and RODPL electrode pairs under both positive and negative li The average electric field intensity, E_{bav} was obtained from the equation,

$$E_{bav} = \frac{U_{b50}}{d} \qquad (5\ 1)$$

where d is the gap distance The maximum electric field intensity at breakdown, E_{bmax} was obtained from the following equation [5 1],

$$E_{bmax} = \frac{U_{b50}}{d\ \eta} \qquad (5\ 2)$$

where η is the degree of uniformity estimated with the help of CSM (Chapter 2)

The measured values of U_{b50} and the calculated values of E_{bav} and E_{bmax} are plotted for varying gap distances as shown in Fig 5 9 to 5 11 for SPSP50, SP50PL and RODPL electrodes respectively The values of η at different gap distances for each of the electrodes were obtained by CSM and plotted on the same figures for comparison It can

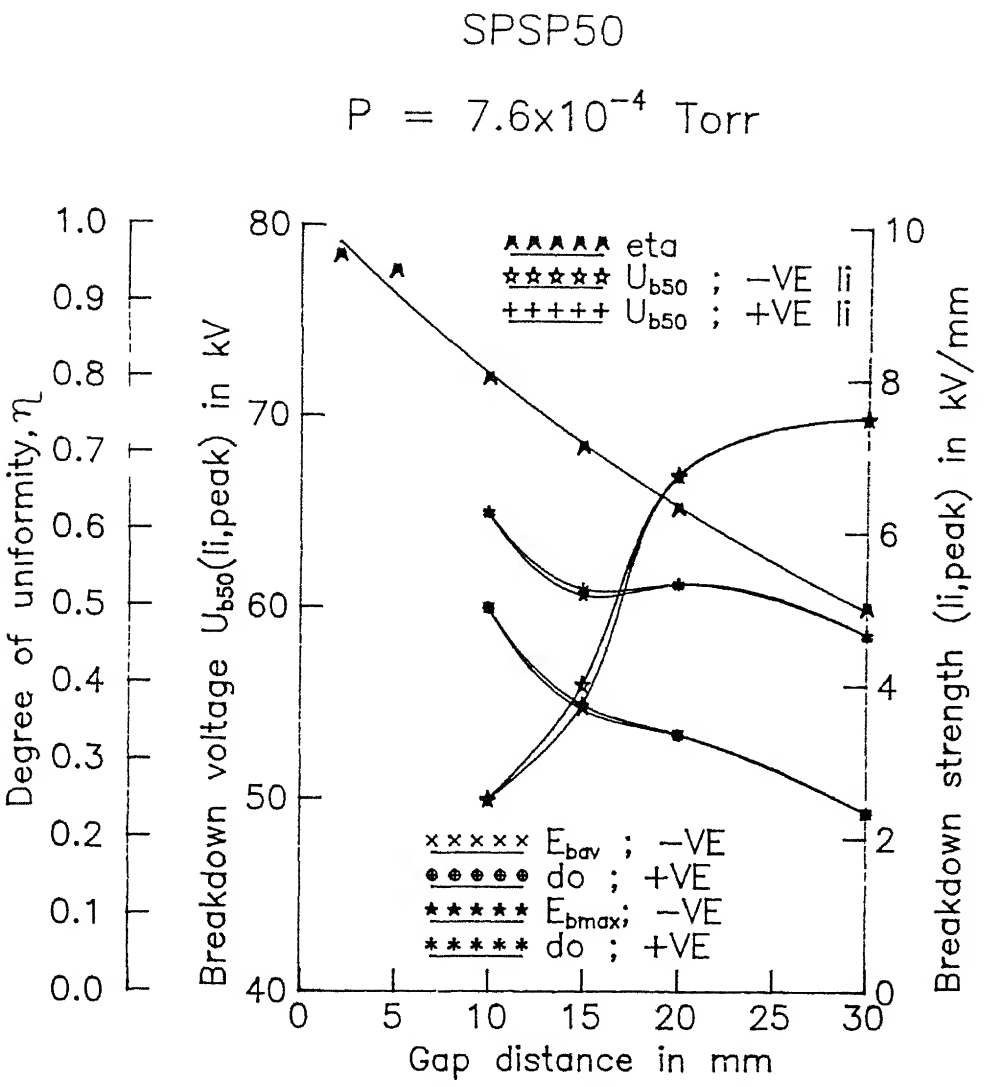

Fig.5.9 Variation of breakdown voltage, breakdown strength and degree of uniformity with respect to gap distance at low vacuum.

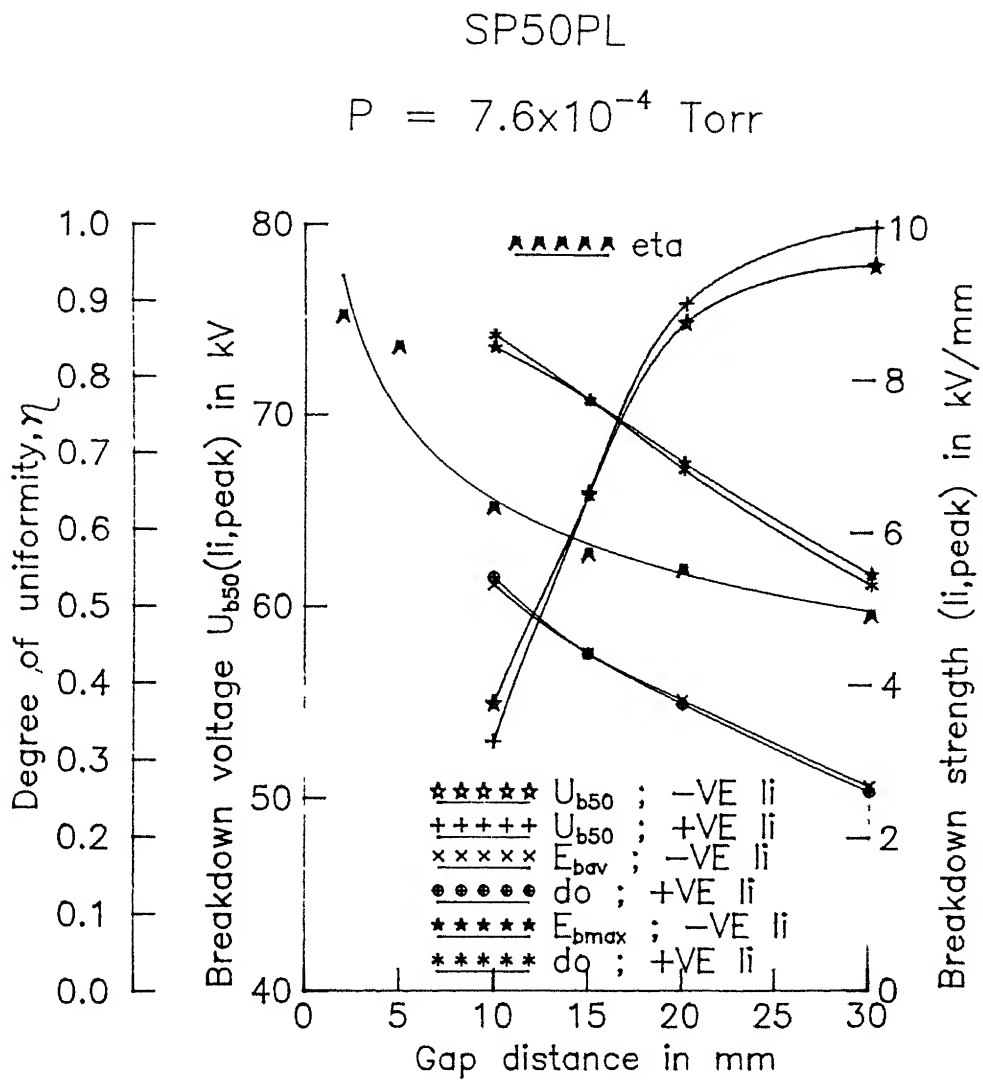

Fig.5.10 Variation of breakdown voltage, breakdown strength and degree of uniformity with respect to gap distance at low vacuum.

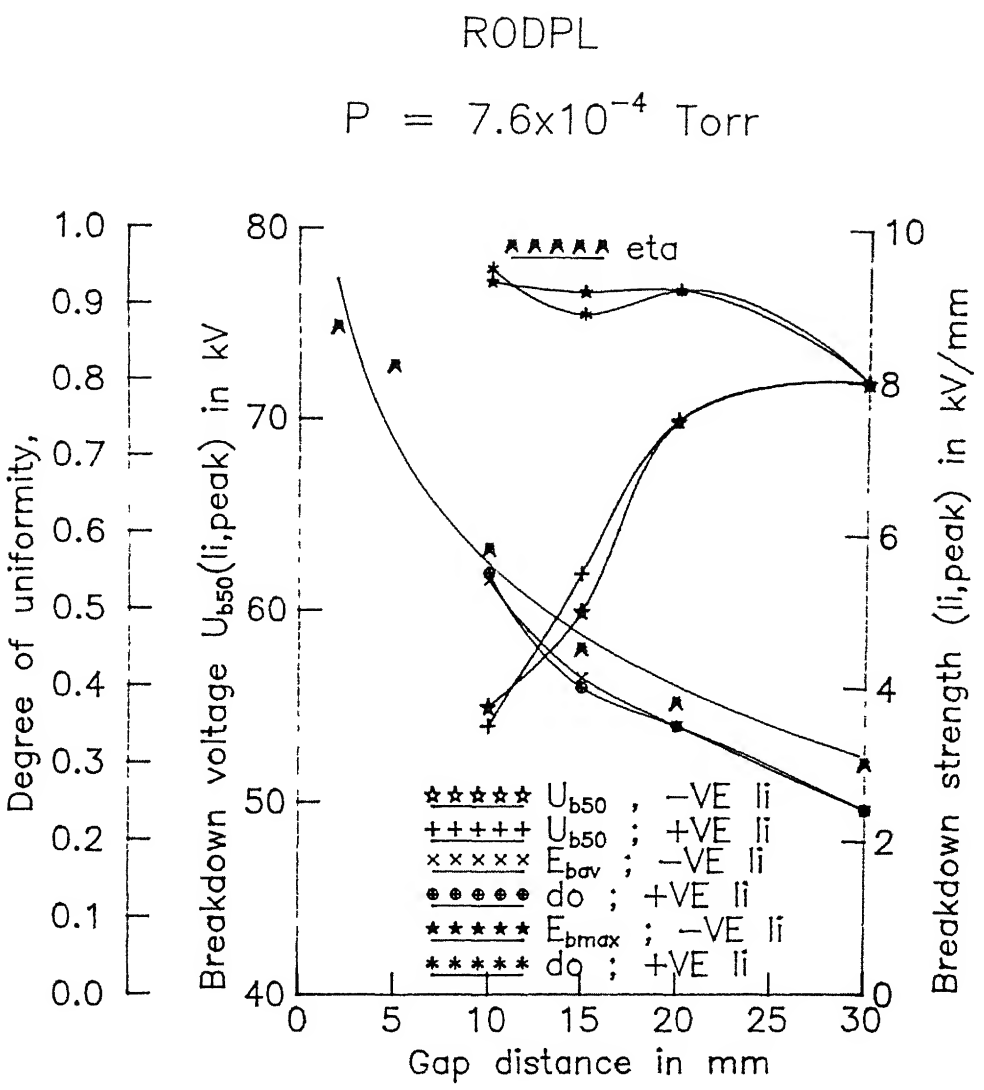

Fig.5.11 Variation of breakdown voltage, breakdown strength and degree of uniformity with respect to gap distance at low vacuum.

be seen from these figures that for all the electrodes, the breakdown voltage increases with the increase of gap distance The breakdown voltage did not increase appreciably on increasing the gap distance beyond 20 mm No appreciable difference in the breakdown voltage could be measured for positive and negative li at low vacuum The average field intensity, E_{bav} and the maximum field intensity, E_{bmax} were found to decrease with the increase in gap distance

5 8 Investigation at high vacuum

The breakdown strength of high vacuum is considerably higher compared to that of low vacuum Therefore it was possible to conduct the investigations over a wide range of gap distances starting from 2 mm to 30 mm The pressure was kept constant at $7\ 6x10^{-6}$ Torr which was the highest vacuum which could be achieved by the vacuum pumping system used

The 50% breakdown voltages, U_{b50} were measured varying the gap distances for SPSP50, SP50PL and RODPL electrode pairs with both positive and negative polarity lightning impulse voltages The average electric field intensity, E_{bav} and the maximum electric field intensity at breakdown, E_{bmax} were calculated by Eqs 5.1 and 5 2.

The measured values of U_{b50} and the calculated values of E_{bav} and E_{bmax} are plotted against gap distance as shown in Fig 5 12 to 5 14 for electrode pairs mentioned above The calculated values of η of the field are also shown for reference It can be seen from these figures that for all the electrodes, the breakdown voltage increases with the increase in gap distance The rate of increase of U_{b50} is lower at longer gap distances compared to that at smaller gap distances The breakdown voltages for positive li are measured to be

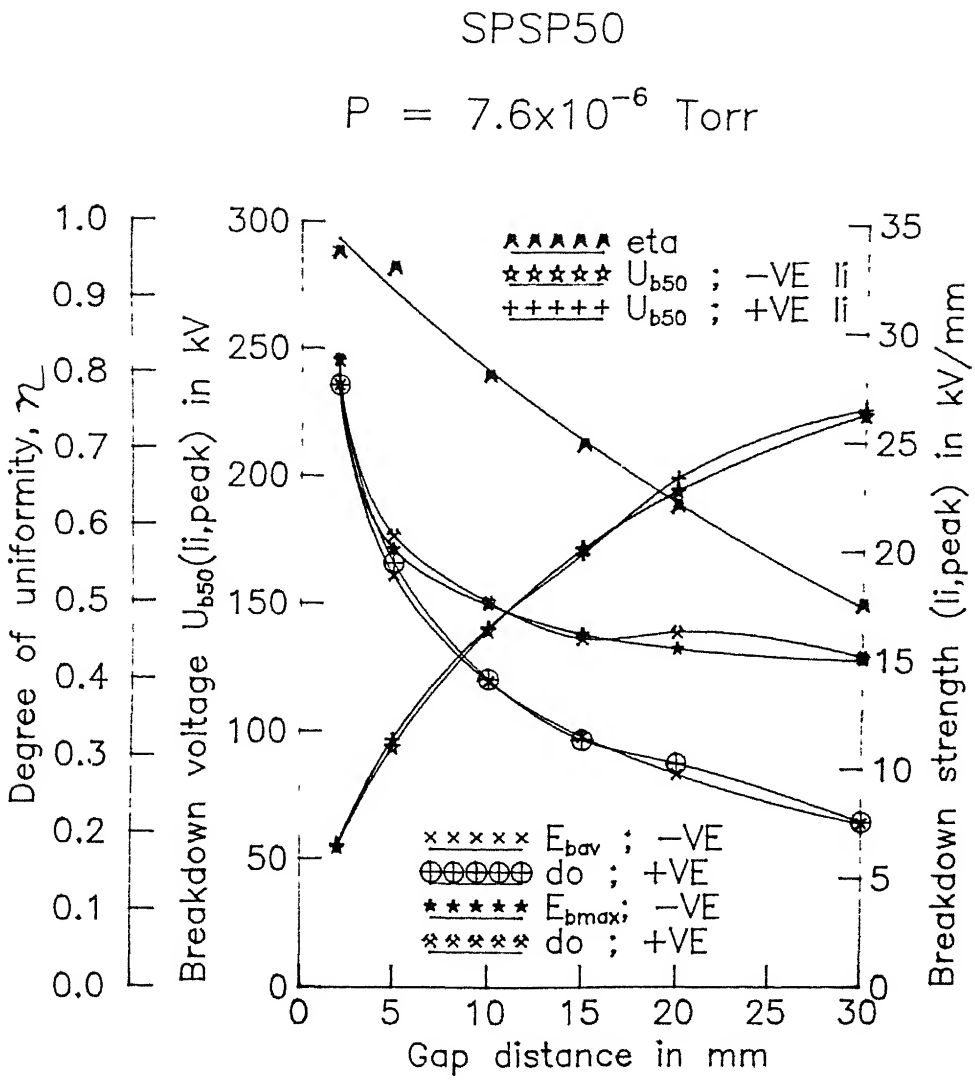

Fig.5.12 Variation of breakdown voltage, breakdown strength and degree of uniformity with respect to gap distance at high vacuum.

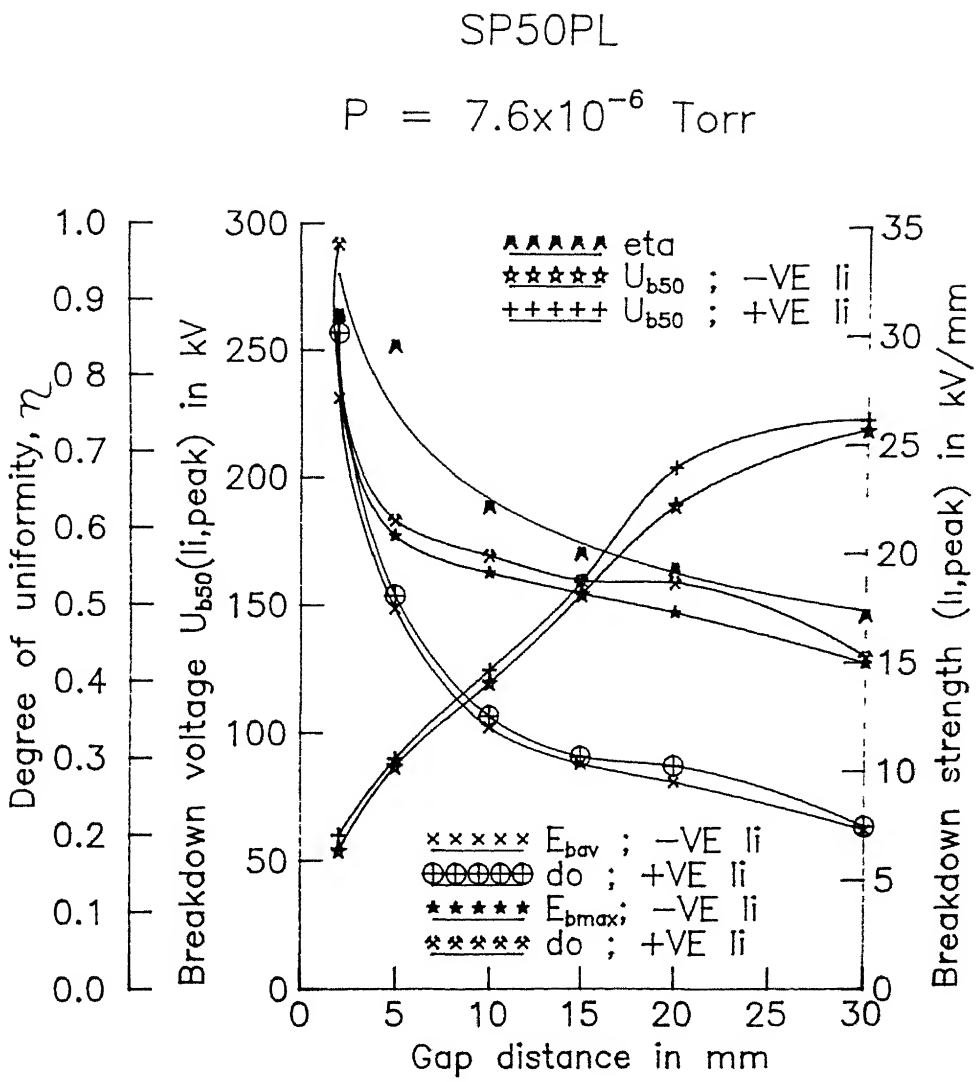

Fig.5.13 Variation of breakdown voltage, breakdown strength and degree of uniformity with respect to gap distance at high vacuum.

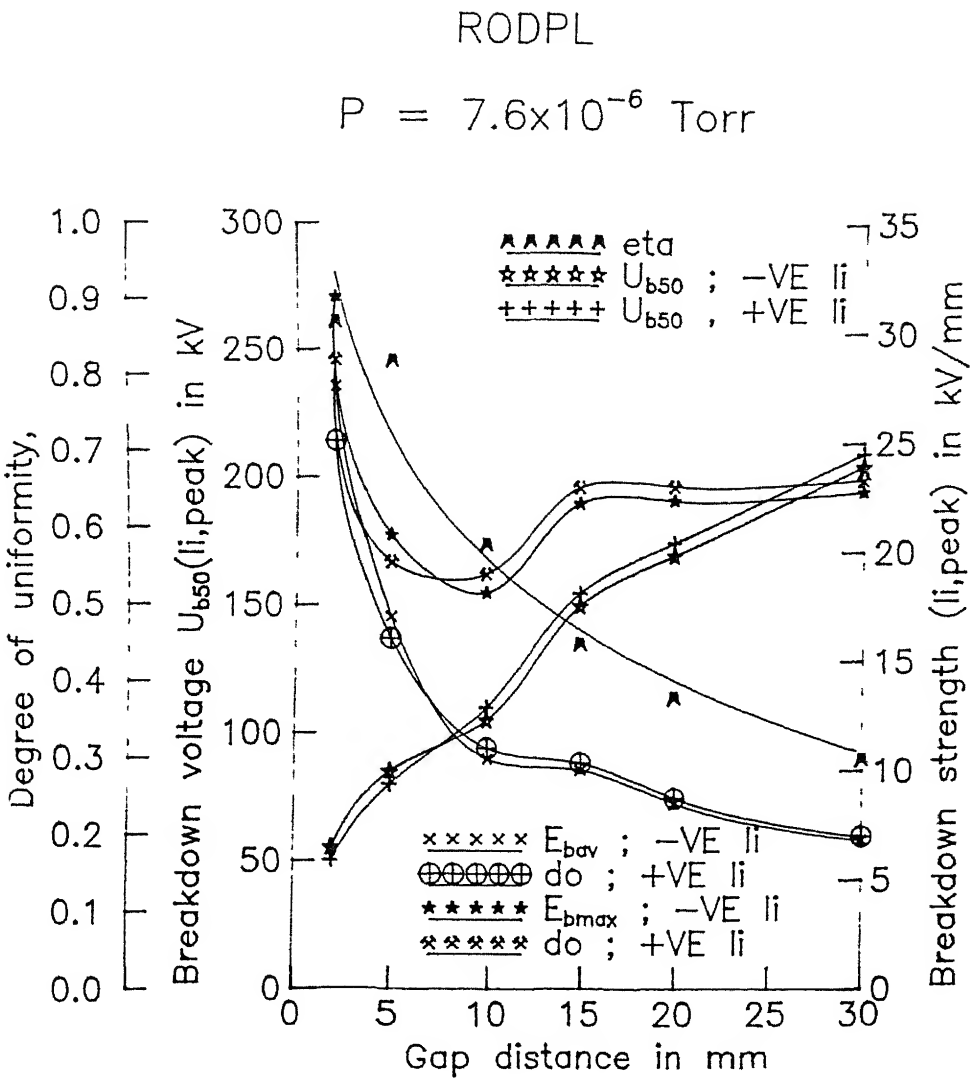

Fig.5.14 Variation of breakdown voltage, breakdown strength and degree of uniformity with respect to gap distance at high vacuum.

slightly greater than that for negative li at this vacuum level The average and the maximum field intensities at breakdown decrease as the gap distance was increased However decrease in E_{bav} is more than in E_{bmax} The value of E_{max} acquires sort of a saturation level as the gap distance was increased beyond 20 mm for SPSP50 and SP50PL electrodes For RODPL electrode, slightly different pattern of change is observed In this case, E_{bav} continues to decrease with the increase in gap distance while E_{bmax} reaches to a minimum at the gap distance of 10 mm after which it increased slightly and acquired a saturation level

5 8.1 Comparison of breakdown voltages measured for different electrode pairs

Comparing Figs 5 12 to 5 14, it can be seen that for the same gap distance, different electrodes have different degree of uniformity and breakdown voltages From these measurements, the variation of breakdown voltage with respect to η are plotted as shown in Fig 5 15 and 5 16 for positive and negative impulse voltages respectively It can be seen from these figures that the breakdown voltage at a particular gap distance and pressure increases as the degree of uniformity of the field increases for both positive as well as negative li

5.9 Effect of pressure on breakdown voltage

The breakdown voltages were measured at three different vacuum levels, that is, at $7\ 6x10^{-4}$, $7\ 6x10^{-5}$ and $7\ 6x10^{-6}$ Torr for SPSP50 electrode pair Variation of U_{b50} with pressure for three gap settings are shown in Fig 5 17 A typical characteristic is seen from this figure that the breakdown voltages for all the gap settings increase as the vacuum level is increased The maximum values of U_{b50} were

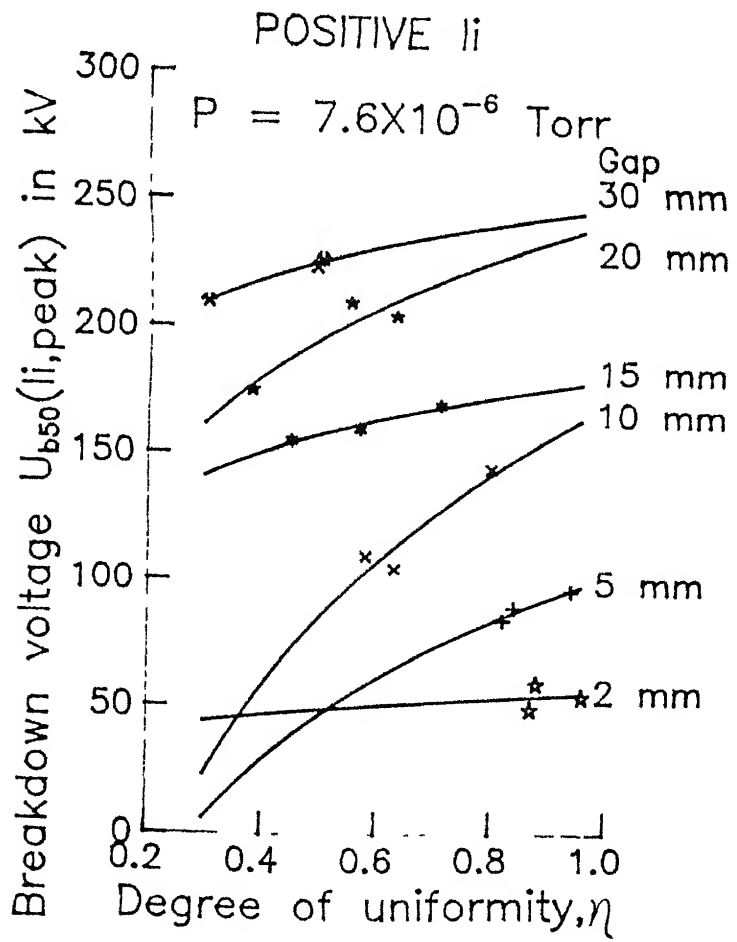

Fig.5.15 Variation of U_{b50} with degree of uniformity at different gap distances for positive impulse voltage.

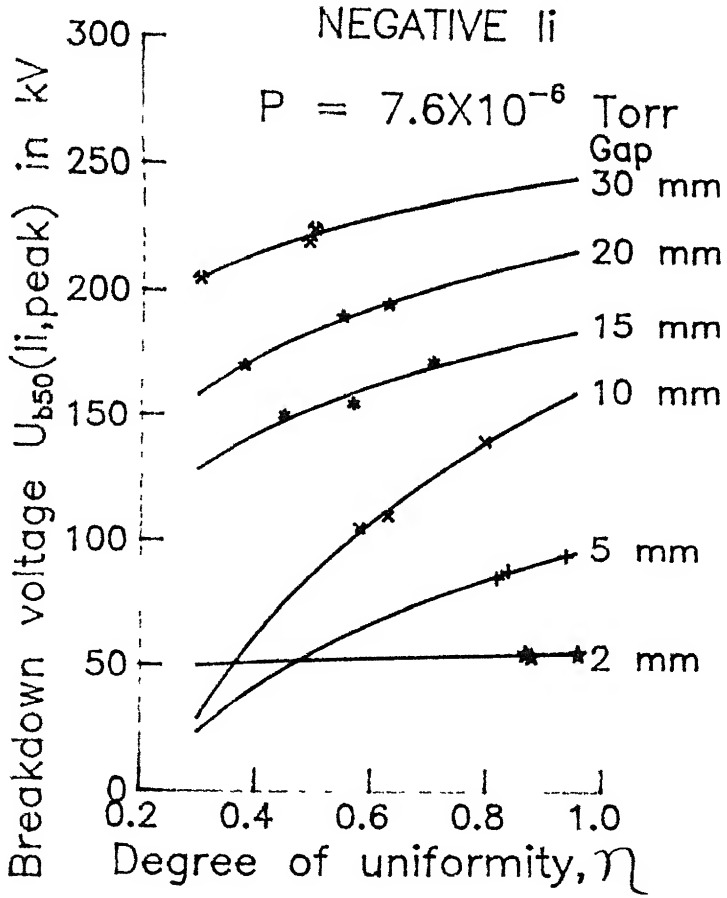

Fig.5.16 Variation of U_{b50} with degree of uniformity at different gap distances for negative impulse voltage.

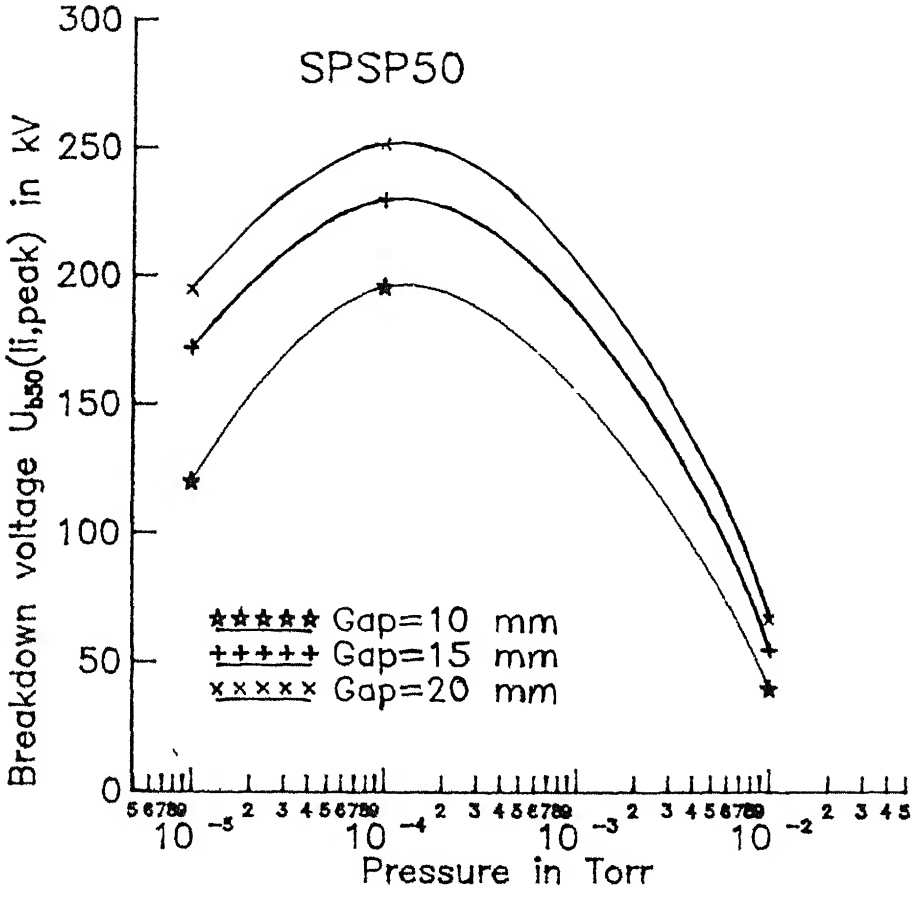

Fig.5.17 Variation of breakdown voltage with pressure.

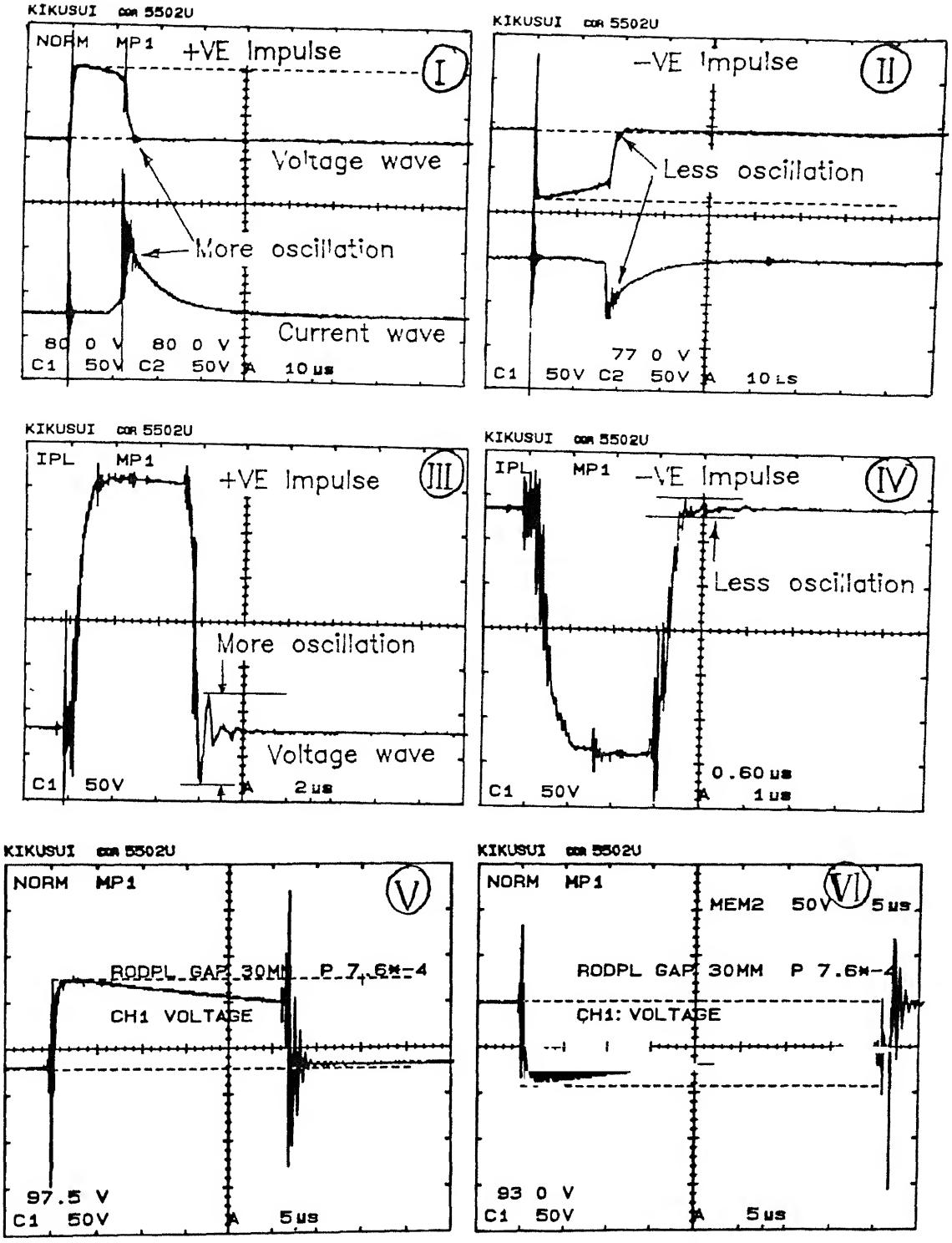

Fig.5.18 Oscillograms showing more spikes on the voltage waveform at the instant of voltage collapse in case of positive lightning impulse.

measured around the pressure of 10^{-4} Torr On increasing the vacuum level further, U_{b50} voltages were measured to decrease around the pressure of 7 6x10^{-6} Torr

5 10 Comparison of positive and negative impulse breakdown

As reported in section 5 8, the breakdown voltages for positive li slightly higher than that for negative impulse Apart from this, some other typical phenomena were observed which are explained in the following In case of positive impulse, intensive oscillations were observed on the voltage as well as current waveforms at the instant when the voltage collapsed due to breakdown Comparatively less oscillations were observed in case of negative li Typical oscillograms showing breakdown under both positive and negative impulse are shown in Fig 5 18 Oscillograms I and II have been taken for SP50PL electrode pair having a gap distance of 2 mm at 7 6x10^{-6} Torr It can be seen that there are comparatively more spikes at the instant when the breakdown is accomplished on both voltage and current waveforms in oscillogram I which is for positive impulse Oscillograms III and IV have been taken for RODPL electrode for a gap distance of 30 mm It can be seen that the magnitude of said oscillations in this case of higher breakdown voltage (for longer gap distance) increase. However such typical difference in voltage oscillations were observed only at high vacuum In case of low vacuum such oscillations were observed for both positive as well as negative li as can be seen from oscillograms V and VI, taken at 7 6x10^{-4} Torr

REFERENCES

5.1 R Arora and W Mosch, "High voltage insulation engineering", Wiley Eastern Ltd , India, 1995

CHAPTER 6

CONCLUSIONS

6 1 Introduction

Vacuum has a very long history to be used as electrical insulation in various apparatus such as X-ray tubes, electronic valves, high frequency capacitors and interrupters etc In power system it is being widely used now in circuit breakers upto 33 kV Developmental work for its use in cryocables is complete The most recent use of vacuum is proposed for its application in space The use of vacuum in low earth orbit (LEO) environment is being investigated presently by SDIO [6 1] The LEO environment constitutes of a low density gas giving rise to its ambient plasma state causing typical problems such as high conductivity, breakdown at low voltage, surface flashover and component malfunctioning etc even for the apparatus which may not be working necessarily at very high voltages

From an extensive literature survey, it was revealed that a fairly good amount of work has been performed in the field of breakdown in vacuum However most of the experimental work has been performed under ideal conditions of vacuum Highly sophisticated methods of electrode preparation and cleaning have been adopted But in practice, the conditions to which vacuum is subjected to high voltage are not ideal Possibility of presence of micro contaminants in the vacuum chamber and that of adsorbates on the electrodes can not

be ruled out [6 2] From the literature survey it appears that not much of investigation has been performed with alternating power frequency voltage Electrodes of different shapes and sizes have been experimented with by different workers making it difficult to correlate their investigation results for a comparative statement In the present work the insulating properties of vacuum have been investigated over a wide range of pressure starting from low vacuum (a few Torr) to high vacuum (10^{-6} Torr) No method of conditioning for the electrodes were adopted Simpler procedures were used for the preparation of electrodes and their cleaning process The experiments were performed under such conditions with both alternating power frequency and lightning impulse voltages Charge Simulation Method has been adopted for the estimation of the electric field and the degree of uniformity for the electrode configurations investigated in this work

6.2 Conclusion

For the kind of investigations, as in this work, CSM has been found to be an appropriate method for the estimation of the degree of uniformity of the field Only point charges have been adopted to simulate the equipotential surfaces of the electrodes which makes the procedure quite simple Although electrodes of regular geometrical shapes used in this work have been considered for the field estimation, this method can be conveniently extended to irregular electrode shapes used in practice

From the results of electric field estimation by CSM, it can be concluded that grounding of one of the electrodes makes the field more nonuniform On the other hand, the field becomes more uniform if the

high voltage electrode has larger radius of curvature The degree of uniformity, η does not worked out to be the same for sphere-sphere, rod-rod or hemisphere-hemisphere electrode pairs in spite of their radii of curvature and gap distances are the same The interchange of the positions of unsymmetrical electrodes such as sphere-plane, plane-sphere, rod-plane, plane-rod etc does not change the value of η in case of symmetrically applied voltage For any electrode pair, the field was found to be more uniform (higher value of η) for symmetrically applied voltage than for asymmetrically applied voltage

In the present work investigation has been performed under the practical conditions of vacuum The same electrodes were used for the investigation under both ac and lightning impulse voltage Comparatively simpler methods of electrode preparation and cleaning were adopted The obtained results have been found to be in good agreement with those obtained by other workers under almost similar conditions A list of breakdown strength of vacuum as obtained by different workers has been given in Table 6 1 along with the results of the present work for comparison It can be seen from the table that the breakdown strength as obtained in the present investigation is less that that obtained by others

While investigating with alternating power frequency voltage, the typical glow phenomena of different appearance could be observed by varying the pressure levels within the range of low vacuum (between a few Torr to 10^{-3} Torr) In this range the breakdown voltages are quite low and are measured to be independent of electrode shape, size and gap distances The minimum breakdown voltage was measured to be 450 Volts (ac, peak) at a pressure of 0 31 Torr In the pressure range between 0 05 and 0 38 Torr, the breakdown voltages were measured

Table 6.1 Breakdown strength of vacuum reported by different workers

Author and Year	Gap distance mm	Voltage type	E_{bmax} V/m
T Shioiri, 1982 [6 3]	12	si,li	$6x10^7$
H Toya, 1989 [6 4]	40	si,li	10^7
M Okawa, 1988 [6 5]	15	si	$6x10^7$
K Tsuruta, 1987 [6 6]	3	si	10^{11}
T Tsutsumi, 1989 [6 7]	2	si	10^{11}
B Mzurek, 1987 [6 8]	2 5	dc	$6x10^7$
H Pursch, 1989 [6 9]	3	dc	$8x10^9$
R Hackam, 1975 [6 10]	1	ac,dc	$4\ 5x10^7$
M A G Khan, 1995	2	ac	$2x10^7$
	2	±li	$3\ 5x10^7$
	30	±li	$1\ 4x10^7$

between 450 to 500 Volts (āc, peak)- At pressures below 0 05 Torr, the breakdown voltage increases rapidly and become function of electrode shape, size and gap distances again

Breakdown voltages were measured at three different pressures i,e, 7 6x10^{-4}, 7.6x10^{-5} and 7 6x10^{-6} Torr for different electrode pairs with both ac and li voltages by varying the gap distances The highest breakdown strengths have been measured in the pressure range of 7 6x10^{-5} Torr Both below and above this pressure, the breakdown strengths were measured to be lower It could be established by calculations that E_{bmax}, the maximum field intensity at breakdown, reduces as the degree of uniformity, η reduces

6.3 Scope of further research

In the present work investigations have been performed with alternating power frequency voltage and lightning impulse It would be worth continuing similar investigations with switching impulse voltages of different waveshapes Due to the constraints of the experimental setup, investigation with ac voltage could be performed for quite small gap distances only upto 3 mm Investigations with ac voltage for longer gap distances are desirable However this will require more elaborate development of the experimental setup

In practice solid insulators are often used in vacuum to mount the high voltage electrodes Problem of surface discharge on the solid insulators is needed to be investigated under different conditions of vacuum and applied voltages

REFERENCES

6 1 P L Rustan, "Strategic Defence Initiative Organigation (SDIO) space insulation technologies", Conference record of the 1992 IEEE International symposium on electrical insulation, Baltimore, USA

6 2 R V Latham, "Prebreakdown electron emission", IEEE Trans on Electrical Insulation, vol EI-18, pp 194-203, 1983

6 3 T Shioiri, I Ohshima, M Honda, H Okumura, H Takahasi, H Yoshida, "Impulse voltage field emission characteristics and breakdown dependency upon field strength in vacuum gaps", IEEE Trans on PAS, vol PAS-101, pp 4178-4184, 1982

6 4 H Toya, T Hayashi, M Yorita and Y Murai, "Numerical modeling to evaluate the withstand voltage of a HV vacuum interrupter", IEEE Trans on Electrical Insulation, vol EI-24, pp 21-30, 1989

6 5 M Okawa, T Shiori, H Okubo, S yanabu, "Area effect on electric breakdown of copper and stainless steel electrodes in vacuum", IEEE Trans on Electrical Insulation, vol EI-23, pp 77-81, 1988.

6 6 K Tsuruta, "Impulse electrical breakdown fields of short vacuum gaps", IEEE Trans on Electrical Insulation, vol EI-22, pp 77-79, 1987

6 7 T Tsutsumi, T Shioiri, H Okubo and S Yanabu, "The effect of mechanical contact on breakdown characteristics in vacuum", IEEE Trans on Electrical Insulation, vol EI-24, pp 921-924, 1989

6 8 B Mazurek, and J D Cross, "An energy explanation of the area effect in electrical breakdown in vacuum", IEEE Trans on Electrical Insulation, vol EI-22, pp 341-346, 1987

6 9 H Pursch, P Siemroyh and B Juttner, "On the nature of prebreakdown emission currents in vacuum interrupters", IEEE Trans on Electrical Insulation, vol EI-24, pp 917-920, 1989

6 10 R Hackam and S K Salman, "Electrical insulating properties of sterling silver electrodes in ultrahigh vacuum", IEEE Trans on Electrical Insulation, vol EI-10, pp 9-13, 1975

125681

EE-1995-D-KHA-INV

A125681